CA8205677/1

AECL-7254

THERMAL-HYDRAULICS IN RECIRCULATING STEAM GENERATORS

THIRST Code User's Manual

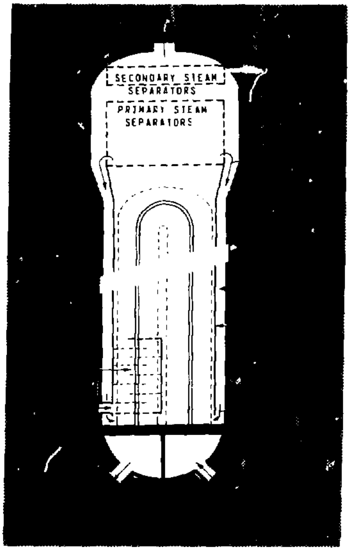

Model of steam generator used for analysis

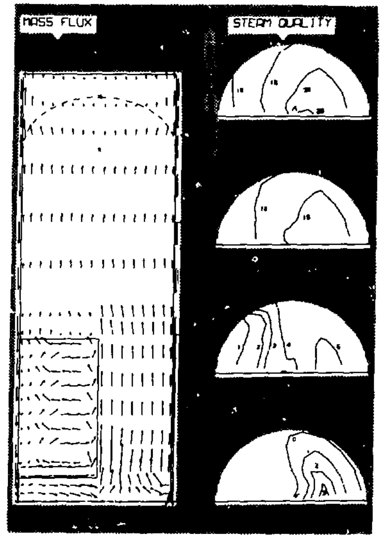

THIRST code results. Profiles of mass flux and steam quality

CARACTÉRISTIQUES THERMOHYDRAULIQUES DES GÉNÉRATEURS DE VAPEUR À RECIRCULATION

Manuel de l'utilisateur du code THIRST

M.B. CARVER, L.N. CARLUCCI, W.W.R. INCH

April 1981 avril

ATOMIC ENERGY OF CANADA LIMITED

THERMAL-HYDRAULICS IN RECIRCULATING STEAM GENERATORS

THIRST Code User's Manual

by

M.B. Carver, L.N. Carlucci, W.W.R. Inch

Chalk River Nuclear Laboratories
Chalk River, Ontario
1981 April

AECL-7254

L'ENERGIE ATOMIQUE DU CANADA, LIMITEE

Caractéristiques thermohydrauliques des générateurs de vapeur à recirculation

Manuel de l'utilisateur du code THIRST

par

M.B. Carver, L.N. Carlucci et W.W.R. Inch

Résumé

Ce manuel décrit le code THIRST et son utilisation pour calculer les écoulements tridimensionnels en deux phases et les transferts de chaleur dans un générateur de vapeur fonctionnant à l'état constant. Ce manuel a principalement pour but de faciliter l'application du code à l'analyse des générateurs de vapeur typiques des centrales nucléaires CANDU. Son application à d'autres concepts de générateurs de vapeur fait l'objet de commentaires. On donne le détail des hypothèses employées pour formuler le modèle et pour appliquer la solution numérique.

Laboratoires nucléaires de Chalk River
Chalk River, Ontario
KOJ 1JO

Avril 1981

AECL-7254

ATOMIC ENERGY OF CANADA LIMITED

THERMAL-HYDRAULICS IN RECIRCULATING STEAM GENERATORS
THIRST CODE USER'S MANUAL

by

M.B. Carver, L.N. Carlucci, W.W.R. Inch

ABSTRACT

This manual describes the THIRST code and its use in computing three-dimensional two-phase flow and heat transfer in a steam generator under steady state operation. The manual is intended primarily to facilitate the application of the code to the analysis of steam generators typical of CANDU nuclear stations. Application to other steam generator designs is also discussed. Details of the assumptions used to formulate the model and to implement the numerical solution are also included.

Chalk River Nuclear Laboratories
Chalk River, Ontario
KOJ 1JO
1981 April

AECL-7254

TABLE OF CONTENTS

TABLE OF CONTENTS (continued)

Page

TABLE OF CONTENTS (continued)

LIST OF FIGURES

LIST OF FIGURES (continued)

1. INTRODUCTION

The THIRST* computer code is the latest in a series of three-dimensional steady state computer codes developed at CRNL for the detailed analysis of steam generator thermal-hydraulics. The original code, designated BOSS**, arose from the DRIP*** program of Spalding and Patankar [1], and was adapted for application to CANDU**** type steam generators [2]. Although the equations to be solved remain the same, extensive changes have been made to the program structure, the numerical computation sequence, the empirical relationships involved, the treatment of the U-bend, and the numerical and graphical presentation of results. The code has therefore been renamed THIRST.

In conjunction with these developments, the program has been used to successfully analyse the thermal-hydraulic performance of a number of different steam generator designs, from CANDU to American PWR nuclear plants. The program has also been used for extensive design parameter surveys. Some results of these analyses have been released in publications [3-7]. Steam generator designs already analysed are summarized in Table 1.1.

As the structure of the THIRST code is now well established, and its flexibility and reliability have been illustrated by extensive application, the time is now appropriate to present the code in a formal manner. It is our intent in this manual to present sufficient details of the THIRST code to permit a new user to run the code, and to obtain parameter survey studies based on variations of a reference hypothetical steam generator design. Suggested approaches to other basic designs are also included.

---

* THIRST: Thermal-Hydraulics In Recirculating STeam Generators

** BOSS: BOiler Secondary Side

*** DRIP: Distributed Resistance In Porous Media

**** CANDU: CANada Deuterium Uranium

Before presenting details of the code implementation, and discussing the input data required, some background knowledge of the nature and function of steam generators must be established.

1.1 Steam Generator Thermal-Hydraulics

The steam generator is a critical component in a nuclear power plant because it provides the interface for heat exchange between the high pressure reactor primary coolant circuit and the secondary turbine circuit. The integrity of this interface must be maintained to prevent mixing of fluids from the two circuits, while thermal interaction must be maximized for efficient transfer of energy to the turbine from the reactor.

Figure 1.1 is a cutaway view showing the salient features of a typical CANDU steam generator. The hot primary fluid from the reactor circulates through the network of tubes, heating the secondary flow which evaporates as it rises inside the shell. Failure of any one of the tubes would lead to expensive downtime for the station. The most likely causes of such tube failure are corrosion and fretting of the tube material. Corrosion can be minimized by regulating secondary fluid chemistry and by optimizing secondary side flow to minimize flow stagnation areas where corrosion tends to be highest. Fretting of tube surfaces due to flow-induced vibrational contact can also be analysed and local flow conditions can be computed with sufficient accuracy. The location of tube supports which minimize vibration can then be specified. In either case, a detailed picture of the flow patterns under operating conditions is required. The THIRST code provides such a picture.

TABLE 1.1

STEAM GENERATOR DESIGNS ANALYSED

	Manufacturer		Nuclear Plant	Thermal Power Rating (MW)
1	Babcock & Wilcox	Pickering	CANDU-PWR	140
2	Babcock & Wilcox	G-2	CANDU-PWR	515
3	Babcock & Wilcox	Pt. Lepreau	CANDU-PWR	515
4	Babcock & Wilcox	Cordoba	CANDU-PWR	510
5	Babcock & Wilcox	Darlington	CANDU-PWR	660
6	Foster-Wheeler	Darlington	CANDU-PWR	670
7	Foster-Wheeler	Wolsung	CANDU-PWR	515
8	Combustion Eng.	Maine Yankee	US-PWR	845
9	Combustion Eng.	System 80	US-PWR	1910
10	Combustion Eng.	Series 67	US-PWR	1260
11	Westinghouse	Model 51	US-PWR	850

TABLE 1.2

PARAMETERS OF A TYPICAL CANDU STEAM GENERATOR

Thermal Rating	600 MW
Primary Inlet Temperature	315°C
Primary Inlet Pressure	10.7 MPa
Primary Inlet Quality	0.034
Primary Flow Rate	2500 kg/s
Feedwater Temperature	180°C
Steam Pressure	5 MPa
Steam Flow Rate	310 kg/s
Recirculation Ratio	5.5
Downcomer Water Level	15 m
Number of Tubes	4850
Tube Bundle Radius	1.3 m
Tube Diameter	0.0125 m

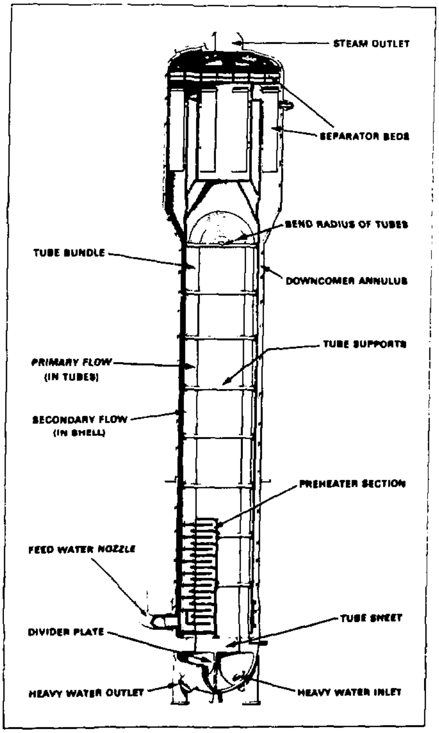

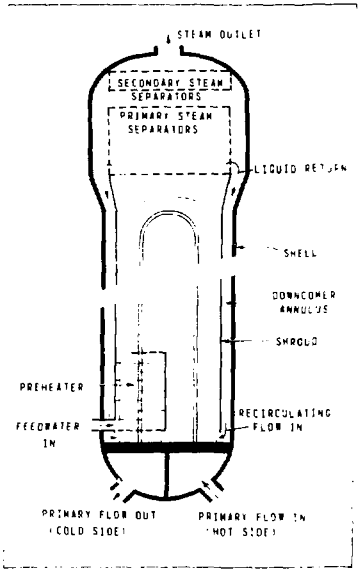

Figure 1.1
Cutaway View of a Steam Generator

Figure 1.2
Simplified Model of the Steam Generator

1.2 The Hypothetical Prototype Steam Generator

Although steam generators developed by different manufacturers share a number of common features, it would be a prohibitive task to attempt to write a computer code which would comprehensively include all possible designs. The bulk of this manual, therefore, describes the standard version of the THIRST code which has been written for analysis of a hypothetical steam generator containing many features common to CANDU designs (Figure 1.1).

In particular, it is a natural circulation steam generator with the following features

- integral preheater
- tube matrix with round U-bends
- annular downcomer with re-entry through specified windows in the circumference

Geometrical specifications and nominal operating conditions of such a hypothetical design are listed in Table 1.2 for a typical 600 MW thermal steam generator.

A simplified diagram of a natural circulation steam generator with integral preheater is given in Figure 1.2. The area inside the shroud is completely filled with tubes except for the central tube free lane between the hot and cold legs and the annulus between the outer tube limit of the bundle and the shroud. The surface of the outer limit of the bundle in the U-bend is spherical.

The primary fluid enters the right side of the sketch flowing up inside the 'hot side' tubes, transferring heat to the secondary fluid en route. The tubes turn through 180° in the U-bend region, and the fluid returns down the cold side. The secondary fluid enters as subcooled water through the integral preheater, where baffles force the flow to cross the tube bank in a zig-zag pattern to enhance heat transfer. At the preheater exit this flow, now raised to saturation temperature, mixes with flow recirculated from the hot side. The resulting mixture undergoes partial evaporation and rises as a two-phase mixture through the remaining bundle section, into the riser, and up into the separator bank. Here the two phases are separated. The steam leaves the vessel to enter the turbines, while the remaining saturated liquid flows through the annular downcomer to the bottom of the vessel. Here it re-enters the heat transfer zone through windows around the shroud circumference.

The downcomer flow entering through the windows on the hot side partially penetrates the tube bundle before turning axially to flow parallel to the tubes. On the cold side, the downcomer flow must pass under the preheater to the hot side before it can turn axially. Thus the downcomer flow converges on the center of the hot side tube bundle.

As this fluid rises through the hot leg it absorbs heat from the tube side fluid. Quality develops very rapidly because the downcomer flow is very close to saturation. Above the top of the preheater, this mixture mixes with the fluid from the preheater.

The tubes are supported by broached plates located along straight portions at the U-tubes. Further lattice supports are located in the U-bend. The baffles in the preheater are drilled plates.

In this design, no feedwater leakage through the thermal plate (floor of the preheater) or the partition plate is allowed. All the feedwater must exit at the top of the preheater.

The primary fluid, heavy water, enters the tube bundle from the reactor circuit as a low quality two-phase mixture. The primary mass flow distribution is determined by the code, although the quality distribution is assumed to be uniform at entry. The secondary fluid is light water. It enters the preheater at subcooled conditions. It is assumed to enter the preheater at a uniform velocity. The driving force for natural circulation is provided by the height of water in the downcomer annulus.

1.3 The THIRST Standard Code and its Intended Application

The THIRST computer code, as evidenced by Table 1.1, can be readily adapted to a number of steam generator designs as the numerical method is extremely robust. The standard THIRST package, however, pertains to a hypothetical steam generator.

The program models a region extending from the face of the tubesheet in Figure 1.2, up to the separator deck, including the downcomer annulus. Symmetry permits analysis of only one half of the vessel.

1.4 The Use of This Manual

The THIRST package is designed to make numerical modelling of steam generator thermal-hydraulics as straightforward as possible. Thus a seasoned user of the code will normally consult only chapters 4 and 5 of this report, which outline in detail the procedures required to layout the computation grid and prepare the input data.

However, to properly accomplish these tasks, the user must first understand the fundamental principles of the relevant mathematical formulation and numerical solution tecnniques. These are summarized in chapters 2 and 3 which follow.

2. FOUNDATIONS OF THE MODEL

The THIRST code computes the steady state thermal-hydraulics of a steam generator by solving the well-known conservation equations in three-dimensional cylindrical coordinates.

This chapter states the equations involved, outlines the overall solution procedure, and lists the assumptions used to formulate the model and the thermal-hydraulic data required.

2.1 The Governing Equations

The THIRST code solves secondary side transport equations having the following general form:

$$\frac{1}{r}\frac{\partial}{\partial r}(\beta r \rho v \phi) + \frac{1}{r}\frac{\partial}{\partial \theta}(\beta \rho w \phi) + \frac{\partial}{\partial z}(\beta \rho u \phi) = \beta S_{\phi} \qquad (2.1)$$

Here v, w, and u are the velocity components in the r, θ and z directions, respectively, β is the volume-based porosity, ρ is the mixture density, S_{ϕ} is the source term corresponding to the transport parameter ϕ. The latter two, for each of the five transport equations, are listed in Table 2.1.

In the table, P is the pressure; R_r, R_{θ} and R_z are the flow resistances per unit volume offered by the tubes, baffles and other obstacles; h is the secondary fluid enthalpy; S_h is the rate of heat transferred per unit volume from the primary to the secondary; and g is the acceleration due to gravity.

TABLE 2.1

Transport Equation	ϕ	S_ϕ	Equation Number
Continuity	1	0	2.2
Radial momentum	v	$-\frac{\partial P}{\partial r} + \frac{\rho w^2}{r} - R_r$	2.3
Angular momentum	w	$-\frac{1}{r}\frac{\partial P}{\partial \theta} - \frac{\rho v w}{r} - R_\theta$	2.4
Axial momentum	u	$-\frac{\partial P}{\partial z} - \rho g - R_z$	2.5
Energy (secondary)	h	S_h	2.6

THIRST also solves the primary side energy equation which for a differential length of tube $\delta \ell$ is given by:

$$G_p \frac{\delta h_p}{\delta \ell} = - \frac{4d\psi}{d_i^2} \tag{2.7}$$

where G_p and h_p are the primary fluid mass flux and enthalpy, respectively, ℓ is the distance along the tube, d is the tube outer diameter, d_i is the tube inside diameter, and ψ is the heat flux at the outer tube surface. The heat flux is calculated from:

$$\psi = U(T_p - T_s) \tag{2.8}$$

where T_p is the primary temperature, T_s is the secondary temperature and U is the overall heat transfer coefficient based on the tube outer area, given by:

$$U = \left(\frac{d}{d_i}\,\frac{1}{h_p} + \frac{d\ \ell n(d/d_i)}{2k_w} + \frac{1}{h}\right)^{-1} \tag{2.9}$$

Here, h_p and h are the primary and secondary heat transfer coefficients, respectively, and k_w is the thermal conductivity of the tube wall material. The source term in equation 2.6 is related to the heat flux by:

$$S_h = \lambda\psi \tag{2.10}$$

where λ is the tube surface area per unit volume.

2.2 Modelling Assumptions

The governing equations are based on the following assumptions and simplifications:

(1) The flow is steady, incompressible and homogeneous.

(2) The shell and shroud walls are adiabatic.

(3) The inside shroud wall is frictionless.

(4) Laminar and turbulent diffusion are negligible in comparison to the frictional resistances and heat source.

(5) The distributed resistances due to the presence of tubes and other solid obstacles are calculated using standard friction factor correlations. Similarly, primary to secondary side heat transfer rates are calculated using empirical heat transfer correlations.

(6) Reductions of flow due to the presence of tubes and other obstacles are accounted for by defining a volume-based porosity.

(7) The primary temperature distribution is calculated from the enthalpy distribution by using a polynomial curve fit (see Chapter 7).

(8) Secondary subcooled values of temperature, viscosity, etc., are calculated by using polynomial curve fits of each parameter expressed as a function of the secondary enthalpy (see Chapter 7).

2.3 Boundary Conditions

Boundary and start-up conditions such as primary flow and temperature, secondary feedwater flow and temperature, downcomer water level, etc., are described in detail in Chapter 4.

2.4 Overview of the Solution Sequence

The numerical solution sequence, apart from some variations discussed later, follows the techniques outlined by Patankar and Spalding in reference [8]. A fair understanding of the mechanics of the technique is required for advanced use of the THIRST code, and Appendix A contains details of the overall formulation.

At this point, however, we present a brief exposition of the philosophy of the method, including only a minimum of mathematics.

THIRST solves the five secondary side transport equations (2.1) in three dimensions to compute distributions of the dependent variables u, v, w, h, and P. The mixture density ρ is calculated from the equation of state $\rho = \rho(h,P)$. The variables are stored in three-dimensional arrays of up to 5000 grid points. This generates about 30,000 simultaneous non-linear differential equations. Obviously, this requires some form of technique which permits the solution to concentrate on portions of the equation set rather than attempting a simultaneous solution. This is accomplished by considering each of the transport equations separately, and then iterating through the full set of equations.

The solution of any given transport equation itself involves developing a finite difference statement of the equation and solving it in an inner iteration, but we will delay considering this until later. Suffice it to say that the transport equations can be reduced to a set of linear matrix equations and written as follows:

Continuity $$A_F U + B_F V + C_F W = 0 \qquad (2.11)$$

Momentum $$D_U U + E_U + F_U P = 0 \qquad (2.12)$$

$$D_V V + E_V + F_V P = 0 \qquad (2.13)$$

$$D_W W + E_W + F_W P = 0 \qquad (2.14)$$

Energy $$Hh + G = 0 \qquad (2.15)$$

State $$\rho = f(P, h) \qquad (2.16)$$

The coefficient matrices A to G are functions involving first estimates of the dependent variables u, v, w, ρ, h, P. We wish to solve equations 2.11 to 2.16 in a sequence that will eventually lead to all six equations being satisfied.

This is accomplished as follows:

i) solve equation 2.12 to get new estimates of U

$$U = -D_U^{-1} \left[E_U + F_U P\right]$$

$$= E_U^* + F_U^* P \qquad (2.17)$$

ii) and iii) operate similarly on equations 2.15 and 2.14 to give

$$V = E_V^* + F_V^* P \qquad (2.18)$$

$$W = E_W^* + F_W^* P \qquad (2.19)$$

The new values of the U,V,W matrices have thus been computed from the initial estimates using the momentum equations. If the original estimates of all the variables were correct, the values would satisfy the continuity equation (2.11). Invariably, however, they will not satisfy (2.11) but will generate a mass imbalance residual R. As pressure is the dominant variable in the momentum equations, it is logical to adjust the pressure matrix in a direction that will reduce R to zero.

A logical method of adjusting pressure is to assess its effect on the velocity components by differentiating equation 2.17 with respect to pressure.

$$\frac{dU}{dP} = F_U^*$$

Thus we can write

$$\begin{aligned} dU &= F_U^* dP \\ dV &= F_V^* dP \\ dW &= F_W^* dP \end{aligned} \qquad (2.20)$$

Now if the pressure adjustment matrix dP in (2.20) is correct, the new velocity matrix

$$U_{NEW} = U_{OLD} + dU \tag{2.21}$$

will satisfy the continuity equation 2.11. Substituting 2.21 and similar equations for V_{NEW} and W_{NEW} in 2.11, then gives rise to the equation

$$\begin{aligned} &AU_{OLD} + BV_{OLD} + CW_{OLD} \\ &+(AF_U^* + BF_V^* + CF_W^*)\, dP = 0 \end{aligned} \tag{2.22}$$

Or more simply:

$$R + (F)dP = 0 \tag{2.23}$$

Equation 2.23 thus illustrates the pressure correction matrix dP required to eliminate the mass imbalance generated by the old velocity values.

Thus the relevant steps are:

iv) compute dP from 2.23

v) compute U, V, W from 2.20 and 2.21

If the equation set were linear, steps iv) and v) would complete the solution. However, the linearized equations contain some remnants of the initial estimate, so steps iv) and v) must be repeated several times.

Finally, the energy equation must also be incorporated:

vi) compute h from equation 2.15

vii) compute ρ from equation 2.16.

The sequence i) to vii) is now repeated to convergence.

The iteration sequence may be summarized as follows:

repeat

i) compute U from equation 2.12
ii) compute V from equation 2.13
iii) compute W from equation 2.14

repeat

iv) compute dP from equation 2.23
v) compute dU, dV, dW from equations 2.20 and 2.21
vi) compute h from equation 2.15
vii) compute ρ from equation 2.16.

In the THIRST program, the outer iteration sequence is orchestrated by the executive routine, which calls a separate routine to perform each of the above steps.

2.5 Thermal-Hydraulic Data

2.5.1 Fluid Properties and Parameters

As mentioned in Section 2.2, equations of state for both the primary (heavy water) and secondary (light water) fluids are required in the analysis. These are incorporated in the THIRST code using relationships derived from standard tables. Full details of these are given in Chapter 7.

2.5.2 Empirical Relationships

In assembling the terms of the differential equations, any thermal-hydraulic code must rely on empirical correlations to approximate a number of phenomena which cannot be prescribed analytically. These empiricisms include correlations for single and two-phase heat transfer and pressure drop in rod bundle arrays and for void fraction.

All correlations used in the THIRST code are summarized in Chapter 7.

3. IMPLEMENTATION FUNDAMENTALS

The previous chapter has discussed the governing equations, developed a suitable solution philosophy, and mentioned the thermal-hydraulic data required to complete the specification of the model. This chapter is concerned with the manner in which these general principles are implemented in the THIRST code. This involves the establishment of the computational grid, the conversion of the partial differential equations to discrete node equations by means of control volume integration, and the technique used to perform the 'inner' solution of individual equations.

The control volume integration and equation solution are of course built into THIRST, but in order to choose an effective grid layout, the user needs some feeling of these procedures.

3.1 The Coordinate Grid

A three-dimensional cylindrical coordinate system is used for obvious reasons. The entire flow domain between the tubesheet and the separator bank is subdivided by planes of constant r, z and θ. The grid arrangement is chosen to suit the geometry and expected flow patterns of the steam generator. Thus it is usually not uniform, but is arranged to provide finer division in the region where steep gradients are expected, for example near the tubesheet.

Following the now classical grid arrangement introduced by Harlow, et al, [9], scalar variables, such as pressure, density and enthalpy are centered at the points of intersection of the grid lines, or nodes. As pressure is the driving force, pressure differences generate velocities between nodes, thus velocities are centered between nodes. The resulting grid arrangement is shown in Figures 3.1 to 3.4. Velocities are considered positive in the direction of the coordinate vector.

3.2 The Control Volumes

Finite difference approximations to the partial differential equations may be derived in many ways. However, the control volume integral approach has proved particularly successful in fluid modelling. This is principally because it easily incorporates variable mesh size, yet rigorously enforces continuity. It does, however, introduce additional complexities, as the finite difference form of each equation must be integrated using a control volume centered on the primary variable concerned. Thus scalars are considered to be constant over control volumes centered at grid points, while the axial momentum equation is integrated over a control volume centered on the U velocity, and the radial and azimuthal momentum equations are centered on V and W, respectively. Typical control volumes for each of these four cases are also shown in Figures 3.1 to 3.4.

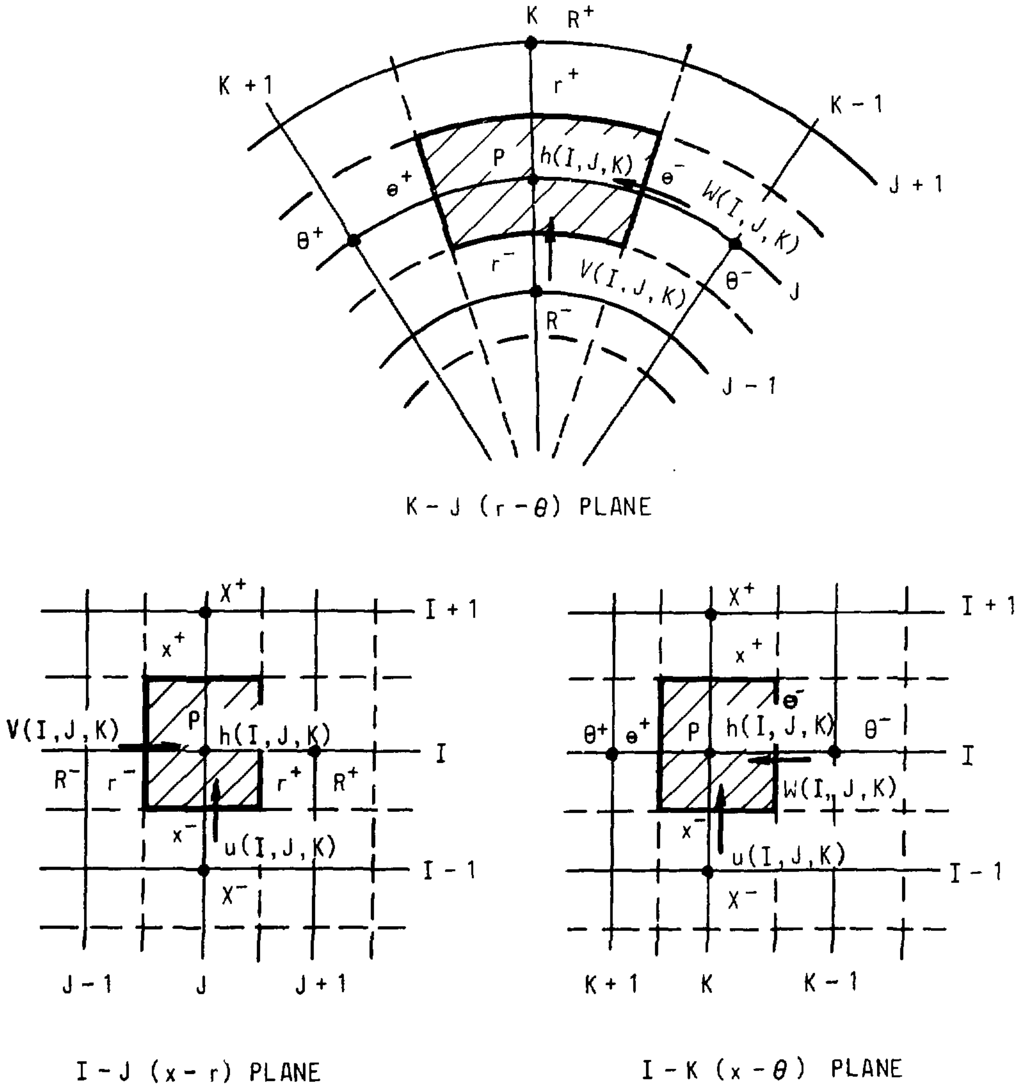

Figure 3.1: Grid Layout showing Scalar and Vector Locations

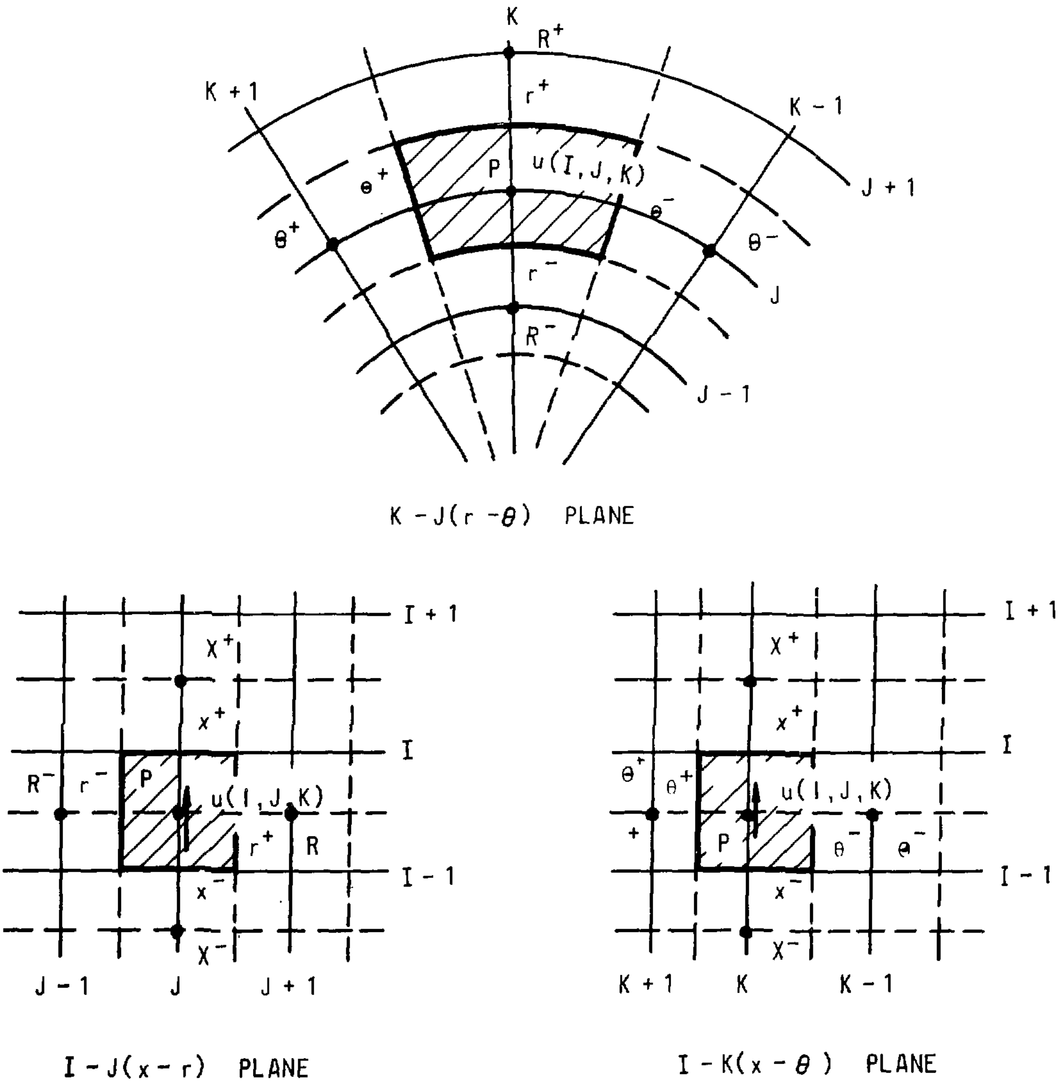

Figure 3.2: Control Volumes for Scalar Quantities

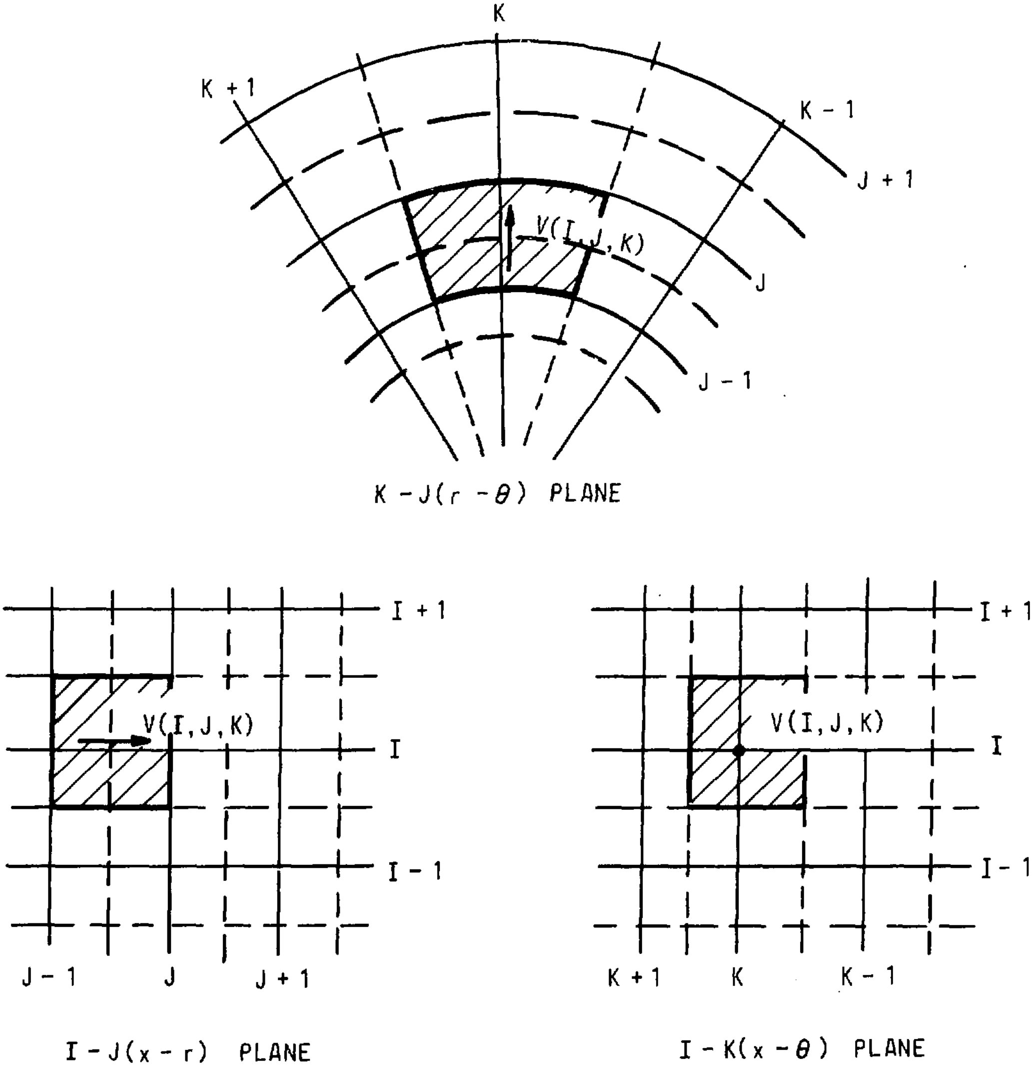

Figure 3.3: Control Volumes for Radial Velocity Vectors

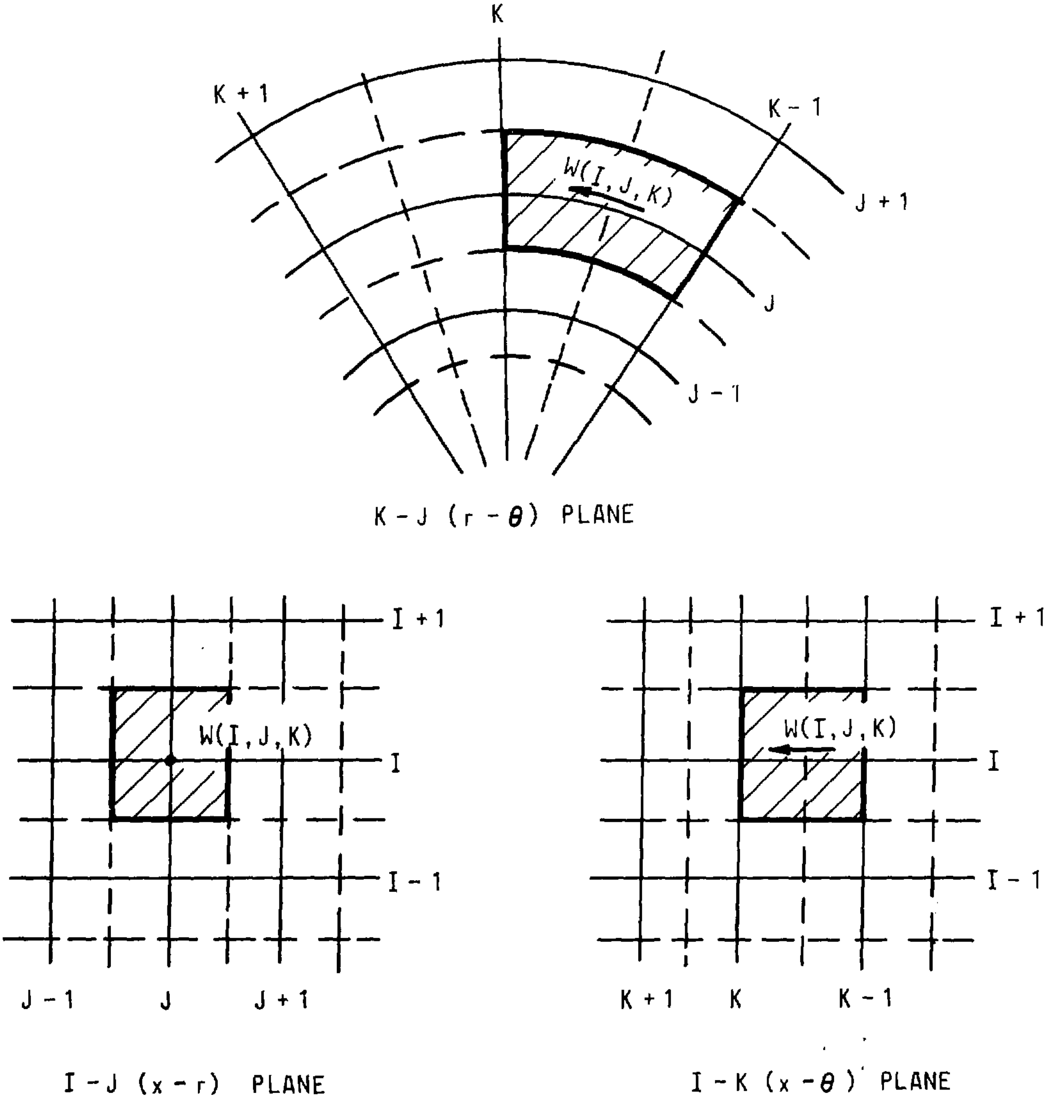

Figure 3.4: Control Volumes for Circumferential Velocity Vectors

3.3 The Control Volume Integral Approach

Although the equations to be solved are integrated over different control volumes, the procedure in each case is completely the same. Thus, each equation may be written in the form of equation 2.1 and integrated

$$\iiint_V \left[\frac{1}{r}\frac{\partial}{\partial r}(\beta r\rho v\phi) + \frac{1}{r}\frac{\partial}{\partial \theta}(\beta\rho w\phi) + \frac{\partial}{\partial z}(\beta\rho u\phi) - \beta S_\phi\right] r dr d\theta dz = 0 \qquad (3.1)$$

Although the integration is done formally by use of Gauss theorem,

$$\iiint_V \nabla\cdot\phi dv = \iint_S (\dot{n}\cdot\phi) ds \qquad (3.2)$$

the result is intuitively obvious from first principles.

It is

$$\left[(\beta r\rho v\phi)_n - (\beta r\rho v\phi)_s\right]\Delta\theta\Delta z + \left[(\beta\rho w\phi)_e - (\beta\rho w\phi)w\right]\Delta r\Delta z + \left[(\beta\rho u\phi)_h - (\beta\rho u\phi)_\ell\right] r\Delta\phi\Delta z = \iiint \beta S_\phi dv \qquad (3.3)$$

The (quantities) obviously represent the flux through the appropriate control volume face, and the [quantities] represent the flux imbalance in each coordinate direction.

3.3.1 Integration of the Source Terms

The source terms are frequently non-linear in ϕ. Integration of these terms is accomplished term by term. The result can be linearized with respect to ϕ and stated in general form as

$$S\,v \equiv S_U + S_P\phi_P \qquad (3.4)$$

Here the term S_P normally contains all coefficients of ϕ_p, and S_U contains remaining terms which are generally (but not always) unrelated to ϕ_p.

Reexamining the equations in Table 2.1, it is apparent that the greater part of the programming in the THIRST code is involved with formulating and integrating the resistance components of the source terms, using the appropriate empirical correlations. This is done in subroutines with the generic name SOURC.

3.3.2 Integration of the Flux Terms

It is apparent from equation 3.3 and figure 3.2 that values at, for example, control volume face n can be obtained to first order accuracy by upwind approximation for any variable A, which assumes that the velocity vector convects scalars from upwind only. Thus if all velocities are positive, inlet flows convect neighbouring scalars, outlet flows convect the control volume scalar. Denoting the coefficients of ϕ by C, and using the upwind approximation, equation 3.3 is reduced to the form

$$C_n\phi_p - C_s\phi_s + C_e\phi_p - C_w\phi_w = S_u + S_p\phi_p \qquad (3.5)$$

where C_i is the flux evaluated at control volume face i.

Collecting terms gives

$$A_p\phi_p = \Sigma A_i\phi_i + S_U$$

$$i = n,s,e,w,h,\ell \qquad (3.6)$$

$$A_n = C_n \qquad A_s = C_s \qquad \text{etc.}$$

$$A_p = \Sigma A_i - S_p$$

Once the coefficients A have been computed, equation 3.6 is the standard linear equation set

$$A\,\phi = B \qquad (3.7)$$

which can be readily solved

$$\phi = A^{-1}B \qquad (3.8)$$

Actually, the size of the matrices prohibits direct solution, so iterative methods are used, and equation 3.8 is solved by an 'inner' iteration.

3.4 The 'Inner' Iteration

The matrices of equation (3.7) are too large to permit direct solution of the equation set by means of (3.8) even when sparse matrix techniques are considered, so an iterative technique is used. It is well known that the solution of equation sets in which the matrix A is tridiagonal can be performed extremely quickly as the algorithm reduces to recursive form.

Equation 3.7 can be converted to tridiagonal form by including, for example, only the coefficients along the r direction on the left-hand side.

$$A_n\phi_n + A_p\phi_p + A_s\phi_s = -(\Sigma A_j\phi_j + S_U)$$
$$j = e, w, \ell, h \qquad (3.9)$$

Similar expressions can be written for the θ and z directions.

$$A_e\phi_e + A_p\phi_p + A_w\phi_w = -(\Sigma A_j\phi_j + S_U)$$
$$j = n, s, \ell, h \qquad (3.10)$$

$$A_h\phi_h + A_p\phi_p + A_1\phi_1 = -(\Sigma A_j\phi_j + S_U)$$
$$j = n, s, e, w \qquad (3.11)$$

A one-dimensional problem can be solved directly by (3.9). A two-dimensional problem is solved by an alternating direction iteration ADI method. This involves solving 3.9 and 3.10 alternately until the solutions converge. A three-dimensional solution requires the solution of 3.11 in addition. This creates several possibilities. For example, 3.9 and 3.10 could be solved for a number of iterations for each time 3.11 is solved. The most suitable strategy depends on the nature of the flow problem. The THIRST code has a number of different strategies designed to promote convergence in three dimensions. These are discussed in Appendix A.

3.5 Stability of the Solution Scheme

The outer iteration scheme discussed in Chapter 2 normally proceeds to convergence in a stable manner, and converges rapidly, providing each inner iteration is stable.

To promote stability of the iterations, three principal devices are incorporated in THIRST. The first, that of under-relaxation, is common to most iteration schemes. The second, upwind weighted differencing, is frequently used to stabilize both steady state and transient thermal-hydraulic calculations [10]. The third concerns the formulation of the source terms to ensure stability.

3.5.1 Under-Relaxation

Because the solution is obtained by iteration, there is a strong likelihood that variable values may fluctuate unduly during the initial stages. It is common practice to stabilize these fluctuations using under-relaxation. Thus if ϕ^N is calculated from 3.9 to 3.11 using previous values ϕ^{N-1}, it is then replaced by

$$\phi^N_{P_{\text{Relax}}} = \alpha\phi^N_{P_{\text{Calc.}}} + (1-\alpha)\phi^{N-1}_{P_{\text{old}}} \qquad (3.12)$$

Relaxation factors α for each equation solution are supplied with the THIRST code, but may be changed by data input if necessary.

In practice, it is possible to impose under-relaxation before attempting the linear equation solution instead of after its completion. This is preferable as it minimizes the chances that the linear equation solution itself may generate unlikely values.

Recall that the equation to be solved is 3.6, or

$$\phi_P = -(\Sigma A_i \phi_i + S_U)/A_P \tag{3.13}$$

Substitution of 3.13 into 3.14 gives

$$\phi^N_{P_{Relax}} = -(\Sigma A_i \phi_i + S_U)(\alpha/A_P) + (1-\alpha)\phi_P^{N-1}$$

or

$$\phi^N_{P_{Relax}} = -(\Sigma A_i \phi_i + \bar{S}_U)/\bar{A}_P$$

when

$$\bar{S}_U = S_U + (1-\alpha)\bar{A}_P \phi_P{}^{N-1}$$

$$\bar{A}_P = A_P/\alpha \tag{3.14}$$

This pre-relaxed equation can obviously be solved using the identical techniques already discussed.

In THIRST, all equations are pre-relaxed in this manner, except for the pressure corrections and density calculation. Equation 2.23 returns a pressure correction rather than the pressure itself. Pressures arising from this correction may be relaxed according to 3.12, but this is not usually necessary. Density may also be relaxed by 3.12.

3.5.2 Upwind Biased Differencing

It is well known that symmetric central difference representation of first derivative terms in transient equations leads to unstable numeric behaviour [10,11]. Stability is usually ensured by incorporating one of two devices in the numeric scheme. The first, artificial dissipation, adds an artificially large viscous term to the equations. The second, upwind differencing uses difference formulae which are asymmetrically weighted towards the upwind or approaching flow direction. Both devices stabilize the computation and, in fact, it can be shown that they are numerically equivalent [11].

Central differencing has the same destabilizing effect in steady state, and computations can be stabilized by the same devices.

Consider, for example, a one-dimensional central difference statement of equation 3.5.

$$C_n \frac{(\phi_N + \phi_P)}{2} - C_s \frac{(\phi_P + \phi_S)}{2} + S_\phi = 0 \tag{3.15}$$

This can be reduced to

$$\phi_P = \frac{C_s \phi_S - C_n \phi_N - 2S_\phi}{C_n - C_s} \tag{3.16}$$

As C_s approaches C_n, the denominator becomes very small, generating undue excursions in ϕ values. In particular if C_s exceeds C_n very slightly, a small increase in ϕ_s gives a large decrease in ϕ_P - an impossible situation.

However, if we add diffusion terms which involve the second derivative, the resulting equation can be shown [13] to be

$$\phi_P = \frac{(D_s + C_s)\phi_S + (D_n - C_n)\phi_N - 2S_\phi}{D_n + D_s + C_n - C_s} \tag{3.17}$$

Note that 3.17 will always be stable providing the diffusion influence $D_n + D_s$ is large enough.

Similarly on physical reasoning alone, one may consider that ϕ is swept primarily in the direction of flux. The simple upwind statement of 3.16 already introduced in section 3.5 is

$$C_n \phi_P - C_s \phi_S + S_\phi = 0$$

This reduces to

$$\phi_P = \frac{C_s \phi_S - S_\phi}{C_n} \qquad (3.18)$$

which will always be stable.

Equation 3.18 is the simplest possible upwind formulation and is equivalent to adding excess viscosity. Its use has been criticized because it can lead to diffusion of the solution, particularly when the flow direction is not normal to the grid axes [14,15]. A number of higher order difference schemes which can be used to give more accuracy may be developed [10,12] and some of these may be implemented in schemes similar to that used in THIRST [15].

In the THIRST code, the simple formulation is retained, however. The large flow resistances and heat sources due to the closely packed tube bundles in the steam generators dominate the computation to such an extent that the differences which would be caused by higher order methods are believed to be minor.

3.6 Notation used in THIRST

Finally, we have up to here been using single subscripts n, s, etc. *for simplicity.* The code, however, is written in cylindrical coordinates and uses terms such as AXM to denote A_{x-}. On this basis, equation 3.6 becomes

$$A_p \phi_p = \Sigma A_i \phi_i + S_U \tag{3.19}$$

where:

$$A_p = A_{r+} + A_{r-} + A_{\theta+} + A_{\theta-} + A_{x+} + A_{x-} + DIVG - SP$$

The upwind formulation can be implemented to consider flow direction automatically in the following manner:

$$A_{r+} = \left|\frac{C_{r+}}{2}\right| - \frac{C_{r-}}{2} \quad ; \quad C_{r+} = (\beta\rho a v)^{\dagger}_{r+} \quad ; \; a = \text{face area}$$

$$A_{r-} = \left|\frac{C_{r-}}{2}\right| + \frac{C_{r-}}{2} \; ; \quad C_{r-} = (\beta\rho a v)_{r-} \tag{3.20}$$

$$A_{\theta+} = \left|\frac{C_{\theta+}}{2}\right| - \frac{C_{\theta+}}{2} \; ; \quad C_{\theta+} + (\beta\rho a w)_{\theta+}$$

etc.,

† C_{r+} = mass flow through control volume face r_+; depending on the transport parameter ϕ; β, ρ, v are either defined at that face or interpolated to that face.

$$DIVG = C_{r+} - C_{r-} + C_{\theta+} - C_{\theta-} + C_{x+} - C_{x-}$$

$\equiv$ net accumulation of mass in the control volume

The table below defines A_i and ϕ_i for each i:

i	A_i	ϕ_i
r+	A_{r+}	ϕ_{R+}
r-	A_{r-}	ϕ_{R-}
θ+	$A_{\theta+}$	$\phi_{\theta+}$
θ-	$A_{\theta-}$	$\phi_{\theta-}$
x+	A_{x+}	ϕ_{X+}
x-	A_{x-}	ϕ_{X-}

Note that this formulation also automatically handles possible extreme cases in which all flow directions but one are in towards (or out away from) a control volume.

3.7 Formulation of the Source Terms

For stability of the inner iteration, it is essential that the coefficients remain positive after the source terms are incorporated. Thus, in 3.20, SP must be negative. Cases in which SP tends to be positive are catered for by artificially augmenting SU. For example, if $S = -K\rho V^2$, one may write $SP_V = -2K\rho|V|$, $SU = +K\rho V^2$; SU will then incorporate the old value of V, and SP will ensure the formulation is both stable and implicit.

This section completes the overall description of the model implementation. The following chapters contain detailed instructions on how to use the code.

4. APPLICATION OF THIRST TO ANALYSE THE PROTOTYPE DESIGN

Specification of the three-dimensional model must include details of all relevant geometrical, fluid flow and heat transfer parameters. It is emphasized that the process of modelling a steam generator relies heavily on diligent assembly of the specifications, optimal choice of grid layout, and of course correct preparation of the input data. This chapter is intended to guide the user step by step through the considerable effort required.

By means of a detailed example, we illustrate the entire procedure required to prepare a THIRST analysis of a particular steam generator design. We assume the user is familiar with the fundamentals discussed in Chapters 2 and 3, and now discuss

Design Specification - the hypothetical steam generator

Grid Selection - arrangement of optimal grid layout

Preliminary Data Specification - procedure for assembling the data specification sheets

Preparation of Input Data Cards

Sample Input Deck

Execution Deck - assembly of a THIRST job and submission to the CIC computer

4.1 Design Specification

The particular case chosen for this example is the hypothetical steam generator discussed in Chapter 1 and shown in Figure 1.2. Design parameters used in the current example are summarized in Table 1.2.

A large number of variations of this design can be investigated using the standard THIRST code by specifying parameter variation through input data.

Designs which deviate from the hypothetical model in major aspects may require code modifications. These are considered in Chapter 5.

4.2 Grid Selection

The first task is to describe the geometry of the design to the computer. This is accomplished by superimposing a cylindrical coordinate grid onto the design, and by specifying the location of flow obstacles in terms of this grid. THIRST accepts a maximum of 40 axial planes, 20 radial planes and 20 circumferential planes; however, due to a storage limitation, the maximum number of nodes must not exceed 4900.

In order to appreciate the selection of grid locations, the user should understand the staggered grid arrangement used in THIRST described in Chapter 3. Essentially, velocities are centered between grid lines in their corresponding direction and centered on grid lines in the other two directions, as shown in Figure 3.1. An axial velocity, for example, has a control element with boundaries as shown in Figure 3.2. The top boundary corresponds to the I plane, the bottom to the I-1 plane. The left side boundary is located midway between the J and J-1 planes. The radial velocity has a control element that extends between J planes and straddles I and K planes. And similarly, the circumferential velocity extends between K-planes and straddles the I and J planes.

4.2.2 Baffles

Figure 4.1 shows how the code handles flow around a typical baffle. We observe a radial flow to the left under the baffle, an axial flow around the baffle followed by a radial flow to the right above the baffle. Note that the baffle lies in the middle of the U velocity control element and the radial control elements lie on either side of the baffle. We can see that axial grid lines must be located such that the baffle plates lie midway between them.

4.2.3 Partition Plate

Figure 4.1 also shows the code treatment of the partition plate. The circumferential velocity W corresponding to the K plane is blocked by this partition plate which is centered between the K and K-1 planes.

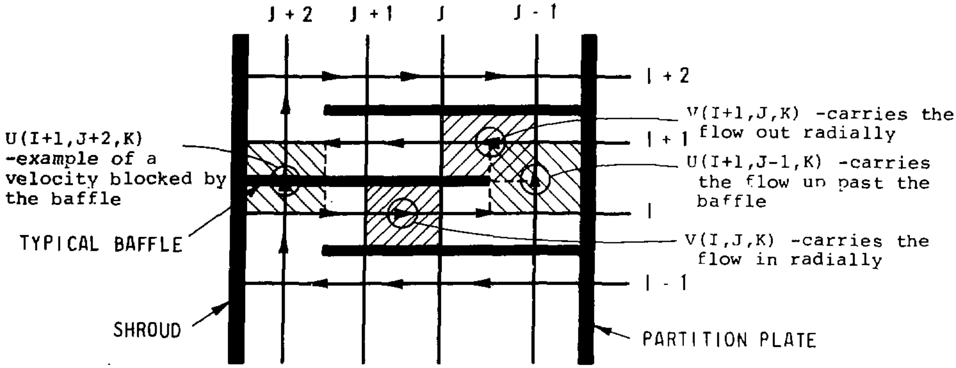

The I-planes are located so that baffles lie midway between them. The location of the J-planes matches the baffle cuts for this particular K-plane; however, the cut will not match other K-planes and the program is set up to handle this.

Figure 4.1: Grid Layout at a Baffle Plate

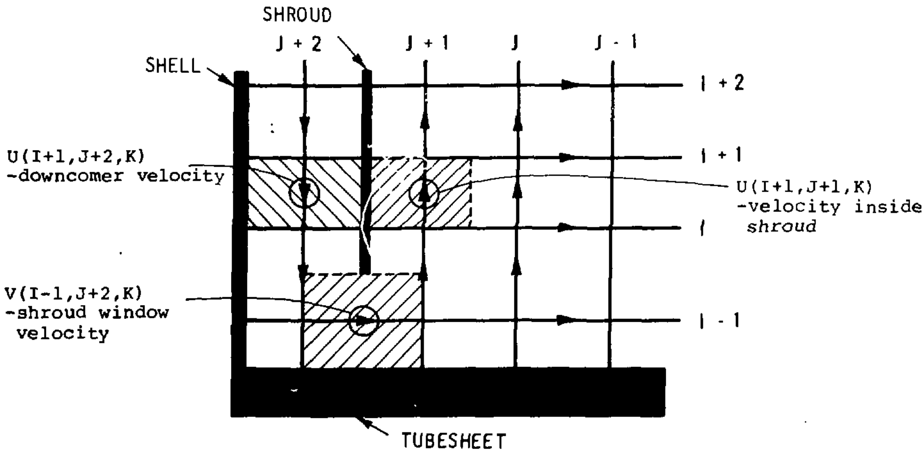

The I and I-1 planes are located so that the top of the window lies halfway between them. The J+1 and J+2 planes center the shroud. Generally, more grid would be located in the shroud window to handle the sudden change in flow direction.

Figure 4.2: Grid Layout at a Shroud Window

4.2.4 Windows

A third example (Figure 4.2) shows the grid layout required near the shroud window opening. The radial grid lines J+2 and J+1 are located to center the shroud. The axial velocity at (I+1, J+2, K) corresponds to the downcomer flow. The radial velocity at (I-1,J+2,K) corresponds to the window flow where the downcomer flow enters the heat transfer area. Thus the location of the shroud and the location of the top of the window governs the I-1,I,J+1 and J+2 grid selections.

4.2.5 Axial Layout (I Plane)

When allocating the grid, the user is advised to start with the axial planes.

Figure 4.3 shows the axial grid layout on the vertical cut of the hypothetical model. One can see the appropriate selection of the axial grid location around the preheater baffles. The tube support plates cannot always be located midway between planes because of the limit on the number of axial grid lines availcble. In such cases, support plates will be effectively seen at lower or higher elevation than their actual location. However, this will not unduly influence the model because the tube support plates do not redirect the flow but simply add to the pressure drop.

Two axial grid planes I=7 and I=8 are positioned so that the top of the shroud window on the hot side is located midway between them. The top of the shroud window on the cold side is lower and thus the I=6 plane is located such that the I=6 and I=7 staggers the top of the cold side shroud window.

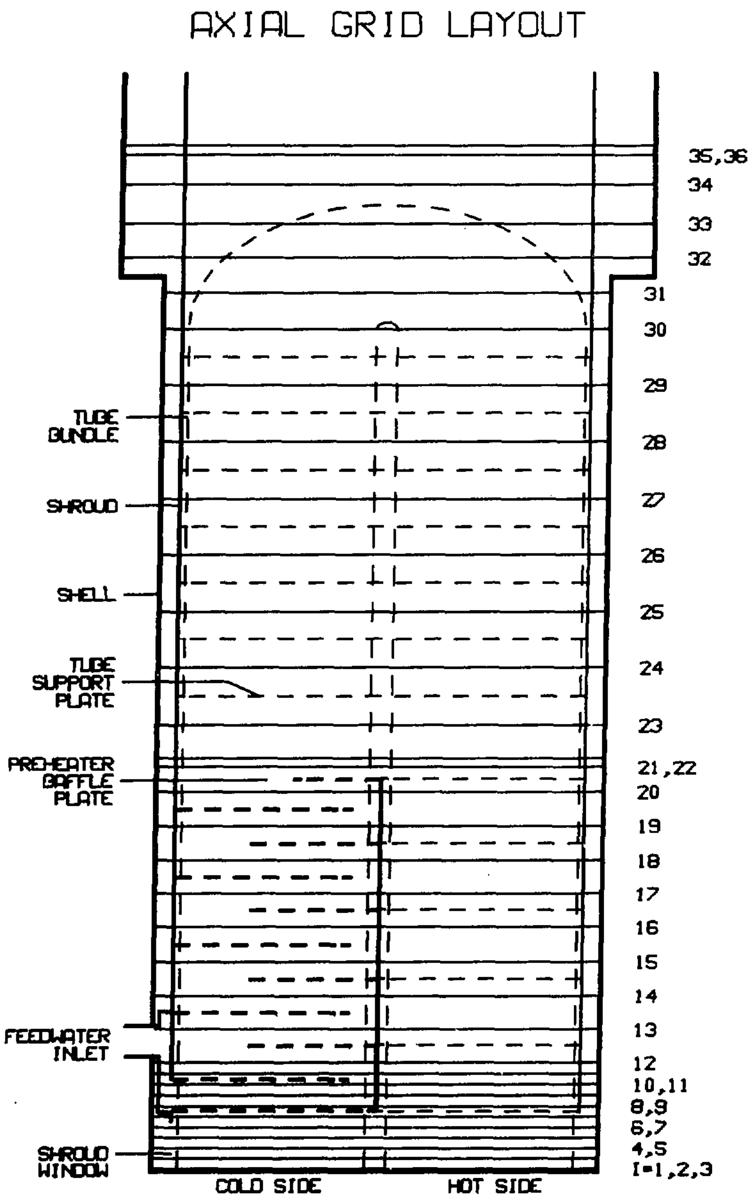

Figure 4.3: Axial Grid Layout

When the axial planes have been allocated to satisfy the axial flow obstacles such as baffles, tube support plates, window openings, etc., the user should then examine areas which are critical to the analysis and ensure that a sufficient number of grid planes are located in these areas. For instance, the region just above the tubesheet at the shroud window is particularly important. The I=2 plane is located just above the tubesheet. The I=3 to I=5 are added to this region to provide more detail. The I=22 plane is added above the preheater to handle the migration of hot side flow to the cold side.

To enable the tracing routine used to calculate the heat transfer in the U-bend, an axial plane must be located at the start of the U-bend curvature. At least 3 additional axial planes should be located in the U-bend to ensure the accuracy of the routine which calculates the pressure drop and heat transfer in the U-bend. Finally the last plane should be located very close to the second last plane so that the axial boundary values which are based on the last internal values can be calculated.

4.2.6 Radial Division (J Planes)

In our example, we have used 36 axial planes. We have now 4900/36 = 136 more nodes available to share between the radial and circumferential directions. Figure 4.4 shows a horizontal cross-sectional cut of our design. Note that only one half of the steam generator is modelled as the design is symmetric about a line dividing the hot and cold sides. The bundle boundaries and baffle plate edges are marked as dashed lines. The shroud and shell locations are shown as solid lines.

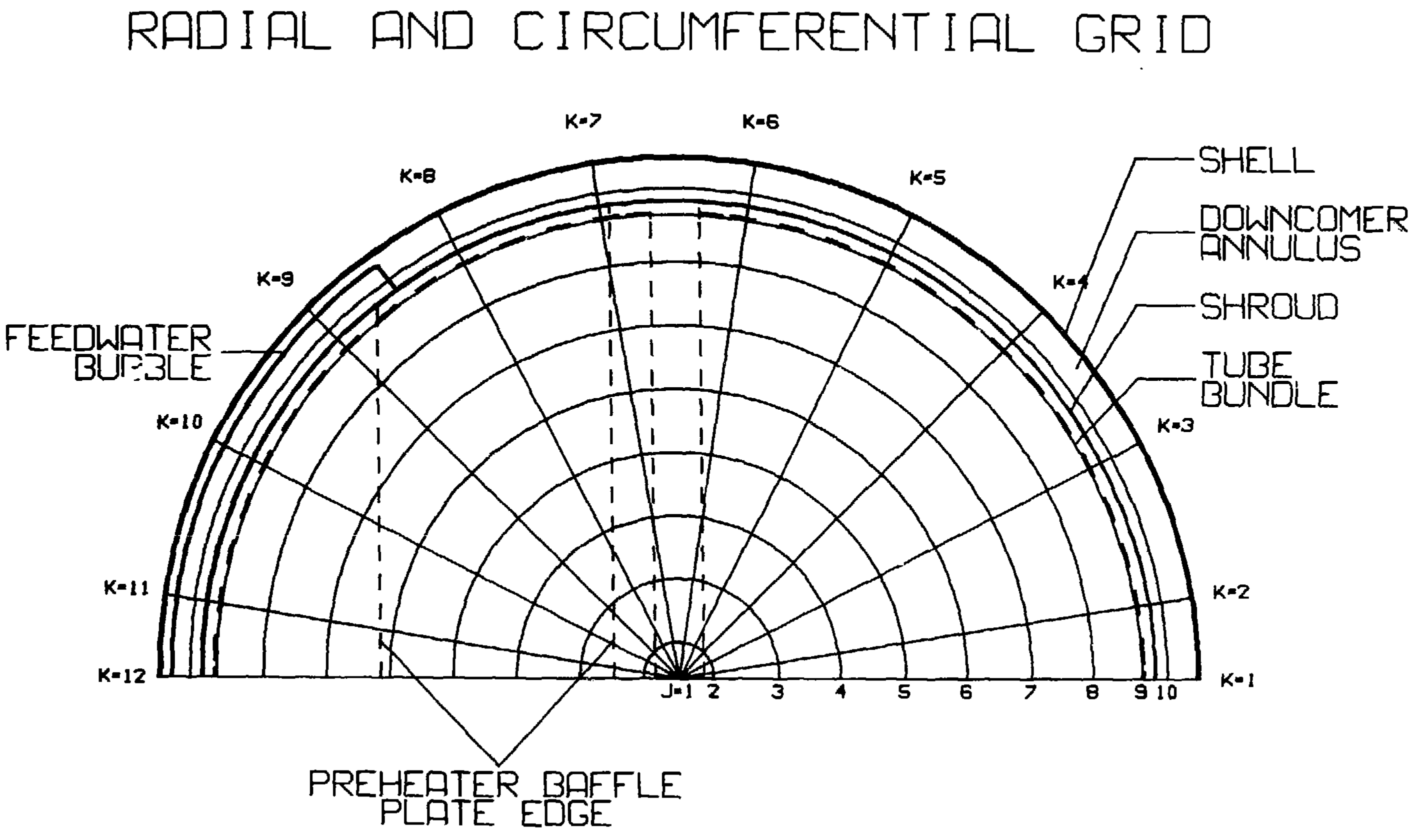

Figure 4.4: Radial and Circumferential Grid

Figure 4.4 also shows the radial grid layout. J=1 corresponds to the center point. The second radial position, J=2, is located very close to the J=1 point because it is the first active point in the radial grid pattern. The J=9 and J=10 points are located so as to center the shroud inner radius, as discussed previously. The J=3 to J=8 points are positioned at equal intervals as specific locations are not dictated by special geometrical features.

4.2.7 Circumferential Division (K Planes)

We have now used 36 x 10 = 360 grid planes and we have 4900/360 ≈ 13 grid planes left to be allocated in the circumferential direction. To simplify the layout, we will only use 12, with equal numbers on the hot and cold side. The code can accept unequal numbers of grid planes on the cold and hot side if the geometry requires it. The K=6 and K=7 planes are located such that they straddle the partition plate. The K=2 and K=11 planes, the first and last internal planes are located fairly close to the boundary points as they are the first active points inside the boundary. The remaining points are spaced equally; however, this is not a requirement, and spacing may be adjusted to fit particular geometrical features.

4.2.8 Final Assessment

This then completes the grid layout. One may find that the number of planes in each direction could be juggled to better model the design. Once the grid layout has been finalized and the geometry of the design described to the code relative to this grid, it is a major undertaking to alter the grid location. Thus it is important at this stage to review the grid selection carefully.

4.3 Preliminary Data Specification

Having examined the design layout and selected the optimum grid location, we must now provide the code with the information required to model the design. This section describes the contents of data sheets. The specification sheets are included in chart form to emphasize that specification must be completed and verified before any actual input data cards are prepared.

Each chart is divided into the following columns:

COLUMN 1:	DATA NO. - for reference purposes
COLUMN 2:	DESCRIPTION
COLUMN 3:	DATA VALUES - to be taken from specifications
COLUMN 4:	REMARKS - any manipulation of the DATA is described or a summary of options is given
COLUMN 5:	VARIABLE NAME - code name used in THIRST
COLUMN 6:	FINAL VALUE - value to be used as data

The data is arranged in functional groups as follows:

GROUP 1:	Preliminary Data (Items 1 - 7)
GROUP 2:	Geometric Data Entered by Grid Indices (Items 8 - 21)
GROUP 3:	Geometric Data Entered by Value (Items 22 - 41)
GROUP 4:	Correlations and Resistances (Items 42 - 60)
GROUP 5:	Operating Conditions (Items 61 - 69)
GROUP 6:	Utility Features (Items 70 - 85)

Items within each group are arranged alphabetically for ready reference.

DATA No.	DESCRIPTION	DATA VALUE	REMARKS	VARIABLE NAME	VALUE
			ITEMS 1 - 7 PRELIMINARY DATA		
1	Controls the use of the restart option (see Section 5.1)	--	RESTART = 1.0 - new run, no RESTART tape used as input RESTART = 2.0 - continue executing from a point reached in a previous run RESTART = 3.0 - attach the data stored on tape from a previous run and print and/or plot the data RESTART = -(1 or 2 or 3) - proceed as above but write the final results on a restart tape	RESTART	
2	Number of axial planes	--	Must be an integer number	NI	
3	Number of radial planes	--	Must be an integer number	NJ	
4	Number of circumferential planes	--	Must be an integer number	NK	
5	Location of axial planes	--	Distance from the secondary side of the tube-sheet surface to each axial plane - in meters	X	
6	Location of radial planes	--	Distance from the center point to each radial plane - in metres	Y	
7	Location of circumferential grid planes	--	The angle (in degrees) from a line passing through the center of the hot side to each circumferential plane	Z	

DATA No.	DESCRIPTION	DATA VALUE	REMARKS	VARIABLE NAME	VALUE
ITEMS 8 - 21 ARE GEOMETRIC DATA ENTERED ACCORDING TO GRID LOCATION USING GRID INDICES					
8	Location of all baffles, tube support plates and thermal plates on the cold side	See layout	This array is set up to indicate which axial velocities are passing through a plate resistance. Each axial plane, I, must be specified as follows· If ICOLD (I) = 1 → no plates ICOLD (I) = 2 → normal tube support ICOLD (I) = 3 → outer baffle plate, see data no. 23 ICOLD (I) = 4 → inner baffle plate, see data no. 22 ICOLD (I) = 5 → thermal plate ICOLD (I) = 6 → differentially broached plate (usually first plate on hot side)	ICOLD	
9	Location of all baffles, tube support plates, etc. on the hot side	See layout	This array is the same as data no. 8 except that it applies on the hot side.	IHOT	
10	Shroud window height on the cold side		The last axial plane lying inside the window on the cold side 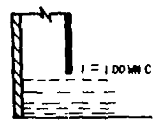	IDOWNC	

DATA No.	DESCRIPTION	DATA VALUE	REMARKS	VARIABLE NAME	VALUE
11	Shroud window height on the hot side		The last axial plane lying inside the window on the hot side 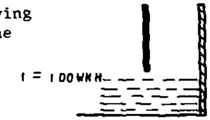	IDOWNH	
12	Top of the feedwater distribution bubble		Last axial plane passing through the distribution bubble 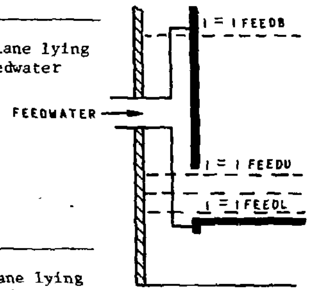	IFEEDB	
13	Feedwater inlet window lower limit		First axial plane lying inside the feedwater window	IFEEDL	
14	Feedwater inlet window upper limit		Last axial plane lying inside the feedwater window	IFEEDU	
15	Height of the preheater		Last axial plane inside the preheater 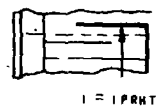	IPRHT	

DATA No.	DESCRIPTION	DATA VALUE	REMARKS	VARIABLE NAME	VALUE
·16	Effective elevation where the downcomer annulus expands		The code treats the conical section as a change in porosity halfway through the expansion. 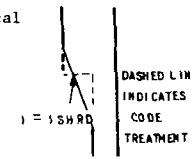	ISHRD	
17	Starting elevation of the U-bend		The I-plane located at the start of the curvature of the U-bend	IUBEND	
18	The radial distance from the center to the effective line dividing the reduced broached side from the normal broached size for differentially broached plates		In some designs the first tube support plate on the hot side is differentially broached to induce flow into the center of the steam generator. The last radial grid line corresponding to the larger diameter holes is used to identify this point. 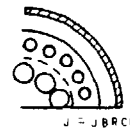	JBRCH	
19	K-plane on the cold side next to the 90° angle	--	K-plane near the center of the modelled region on the cold side 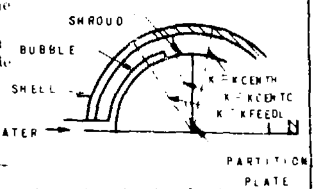	KCENTC	
20	K-plane on the hot side next to the 90° angle	--	As 19 but on hot side	KCENTH	
21	Angle at which the feedwater distribution bubble starts		K-plane that lies just inside the feedwater distribution bubble	KFEEDL	

DATA No.	DESCRIPTION	DATA VALUE	REMARKS	VARIABLE NAME	VALUE
	ITEMS 22 - 41 ARE GEOMETRIC DATA ENTERED AS ACTUAL NUMBERS				
22	Distance from the partition plate to the edge of the inner baffle (m)		Used to determine which control volumes contain the baffle plate. Control volumes which are partially exposed to the baffle (partly filled) have a weighed impedance. 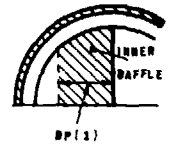	BP(1)	
23	Distance from the partition plate to the edge of the outer baffle (m)		Used as above 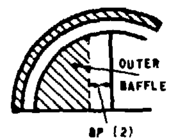	BP(2)	
24	Distance from the partition plate to the edge of the inner baffle at the exit of the preheater (m)		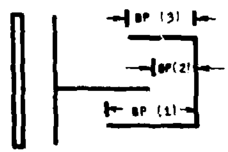	BP(3)	
25	One half of the width of tube free lane between the hot and cold side (m)		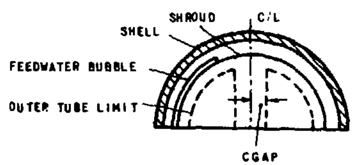	CGAP	

DATA No.	DESCRIPTION	DATA VALUE	REMARKS	VARIABLE NAME	VALUE
26	Outer diameter of the tubes (m)			DIA	
27	Inner diameter of the tubes (m)			DIAIN	
28	Hydraulic equivalent diameter in the downcomer annulus at the feed-water bubble (m)	Shell inner diam.= Outer bubble diam.=	EDFEED = $D_{SHELL}-D_{BUBBLE}$ EDFEED = $D_{SHELL} - D_{BUBBLE}$ 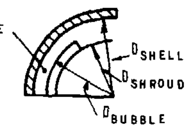	EDFEED	
29	Hydraulic equivalent diameter for the normal downcomer annulus below the conical section (m)	Shell inner diam.= D_{SHELL} Shroud outer diam.= D_{SHROUD}	EDNORM = $D_{SHELL}-D_{SHROUD}$	EDNORM	
30	Hydraulic equivalent diameter for the downcomer annulus above the conical expansion zone applies at I planes greater than ISHRD (see data no. 14) (m)	Upper shell inner diam. = D_{USHELL} Upper shroud outer diam. = $D_{USHROUD}$	EDSHRDX = $D_{USHELL} - D_{USHROUD}$	EDSHRDX	
31	Total heat transfer area (m^2)			HTAR	
32	Distance between the outermost tube and the shroud inner surface (m)		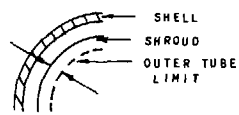	OGAP	

DATA No.	DESCRIPTION	DATA VALUE	REMARKS	VARIABLE NAME	VALUE
.33	Porosity in the downcomer at the feedwater bubble	Shell inner radius $= R_{SHELL}$ Bubble outer radius $= R_{BUBBLE}$ Shroud outer radius $= R_{SHROUD}$	Normally the downcomer porosity is equal to 1 indicating that the area is entirely open. For the region around the bubble, one has to calculate a porosity which when multiplied times the regular downcomer area will give the reduced area 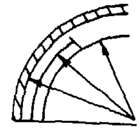 $PFWB = \frac{(R^2_{SHELL} - R^2_{BUBBLE})}{(R^2_{SHELL} - R^2_{SHROUD})}$	PFWB	
34	Distance between tubes (PITCH)			PITCH	
35	Porosity in the downcomer annulus above the expansion region	Inner radius of the upper shell section $= R_{SHELL_{UP}}$ Outer radius of upper shroud $= R_{SHROUD_{UP}}$ Lower shell inner rad. $= R_{SHELL_{LO}}$ Lower shroud outer rad. $= R_{SHROUD_{LO}}$	As with data no. 28, porosity is used to correct the flow area $PSHRD = \frac{(R^2_{SHELL_{UP}} - R^2_{SHROUD_{UP}})}{(R^2_{SHELL_{LO}} - R^2_{SHROUD_{LO}})}$	PSHRD	
36	Inner radius of the shroud			RADIUS	

DATA No.	DESCRIPTION	DATA VALUE	REMARKS	VARIABLE NAME	VALUE
37	Calculated inner radius of the shell (m)	Inner radius shell= R_{SHELL} Outer radius shroud = $R_{OUT_{SHRD}}$ Inner radius shroud = RADIUS	The code ignores the thickness of the shroud. To maintain the correct downcomer area, the inner radius of the shell has to be reduced to compensate for the added area contributed by the shroud thickness. $(R_{SHELL}^2 - RADIUS^2)\pi = (R_{SHELL}^2 - R_{OUT_{SHRD}}^2)\pi$	RSHELL	
38	Height of thermal plate above level tubesheet (m)			TPLATE	
39	Tubesheet thickness (m)			TUBSHET	
40	Height of the downcomer water above the tubesheet (m)			XDOWN	
41	Height at which the two-phase mixture can be assumed to be separated (relative to tubesheet)		This is used to calculate the gravity head inside the shroud. Generally, one could take the elevation halfway along the separator.	XVANE	

DATA No.	DESCRIPTION	DATA VALUE	REMARKS	VARIABLE NAME	VALUE
			ITEMS 42 - 60 CORRELATIONS AND RESISTANCES		
42	**k loss factor for the centerline between the hot and cold side, AKDIV(I)**	See layout	This array is used to indicate the location of the partition plate AKDIV(I) = 1.0 E+15, the U-bend supports AKDIV(I) = k, or indicate where no obstacles occur AKDIV(I) = 0. These loss factors are used to calculate the pressure loss relationship for the circumferential velocity between the hot and cold sides due to plates or supports; the tubes are handled independently.	AKDIV(I)	
43	**Parameter for selecting two-phase multipliers**	--	If ITPPD = 1-THOM used for parallel, cross and area change If ITPPD = 2-BAROCZY-CHISHOLM used for parallel, cross and area change If ITPPD = 3 - Separate correlations used See Section 7.3	ITPPD	
44	**Parameter for selecting void fraction correlation**	--	If IVF = 1, homogeneous correlation If IVF = 2, Chisholm correlation If IVF = 3, Smith correlation	IVF	

DATA No.	DESCRIPTION	DATA VALUE	REMARKS	VARIABLE NAME	VALUE
45	k shock loss factor for the baffle plate resulting from area change (contraction and expansion)	Approach Area Device Area Device Loss Factor	The loss for the baffle plate $= (AKBL + f\frac{L}{D}) \frac{\rho v^2}{2}$ This data is the AKBL portion which is the pressure drop due to the contraction into the annulus between the drilled plate and the tube. It is based on the approach area. $AKBL = k_{DEVICE} * \left(\frac{A_{APPROACH}}{A_{DEVICE}}\right)^2$ (Also see data no. 58)	AKBL	
46	k loss factor for the tube support broached plate - based on shock loss due to area change	Same as data no. 45	The tube support plates result in a pressure drop due to an area change. This value is based on the approach area.	AKBR	
47	k loss factor for the larger broached holes in a differentially broached plate	Same as data no. 45	In some designs, the first plate on the hot side has smaller broached holes near the shroud and larger broached holes near the center to encourage flow penetration. This factor is for the area change in the central larger holes.	AKBRL	
48	k loss factor for the smaller broached holes in a differentially broached plate	Same as data no. 45	Shock loss for the outer small broached holes. See data no. 18 for the radial position where the hole size changes.	AKBRS	
49	Shock loss k factor for the THERMAL plate	Same as data no. 45	For some designs the tubes are not rolled into the thermal plate and leakage through the plate may occur. The pressure loss relationship is $(AKTP + f\frac{L}{D}) \frac{\rho v^2}{2}$ a shock loss and a friction loss. This data no. deals with the shock loss. Again it is based on the approach area	AKTP	

DATA No.	DESCRIPTION	DATA VALUE	REMARKS	VARIABLE NAME	VALUE
50	Shock loss k factor for the shroud window on the cold side	Window area = A_w Annular Area = A_{an} 90° Elbow Loss = k_{90} Expansion Loss = k_{exp}	This pressure loss relationship is based on a 90° flow direction change and an expansion from the downcomer annulus into the shroud window. Both $k_{90°}$ and k_{exp} are based on A_{an}: $AKWINDC = (k_{90°} + k_{exp}) \left(\frac{A_w}{A_{an}}\right)^2$	AKWINDC	
51	Shock loss k factor for the shroud window on the hot side	Same as data no. 50	Because the shroud window height may differ between the hot and cold side, a second loss factor may be required.	AKWINDH	
52	Area ratio multiplier to determine Reynold's number in gap in baffles. (See also data no. 58)	Approach area = A_{ap} Gap area = A_g Diametrical clearance = c	The local Reynolds number is: $R = \frac{\rho * v_{loc} * c}{\mu} = \frac{\rho * ARATB * V_{app} * c}{\mu}$ where: $ARATB = (A_{ap}/A_g)*c$	ARATB	
53	Area ratio multiplier to determine Reynold's number in gap in thermal plate	See data no. 52	$ARATTP = (A_{ap}/A_g)*c$	ARATTP	

DATA No.	DESCRIPTION	DATA VALUE	REMARKS	VARIABLE NAME	VALUE
54	Loss factor calculated for the two-phase flow from the last modelled plane inside the shroud to the separator exit, k_{sep} is normally given by the manufacturer. k_c (based on V_{sep}) is calculated by user, and is generally much less than k_{sep}.	Separator Loss Factor $= k_{sep}$ Contraction Factor $= k_c$ A_{pp} = total flow area before entering separator A_{sep} = total separator area	To calculate the recirculation ratio the flow from the last modelled plane inside the shroud to the last modelled plane outside the shroud is modelled one-dimensionally. CON1 is a combination of the loss factors for the two-phase mixture. It is based on the total flow as shown below. CON2 (data no. 55) is the loss factor for the saturated liquid flowing out of the separators. 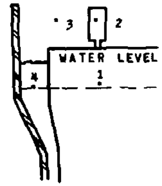 From (1) to (2) - area contraction into separators. $\Delta P = k_c \frac{\bar{\rho} V_{SEP}^2}{2}$ where V_{SEP} = velocity in separator $FLOW = \bar{\rho}\, A_{SEP}\, V_{SEP}$ $\Delta P = k_c \frac{\bar{\rho}}{2} * \frac{FLOW^2}{\bar{\rho}^2 A_{SEP}^2} = \frac{k_c}{A_{SEP}^2} * \frac{FLOW^2}{2\bar{\rho}}$ From (2) to (3) - separator loss $\Delta P = k_{SEP} \frac{\bar{\rho} V^2}{2} = \frac{k_{SEP}}{A_{SEP}^2} * \frac{FLOW^2}{2\bar{\rho}}$ $CON1 = \frac{k_c}{A_{SEP}^2} + \frac{k_{SEP}}{A_{SEP}^2}$ $V_{SEP} = \frac{A_{APP}}{A_{SEP}} * V_{APP}$	CON1	

DATA No.	DESCRIPTION	DATA VALUE	REMARKS	VARIABLE NAME	VALUE
55	Loss factor calculated for the separated liquid flowing from the water level to the last modelled plane in the downcomer.	--	This loss is assumed to be a frictional loss and treated as flow in a pipe. $\therefore \Delta P = f\frac{L}{D}\ \frac{\rho v^2}{2} = f\frac{L}{D} * \frac{1}{A_{DC}^2}\ \frac{FLOW^2}{2\rho} = \frac{CON2*FLOW^2}{2\rho}$ where $CON2 = f\frac{L}{D}\ (\frac{1}{A_{DC}})^2$ L = XDOWN-X(L)→see data no. 39 D = Hydraulic Diam. = Diam. Clearance A_{DC} = Downcomer Area ρ = Saturation Density of Water $f = \frac{0.316}{R_e}$ R_e is based on an estimate at the velocity calculated from a recirculation ratio estimate. $R_e = \frac{D_H \rho V}{\mu} \rightarrow V = \frac{RECIR * FLOWC}{\rho * A_{DC}} = \frac{FLOW}{\rho * A_{DC}}$	CON2	
56	Parameter used to optimize the estimate of the recirculation ratio.	--	This ratio provides the code with an estimate of how the pressure drop through the modelled region changes with recirculation ratio (i.e., total flow). The code uses this value to estimate the recirculation ratio needed to balance the pressure loss against the driving head. CON4 is set at 2000. If severe convergence problems are encountered, other estimates (i.e., 2000 $\pm$ 1000) should be tried.	CON4	

DATA No.	DESCRIPTION	DATA VALUE	REMARKS	VARIABLE NAME	VALUE
57	Thermal conductivity of the tube wall material (W/(m·°C))		Obtain from material property data.	CWALL	
58	Friction pressure loss for the baffle plate	Baffle thickness = L Diametrical clearance = D Area approach = A_{APP} Area gap = A_{GAP}	Also see data no. 45 and 52. $\Delta p = [AKBL + \frac{fL}{D}] \frac{\rho V^2}{2}$ The variable is concerned with the second term - the frictional loss. $f = .316/R_e^{.25}$ L = thickness of baffle D = diametrical clearance Because this loss is based on approach velocities, the area correction is included. Thus $FLDB = .316 * \frac{L}{D} * \left(\frac{A_{APP}}{A_{GAP}}\right)^2$ $\therefore\ \Delta P = [AKBL + FLDB * R_e^{-.25}] * \frac{\bar{\rho} V_{APP}^2}{2}$	FLDB	

DATA No.	DESCRIPTION	DATA VALUE	REMARKS	VARIABLE NAME	VALUE
59	**Friction pressure loss for the thermal plate**	See data no. 58	This variable stored the friction coefficients mentioned in data no. 49 and 53. $\Delta p = \left[AKTP + \frac{fL}{D} * \left(\frac{A_{APP}}{A_{GAP}} \right)^2 \right] \frac{\bar{\rho} V_{APP}^2}{2}$ $FLDT = \frac{fL}{D} * \left(\frac{A_{APP}}{A_{GAP}} \right)^2$ $\therefore \Delta P = [AKTP * FLDT * R_e^{-.25}] \frac{\bar{\rho} V_{APP}^2}{2}$	FLDT	
60	**Resistance due to fouling on the external surface of the tube**		Fouling is assumed to act uniformly over the tube surface	RFOUL	
	ITEMS 61 - 69 ARE OPERATING CONDITIONS				
61	**Feedwater flow rate (kg/s)**		This is the total steam generator feedwater flow rate.	FLOWC	
62	**Reheater flow rate (kg/s)**		Some designs include a reheater circuit. The flow returning from the reheater is assumed by the code to enter the steam generator at the top of the downcomer. If there is no reheater circuit, set this value to zero.	FLOWRH	
63	**Primary flow rate (kg/s)**		Flow rate for the whole unit	FLOWTU	
64	**Saturation pressure of the primary (MPa)**		Used to calculate primary properties	PPRI	

DATA No.	DESCRIPTION	DATA VALUE	REMARKS	VARIABLE NAME	VALUE
65	Saturation pressure of the secondary (MPa)		Used to calculate secondary properties. Take the value at the normal water level.	PSEC	
66	Inlet quality of the primary fluid		For a two-phase mixture, it is the actual quality. For a subcooled primary flow this value is calculated using $QLTU = \frac{\text{Enthalpy of Liquid-Saturation Enthalpy}}{\text{Latent Heat}}$	QLTU	
67	Initial estimate of recirculation ratio (°C)		The recirculation ratio is not adjusted for the first 9 steps to allow the flow to settle out. This value serves as an initial condition.	RECIR	
68	Temperature of the feedwater (°C)			TINC	
69	Temperature of the reheater return flow			TRH	
ITEMS 70 - 85 ARE UTILITY FEATURES AVAILABLE TO THE USER					
70	The horizontal lines of data which are to be included on the vertical cut plots	--	In areas where I planes are concentrated, one may decide to leave out some I lines from vertical plots so that the plotted arrows do not overlap. Normally all the lines would be plotted. IF IIPLOT(I) = 1 - plot the line IF IIPLOT(I) = 0 - skip the line Note: IIPLOT(I) must have NI entries	IIPLOT	

DATA No.	DESCRIPTION	DATA VALUE	REMARKS	VARIABLE NAME	VALUE
71	Selection of the I position for which the hot side and cold side mass flow will be calculated and printed out	--	A subroutine MASSFLO has been set up to calculate the mass flow in the axial direction for selected planes. This information is printed out any time the axial velocities or densities are adjusted. Any number of I planes may be specified up to NI.	IMASSF	
72	Selection of the K-planes to be plotted.	--	This variable allows the user to select any number of the circumferential planes for plotting. Note the K=2 and K=N planes are automatically plotted to give the first frame and should not be requested again.	IPLOTK	
73	Selection of the I axial planes to be plotted	--	The plotting routine is set up to plot up to a maximum of 8 horizontal cuts. This variable is used to specify the I planes of interest. For example, If IPLOTI = +10, the 10th plane will be plotted to the right of the vertical cuts - see Section 6.3 for more details If IPLOTI = -10, the 10th plane will be plotted on the left of the vertical plot. Note there must be only 4 specified for the left side (negative number) and 4 specified for the right side (positive number).	IPLOTI	

DATA No.	DESCRIPTION	DATA VALUE	REMARKS	VARIABLE NAME	VALUE
74	Select the variables to be printed out	--	This parameter allows the user to trim the output down to variables of specific interest. If IPRINT = 1, the variable is printed. If IPRINT = 0, the variable is skipped. The order of variable storage: IPRINT(1) = axial velocity IPRINT(2) = radial velocity IPRINT(3) = circumferential velocity IPRINT(4) = mass flux IPRINT(5) = steam quality IPRINT(6) = primary temperature IPRINT(7) = tube wall temperature IPRINT(8) = static pressure IPRINT(9) = density of mixture IPRINT(10) = local heat flux IPRINT(11) = porosity	IPRINT	
75	Relaxation factors	--	The order of variable storage: RELAX(1) = axial velocity RELAX(2) = radial velocity RELAX(3) = circumferential velocity RELAX(4) = pressure correction RELAX(5) = enthalpy RELAX(6) = (inactive) RELAX(7) = tube wall temperature RELAX(8) = pressure RELAX(9) = density RELAX(10) = wedges and rings RELAX(11) = (inactive)	RELAX	
76	Contour intervals for the plotting routines	--	Allows the user to specify the quality contours of interest. Can have up to 15 values. Zero values at the end of the array are ignored.	TCON	
77	Last execution step	--	Sets the last execution step. On completion of LASTEP iterations, the computation ceases and detailed printing and plotting starts.	LASTEP	

DATA No.	DESCRIPTION	DATA VALUE	REMARKS	VARIABLE NAME	VALUE
78	Parameter to specify when, during the execution, plots are to be made	--	IF PLOTO = 0, plots are never made IF PLOTO = 1, plots are made at the end of the job IF PLOTO = 2, plots are made after each iteration Note: If PLOTO = 2, a very long plot file will be produced. Careful selection of values for IPLOTI and IPLOTK are necessary. (data no. 72 and 73)	PLOTO	
79	Parameter to specify when, during the execution, the variables specified in IPRINT will be printed out	--	PRINTO is set up the same as PLOTO in data no. 78. Note that PRINTO and PLOTO may be reset in the logic to turn the PLOTTING and PRINTING routines on or off.	PRINTO	
80	Parameter for overriding the time limit routine	--	THIRST has been set up to print out all the variables, make plots and write a RESTART tape if the execution or INPUT/OUTPUT time has been reached. To suppress this feature, set TIMELT to zero.	TIMELT	
81	Width of the plotting frame when I-planes are to be plotted both on the left and on the right of the vertical cut (see data no. 73)	--	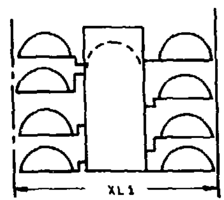	XL1	
82	Width of the plotting frame when only I-planes are plotted on the right side of the vertical cut	--	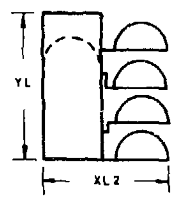	XL2	
83	Height of the plotting frame	--		YL	

DATA No.	DESCRIPTION	DATA VALUE	REMARKS	VARIABLE NAME	VALUE
84			Extra integer input locations. Data put into these variables is common to all subroutines	IEXTRA(I) I=1,9	
85			Extra real input locations.	REXTRA(I) I=1,9	

4.4 Preparation of the Input Data Cards

Once the data specification sheets have been completed, it is a straightforward matter to transpose the requisite information into data card form.

In THIRST, the data is all processed through a routine called READIN. READIN not only reads the data into core, but also performs a detailed check on the completeness and precision of the data supplied.

The course of execution of the program is directed by the RESTART feature which is described in Section 5.2.

The input cards are assembled from the variable names and values already detailed in the last two columns of the charts in Section 4.3, immediately preceding.

The cards must adhere to the following rules:

(1) The first card must contain the title (1 to 40 columns) and the RESTART value (word RESTART in columns 50 to 59 and value in 60 to 69). If the RESTART name and value are not included, READIN assumes a RESTART value of 1.

(2) All succeeding cards are read with the following format statement

```
FORMAT (A9, 6 (A9, 1X), A9)
```

The input cards for data arrays or single variables are,

	10	20	30	40	50	60	70	80
ARRYN	NN 1	-1.	6.2	8750.5	1.0E+20	-.0068	-6.8E-4	
NAM1	1	NAM2	-1	ANAM3	1.3456789	ANAM3	180040.7	

(NN is the number of entries in the array called ARRYN. It is only required for arrays IMASSF, IPLOTI and IPLOTK.)

(3) The second card must contain the number of grid points NI, NJ, NK, selected for each direction to provide READIN with the counters for checking array data.

(4) From this point onwards, the data may appear in any order since the variable name is always included with the data. READIN treats each variable name and the corresponding data as a variable set.

(5) It is possible that after a data deck is prepared, some temporary changes are found necessary. In this case, a data item may be changed in situ in the deck, or a single card with the changed variable may be inserted immediately after the NINJNK card. In such cases of multiple definition the definition encountered earliest in the deck takes precedence, so the new value will be used.

4.5 Sample Input Data Deck

The data deck sheets in Table 4.2 have been prepared from the specification sheets of Section 4.3 according to rules outlined in Section 4.4.

THIRST INPUT DATA SHEET

PAGE 1

1	10	20	30	40	50	60	70
HYPOTH	ETICAL 600	MW STEAM	GENERATOR		RESTART	-1	
NI	36	NJ	10	NK	12		
AKDIV							
1.0E-10	1.0E-10	1.0E-10	1.0E-10	1.0E-10	1.0E-10	1.0E15	1.0E15
1.0E15	1.0E15	1.0E15	1.0E15	1.0E15	1.0E15	1.0E15	1.0E15
1.0E15	1.0E15	1.0E15	1.0E15				
					1.8	1.8	1.8
1.8							
BP							
0.83	0.18	0.56					
ICOLD							
1	1	1	1	1	1	1	5
1	1	3	1	4	3	4	3
4	3	4	3	7	1	1	2
2	2	2	2	2	2	1	1
1	1	1	1				
IHOT							
1	1	1	1	1	1	1	6
1	1	1	1	2	1	2	1
2	1	2	1	2	1	1	2
2	2	2	2	2	2	1	1
1	1	1	1				
IIPLOT							
0	1	0	1	0	1	0	1
0	1	1	0	1	1	1	1
1	1	1	1	1	1	1	1
1	1	1	1	1	0	1	0
1	1	1	0				
IMASSF	33						

THIRST INPUT DATA SHEET

PAGE 2

1	10	20	30	40	50	60	70
3	4	5	6	7	8	9	10
11	12	13	14	15	16	1[illegible]	1[illegible]
19	20	21	22	23	24	[illegible]	26
27	28	29	30	31	32	[illegible]	3[illegible]
35							
IPLOTI	8						
2	-6	14	-21	25	-32	3[illegible]	-[illegible]5
IPLOTK	8						
3	4	5	6	7	9	9	10
IPRINT							
1	0	0	0	0	0	0	0
0	0	0					
RELAX							
.5	.5	.5	1.	1.	1.	.25	.5
.5	.2	1.					
TCON							
0.0	0.01	0.02	0.03	0.05	0.1	0.15	0.2
0.22	0.25	0.3	0.35	0.4	0.5		
X							
0.0	0.01	0.12	0.23	0.34	0.45	0.56	0.67
0.78	0.89	1.0	1.11	1.46	1.[illegible]	[illegible].[illegible]6	2.51
2.86	3.21	3.56	3.[illegible]	4.1[illegible]	[illegible]	4.[illegible]	5.[illegible]4
5.78	6.36	6.94	7.[illegible]	[illegible]	[illegible]	[illegible]	9.4[illegible]
9.8	10.2	10.5	10.6				
Y							
0.0	0.1	0.27565	0.451	0.[illegible]	[illegible]	[illegible]	1.[illegible]
1.2845	1.3575						
Z							
0.0	9.0	27.0	45.0	63.0	[illegible]	[illegible]	11[illegible].

THIRST INPUT DATA SHEET

PAGE 3

1	10	20	30	40	50	60	70
135	153	1.71E+02	1.8E+02				
AKBL	1600	AKBR	1.5	AKBRL	1.0	AKBRS	6.0
AKTP	1600	AKWINDC	10	AKWINDH	13	ARATB	1.27045E-2
ARATTP	0.0	CGAP	0.07	CON1	0.9495	CON2	.1156
CON4	2000	CWALL	16.7	DIA	0.015875	DIAIN	.0136009
EDFEED	0.065	EDNORM	0.22	EDSHRDX	0.8	FLDB	21000
FLDT	1600	FLOWC	306.18	FLOWRH	23.7	FLOWTU	2484.93
HTAR	4550	IDOWNC	6	IDOWNH	7	IFEEDB	13
IFEEDL	8	IFEEDU	10	IPRHT	20	ISHRD	31
ITPPD	1	IUBEND	30	IVF	1	JBRCH	4
KCENTC	7	KCENTH	6	KFEEDL	9	LASTEP	60
OGAP	0.03	PFWB	0.3125	PITCH	0.024511	PLOTO	1
PPRI	9.879	PRINTO	1	PSFC	5.1	PSHRD	10.1
QLTU	0.044	RADIUS	1.321	RECIR	5.3	RFOUL	2.642E-5
RSHELL	1.44	TINC	176.67	TPLATE	0.615	TRH	251.67
TUBSHET	0.419	XDOWN	15.0	XL1	9	XL2	6.25
XVANE	16.0	YL	6				

4.6 The Standard Execution Deck

At this point, the major effort of preparing the data deck is complete. It is now necessary to enter the THIRST job into the computer system.

Execution control cards can vary between CDC computer installations. However, the following decks are included as examples, and operate satisfactorily on the CRNL system. For a full explanation of CDC control cards, see references 13 and 14.

The decks consist of the following:

JOBCARD containing job name and account information
CONTROL CARDS directing execution
7/8/9 END OF RECORD CARD
DATA DECK
7/8/9 END OF RECORD CARD
6/7/8/9 END OF JOB CARD

Card	Content	Explanation
1	JOBNAME, BXXX-YYY, Tttt,IOiii.	JOBNAME - 7 character job name
2	ATTACH, THIRST, ID=THIRST, CY=1.	Attach THIRST object code
3	THIRST.	Execute THIRST code

Card	Content	Explanation
4	7/8/9 END OF RECORD CARD	
5 to N	COMPUTER DATA DECK	
N+1	7/8/9 END OF RECORD CARD	
N+2	6/7/8/9 END OF JOB CARD	

The above simple execution deck will execute the standard THIRST code without reading or saving any RESTART data. Advanced Execution Decks are discussed in Section 5.5.

4.7 Job Submission

A complete listing of the entire deck is given in Figure 4.5. This may now be submitted to the CRNL system.

As turnaround time for a large job is not particularly fast, we discuss in Chapter 5 some additional features of the code. Our output will appear in Chapter 6.

```
THIRST,B652-EXAMPL,T50C,IO100.
ATTACH(OLDPL,THIRSTPL,ID=THIRST)
UPDATE(C=DISC)
FTN(I=DISC,B=THIRMOD)
ATTACH(THIRST,ID=THIRST)
COPYL(THIRST,THIRMOD,THIRST2)
ATTACH(TAPE60,THIRSTDATA,ID=THIRST)
ATTACH(PLOTLIB)
LDSET(LIB=PLOTLIB,SUBST=PLOT-PLT)
THIRST2(PL=30000)
IFE,R1.NE.0,JUMP.
COMMENT.   CATALOG RESTART TAPE
CATALOG(TAPE60,THIRSTDATA,ID=THIRST)
ENDIF(JUMP)
7/8/9
*IDENT HYPOTH
*D KOMON.1
      COMMON F(4320,13)
7/8/9
   HYPOTHETICAL 600 MW STEAM GENERATOR            RESTART    -1
NI         36          NJ          10          NK          12
AKDIV
1.0E-10    1.0E-10     1.0E-10     1.0E-10     1.0E-10     1.0E-10     1.0E15     1.0E15
1.0E15     1.0E15      1.0E15      1.0E15      1.0E15      1.0E15      1.0E15     1.0E15
1.0E15     1.0E15      1.0E15      1.0E15
                                                           1.8         1.8        1.8
1.8
BP
0.83       0.18        0.56
ICOLD
1          1           1           1           1           1           1          5
1          1           3           1           4           3           4          3
4          3           4           3           7           1           1          2
2          2           2           2           2           2           1          1
1          1           1           1
IHOT
1          1           1           1           1           1           1          6
1          1           1           1           2           1           2          1
2          1           2           1           2           1           1          2
2          2           2           2           2           2           1          1
1          1           1           1
IIPLOT
0          1           0           1           0           1           0          1
0          1           1           0           1           1           1          1
1          1           1           1           1           1           1          1
1          1           1           1           1           0           1          0
1          1           1           0
IMASSF     33
3          4           5           6           7           8           9          10
11         12          13          14          15          16          17         18
19         20          21          22          23          24          25         26
27         28          29          30          31          32          33         34
35
IPLOTI     8
2          -6          14          -21         25          -32         33         -35
IPLOTK     8
3          4           5           6           7           8           9          10
IPRINT
1          0           0           0           0           0           0          0
0          0           0
RELAX
.5         .5          .5          1.          1.          1.          .25        .5
.5         .2          1.
TCON
0.0        0.01        0.02        0.03        0.05        0.1         0.15       0.2
0.22       0.25        0.3         0.35        0.4         0.5
X
0.0        0.01        0.12        0.23        0.34        0.45        0.56       0.67
0.78       0.89        1.0         1.11        1.46        1.81        2.16       2.51
2.86       3.21        3.56        3.91        4.17        4.26        4.61       5.194
5.78       6.36        5.94        7.53        8.12        8.7         9.07       9.44
9.8        10.2        10.5        10.6
Y
0.0        0.1         0.27565     0.4513      0.6269      0.8026      0.978      1.1539
1.2845     1.3575
Z
0.0        9.0         27.0        45.0        63.0        8.1E1       9.9E1      117.
135        153         1.71E+02    1.8E+02
AKBL       1600        AKBR        1.5         AKBRL       1.0         AKBRS      6.0
AKTP       1600        AKWINDC     10          AKWINDH     13          ARATB      1.2705E-2
ARATTP     0.0         CGAP        0.07        CON1        0.9495      CON2       .1150
CON4       2000        CWALL       16.7        DIA         0.015875    DIAIN      .0136009
EDFEED     0.065       EDNORM      0.22        EDSHROX     0.8         FLOB       21000
FLOT       1600        FLOWC       306.18      FLOWRH      23.7        FLOWTU     2484.93
HTAR       4550        IDOWNC      6           IDOWNH      7           IFEEDB     13
IFEEDL     8           IFEEDU      10          IPRHT       20          ISHRD      31
ITPPD      1           IUBEND      30          IVF         1           JBRCH      4
KCENTC     7           KCENTH      6           KFEEDL      9           LASTEP     60
OGAP       0.03        PFWB        0.3125      PITCH       0.024511    PLOTO      1
PPRI       9.879       PRINTO      1           PSEC        5.1         PSHRD      10.1
QLTU       0.044       RADIUS      1.321       RECIR       5.3         RFOUL      2.642E-5
RSHELL     1.44        TINC        176.67      TPLATE      0.615       TRH        251.67
TUBSHET    0.419       XDOWN       15.0        XL1         9           XL2        6.25
XVANE      16.0        YL          6
7/8/9
```

Figure 4.5: Execution Deck

5. SOME FEATURES OF THE THIRST CODE

While the instructions included in the previous chapter are sufficient to prepare an input deck, an understanding of some additional features of THIRST is required for advanced use of the code. This chapter describes some of the THIRST input and output options.

5.1 The RESTART Feature

RESTART has been introduced very briefly in chapter 4. This feature was included in THIRST to reduce the repetition required in making several runs with only slight data modification, and to enable results to be stored so that later printouts and plots can be made without re-executing.

In THIRST, all the variables are initialized in START with, at best, a rough guess. Using RESTART, the variables can be initialized with results saved from a previous run, resulting in improved convergence.

RESTART has been set up so that a user can stop, at say the twentieth step, examine the results and then proceed further if desired. The user can also run the code, examine the results, make logic or input changes and continue running the program, or merely change the plotting or numbering parameters, and produce new output without executing the program.

The RESTART variable can have six values, three positive and three negative.

RESTART=1 is used for a new run in which all variables and arrays are initialized with rough guesses by the program. All routines are executed to attain a solution. RESTART must always be set to 1 if the number of grids or the grid layout is changed.

RESTART=2 is used to continue an old run. All the variables in common blocks are set to values calculated in a previous run, which has been stored on a RESTART tape. New values for selected variables can be entered by including these in the input deck, they then replace any stored values. Variables which are not to be changed are omitted from the input deck. The new run is then executed until a total of LASTEP iterations have been completed.

RESTART=3 is used mainly to obtain new output from a previously completed run. With this option, all parameters except those read in to specify the type of output required are set to their values from the RESTART tape. The EXEC routine then passes the control directly to the OUTPUT routine for the summary of the last step, and a printout of all arrays requested through the IPRINT(NN) parameter. Finally, if PLOTO $\neq$ 0, the plot routine generates the plots requested by IPLOTI and IPLOTK. After this output, the program terminates; no further execution is attempted.

RESTART=-n writes a RESTART tape on completion of a run. The absolute value of n (i.e., $|n| = 1,2,3$) determines the initial conditions for the run. On completion, a tape is written through the WSTART routine ready for subsequent reading with $|\text{RESTART}| > 1$.

Saving and Accessing a RESTART Tape

In WSTART a special global parameter "R1" is set to 0 when the tape is written. A set of statements can be included in the execution control cards to catalog the tape if this global parameter is set.

```
IFE(R1.NE.0)JUMP
CATALOG(TAPE50, THIRSTDATA, ID=THIRST)
ENDIF(JUMP)
```

If R1=0, control jumps past the CATALOG card to the ENDIF(JUMP) card. If WSTART has set R1=0, the CATALOG card is executed and the RESTART tape is stored under the name THIRSTDATA, ID=THIRST and CY=n, the lowest available number. Thus each time a RESTART tape is made, a new THIRSTDATA file is created. The user will have to exercise strict management of these files to avoid confusion and the creation of unnecessary files.

To RESTART from this tape, the user includes the card

```
ATTACH(TAPE50, THIRSTDATA, ID=THIRST, CY=n)
```

before the execution card in the JOB control statements. The information stored on this file will then be used in the RESTART routine to initialize the arrays and the variables providing RESTART is set at 2 or 3 in the input deck.

5.2 The READIN Feature

To assist the user with the entry of data into the code, a subroutine called READIN has been written . READIN extracts the variable name and its value from the data cards. As each piece of data is associated with the computer variable name, READIN can:

(a) ensure that all the data required are provided and determine which data are missing

(b) allow the user flexibility in choosing the order of the data

(c) initialize the variables with values on the restart tape.

READIN is set up to accept the title card with the RESTART value as the first card. The title can be set up to 40 characters in columns 1 - 40. The word RESTART should be located in columns 50 - 58 and the RESTART value in columns 60 - 68. If the RESTART name and value are left off, READIN assumes a value of 1.

If RESTART is set to 1, the second card must specify NI, NJ and NK. These variables specify the array sizes for all the variable arrays except IMASSF, IPLOTI and IPLOTK. If NI, NJ and NK are not specified, an error message is sent and the run terminates.

If the RESTART is set at ± 2 or ± 3, the run will continue from a point reached in an earlier execution. Because the values are stored in matrix arrays, the number of grids in each direction must remain fixed. Therefore, any attempt at re-specifying the number of grids, i.e., changing the value of NI, NJ or NK, is ignored.

All the remaining data can be introduced in any order. In our examples, we have elected to group the data according to its usage, i.e., geometric, correlation-related, operating conditions and input/output parameter selection.

READIN contains lists of all the variables required by the code. As the data cards are read, READIN searches through the list to match input variable names with the ones on its list. If the subroutine can make the match, it stores the data in the variable and removes the variable name from the list.

If READIN cannot match an input variable to one on its list, it issues the following message:

*** X CANNOT MATCH X <u>VARNAME</u> <u>DATA</u> ***

This message contains the input variable name and its value so the user can trace the nature of the error. This error could result from a misspelling of the variable name, from reading the same variable twice, or using improper data. This error does not result in a termination of the run. If a variable appears twice, READIN stores the first value and disregards the second. If a variable is mispelled, READIN ignores the variable and its value, and thus the intended variable name will not be removed from the list.

When the end of the input deck (END OF FILE) is encountered, READIN checks that all the variables on its list have been initialized. Some variables may not be stroked off because they are either mispelled or simply left out. If a variable name remains, but has not been initialized, READIN issues one of the following messages:

* THE FOLLOWING VARIABLE(S) HAVE NO INPUT DATA: VARNAME *

or * THE FOLLOWING ARRAY(S) HAVE NO INPUT DATA: VARNAME *

READIN then checks the value of RESTART and:

If (RESTART=±1) - READIN terminates the run

If (RESTART=±2 or ±3) - READIN uses the values stored on the tape made from a previous run and continues executing, thus only variables to be changed are required as input data.

5.3 Time Limit Feature

If the code senses that insufficient time remains to complete another iteration step and to print and plot the output, it will automatically call FPRINT for a printout, and call the WSTART routine to write a RESTART tape. The user can subsequently attach the RESTART tape and continue executing with additional time.

Both execution time and input/output time are monitored, but the time limit feature can be suppressed by setting the parameter TIMELT to zero. If TIMELT is not set in input or is set to 1 in the input deck, time remaining is checked at the end of each iteration.

The statements:

```
IFE(R1.NE.0)JUMP
CATALOG ( ----
ENDIF(JUMP)
```

should be included in the job control deck to catalog a RESTART tape when a time limit is encountered.

5.4 Advanced Execution Deck

The simple execution deck introduced in Chapter 4 is sufficient to run a standard WHIRST job in which no RESTART tape is read or saved. For more advanced use, we now include an execution deck which will permit the use of a RESTART tape, and also permit certain code changes to be made, using the CDC program library editor, UPDATE.

This "advanced use" deck contains three major segments:

(i) job control statements
(ii) update correction set
(iii) input data

Because the function of each section in the execution deck is different, they will be explained separately. It is assumed that the reader has a basic understanding of the job card sequence and the update routines available through the computing system. A listing of the execution deck without explanations is shown in Appendix C.

5.4.1 Job Control Statements

Card No.		Explanation
1	THIRST, B652-EXAMPLE,T500,I0100	
2	ATTACH(OLDPL,THIRSTPL,ID=THIRST)	Attach the code stored on file name THIRST
3	UPDATE(C=DISC)	Update the file THIRST with any code changes in the associated correction set and list on disc
4	FTN(I=DISC, B=THIRMOD)	Compile the file THIRST from DISC. Store compiled file on THIRMOD
5	ATTACH(THIRST, ID=THIRST)	Access standard THIRST code
6	COPYL(THIRST, THIRMOD, THIRST2)	Merge modifications and standard code to create new program THIRST 2
7	ATTACH(PLOTLIB)	Attach library plotting package
8	COMMENT.	
9	LDSET(LIB=PLOTLIB, SUBST=PLOT-PLT)	

Card No.		Explanation
10	ATTACH(TAPE60, THIRSTDATA, ID=THIRST)	This card is required only when the RESTART option is used (ABS(RESTART). GT.1) The data catalogue from a previous run under file name THIRSTDATA with ID= THIRST and for CY=1 will be attached and used to initialize the variables. If RESTART is 1, this card will have no useful purpose and should be omitted.
11	THIRST2(PL=30000)	Execute the job and set the printing limit at 30000 print lines
12	IFE(R1.NE.0)JUMP.	If a RESTART tape has been written either through a time limit or a negative value of RESTART then R1 is set to one. If the program has not written a data RESTART tape then R1 = 0 and the execution jumps to ENDIF (JUMP). Thus this card controls the sequence to CATALOG only when the data RESTART tape exists.

Card No.		Explanation
13	CATALOG(TAPE60, THIRSTDATA, ID=THIRST)	Catalog the RESTART tape
14	ENDIF(JUMP)	Point to which the IFE( ) card directs control
15	7/8/9	End of record card

To enable the computer to allocate storage, the size of the grid layout must be specified in the EXEC routine. The following update correction may be used to change this allocation and is included for example purposes.

Card No.		Explanation
16	*D EXEC.4	Delete the fourth card in EXEC
17	COMMON F(4320,13)	Reserve 13 arrays (11 variables plus 2 working spaces). Each array contains NI*NJ *NK = 36*10*12 = 4320 storage places
18	7/8/9	END OF RECORD

5.4.2 Input Deck

Unless the changes made above incorporate new input data, no form changes in the deck of Chapter 4 are required.

6. THIRST OUTPUT

In this chapter, we present the basic output obtained from the THIRST code. Possible variations of output are also discussed. Output from THIRST is in both printed and graphical form. The following paragraphs refer to sample output which appears consecutively at the end of this section starting on page 99.

6.1 Printed Output Features

6.1.1 Preliminary Output

After the program logo, THIRST prints out the values in the input deck. The arrays are printed first, the single integer values second and the single real values last. All the error messages related to the input are printed out in this section, Figure 6.1.

The next section of the printed output contains a summary of all the input received by the code for this run and a summary of the properties which THIRST has calculated from curve fits.

Figures 6.2.1 to 6.2.3 contain:

(a) Operating Conditions
- Primary
- Secondary

(b) Properties as Calculated by THIRST (using Curve Fits)
- Primary Saturation Values
- Secondary Saturation Values
- Secondary Subcooled Inlet Properties

(c) Output Selection and Control Parameters

(d) Geometrical Parameters

Figure 6.3 contains:

(a) <u>The Grid Locations for Scalar and Vector Components</u>
- The Axial Positions in Metres
- The Radial Positions in Metres
- The Circumferential Positions in Degrees

(b) <u>Primary Fluid Flow Distribution per Typical Tube in kg/s</u>

All the above output is generated in START before the iteration procedure begins. The user has no control over the format without altering the program logic.

6.1.2 <u>Individual Iteration Summary</u> (Figures 6.4.1 to 6.4.5)

During the progression of the solution to convergence, the following information is summarized on one page for each outer iteration.

(a) <u>Iteration</u>: At the beginning of each iteration prior to any further calculation, the EXEC routine prints the outer iteration number.

(b) <u>New Estimate of RECIR (only after the ninth step)</u>: After the ninth iteration, the program begins to calculate the RECIRculation ratio. Because the solution technique is iterative, the value will change until the solution approaches convergence.

(c) <u>Mass Flows at Planes of Interest</u>: The mass flows are calculated at I-planes selected by the user. The user can choose any or all of the I-planes by using the IMASSF parameter (see data no. 71, Table 4.1). The mass flow information is preceded by a line indicating the point within the iteration step at which these calculations were performed. The mass flows at designated I-planes are plotted in five columns of eight entries each for a maximum of forty positions, if required. The mass flows are given for both the hot and cold side. The calculations are made in MASSFLO. MASSFLO is called whenever the axial velocity or local density is changed.

(d) Summary of Overall Performance Variables and the Convergence Indicators: At the end of an iteration step, a summary of the overall performance variables and the convergence indicators are printed. The user has no direct control over this format. The information provided includes:

RECIR	Recirculation ratio used for this iteration
PRESS DROP in Pa	is the pressure drop between the average pressure at the last I-plane (L-plane) inside the shroud and the average pressure at the last I plane (L-plane) outside the shroud in the downcomer.
PRIM H.T. in MW	is the net amount of heat given up by the primary fluid

SEC H.T. in MW — is the amount of heat picked up by the secondary. This includes the heat required to raise the feedwater and reheater drain flows to saturation, plus the heat absorbed in evaporating the secondary liquid.

NOTE — PRIM H.T. should equal SEC H.T. when convergence has been achieved.

AVG/OUTLET/QUAL — average outlet quality

SUMSOURCE — is the summation of the absolute value of the mass imbalance for each control volume normalized by dividing by the total flow. This indicator should approach zero with convergence.

MAXSOURCE (2,7,11) — is the largest mass imbalance normalized by dividing by the total flow in the modelled region. The location is given in the brackets as I=2, J=7, K=11. If the location remains fixed, and the imbalance is significant, the use should examine the region for a possible error in that area.

(e) Summary of Local Values: The last section of the iteration by iteration printout summarizes local values at strategic locations in the model. The locations are fixed in the code at such points as window inlets, above the preheater, in the downcomer, etc.

Three sets of variables - AXIAL VELOCITY, CROSS FLOW VELOCITIES and THERMAL VALUE are printed. The location of each variable is described including its (I,J,K) coordinates. If the user wishes to change the locations to be printed, the OUTPUT subroutine must be altered.

The overall values (d) and local values (e) are printed out in OUTPUT. OUTPUT can be called at any point in the execution if the user desires to. At present it is called at the end of each iteration step.

6.1.3 Detailed Array Printout (Figure 6.5)

The last type of printed output, again under user control, is the complete printout of selected variables at every active node in the model. The format for the printout is

```
          XXXXXXXXXX  VARIABLE NAME (1)  XXXXXXXXXX

                                K=2
      I=2     J=2     J=3     J=4  -------------------------J=M
      I=3
      I=4
       ↓
      I=L
```

```
                              K=3
I=2    J=2    J=3    J=4 -------------------------J=M
I=3
I=4

I=L



                              K=N
I=2    J=2    J=3    J=4 -------------------------J=M
I=3
I=4

I=L
```

XXXXXXXXXX VARIABLE NAME (2) XXXXXXXXXX

etc.

This printout can be very long depending on how many variables are specified for printout. Figure 6.5 shows the first page of a detailed array printout of axial velocity obtained by setting IPRINT(I) to 1. Each selected variable takes a similar format and each generates five pages of output for K=12, so the feature should be used with caution. Variables to be printed may be selected by the input variable IPRINT.

If IPRINT(NV) is entered non zero, the array of values for variable NV is printed, where NV is selected as follows:

NV = 1 - axial velocity
NV = 2 - radial velocity
NV = 3 - circumferential velocity
NV = 4 - mass flux
NV = 5 - steam quality
NV = 6 - primary temperature
NV = 7 - tube wall temperature
NV = 8 - static pressure
NV = 9 - density
NV = 10 - heat flux
NV = 11 - porosity

This printout is generated by the FPRINT subroutine. The PRINTO parameter calls FPRINT as follows:

If PRINTO = 0 - the FPRINT array is never called
- this would be used where the user is interested in the plots only

If PRINTO = 1 - che FPRINT array is called after exit from the iteration loop at the end of the run

If PRINTO = N - the FPRINT array is called every (N-1) iteration steps. This tends to create large output files and thus is only used for debugging p.rposes. Careful selection of the IPRINT (NV) parameter is suggested.

6.2 Graphical Output Features

The plot routines have been set up to produce:

(a) quality contours
(b) velocity vectors
(c) mass flux vectors

for any planes of interest.

Quality contour values are specified by TCON in the input deck. Up to 15 contour intervals are allowed. If less than 15 contours are desired, then set the remaining position of the TCON array to zero and the plotting subroutine ignores them. Velocity vectors are determined by first interpolating each velocity component to the grid nodes. The two velocity components lying in the plane of interest are added vectorially. The resultant vector is printed as an arrow with its length indicating magnitude and angle indicating direction. Mass flux contours are determined by multiplying the velocity vector calculated earlier by the local density.

Two plotting formats are available to the user:

(a) Full Diameter/Horizontal Cut Composite
(b) Vertical Cut Composite

Full Diameter/Horizontal Cut Composite

This composite includes plots of values of the K=2 and K=N planes which lie next to the line of symmetry. These are put out by the plot routine automatically. Included on this frame are up to eight horizontal cuts through the modelled region corresponding to eight axial lines specified by the IPLOTI parameter. The selection of horizontal cuts is made by the user in the input deck, by specifying the number of desired I-planes (maximum of eight). A negative sign in front of the specified I-plane positions the plot on the left of the Full Diameter Plot, otherwise the plot appears on the right of the Full Diameter Plot. No more than four I-plots for the left and four for the right may be specified. If only four I-planes are specified, all the plots should appear on the right as the plotting routine will reduce the frame size. Examples of this composite are given in Figure 6.6, which depicts quality, velocity and mass flux profiles consecutively.

Vertical Cut Composite

The second plot format is a composite of four vertical cuts corresponding to circumferential planes. The number and indices of K-planes to be plotted are specified by the parameter IPLOTK. There is no limit on the number of K-planes to be selected. Examples of this composite for quality, velocity and mass flux profiles are given in Figure 6.7.

In some grid layouts, axial planes are grouped together to provide greater detail. Unfortunately, when velocity or mass flux vectors are plotted, they tend to overlap. To ensure clarity of the plots, an additional plot parameter called IIPLOT has been introduced. If IIPLOT (I) = 1, the values on that I-plane are included on the vertical cut plots. If IIPLOT (I) = 0, the corresponding I-plane values are left off the plot.

The user has control over the plotting frame size. For the first composite, the width is specified by "XL1" and "XL2". If horizontal plots are made on the left and on the right of the vertical cut, the routine uses the wider plotting frame specified in XL1. If other horizontal plots appear only on the right, the routine uses the narrow plot XL2. The height for all plots is YL. The length to width ratios of the plots may not be in proportion to the actual design, as the width may be increased to add clarity. Scaling factors are determined by the code.

The plotting routines can be called at any point in the code by the statement CALL CONTOUR. The parameter PLOTO has been introduced to control the calling of the plot routines.

If PLOTO = 0 - the plot routine is never called. This may be used where the user wants only a printout.

If PLOTO = 1 - the plot routine is called at the end of the program.

If PLOTO = 2 - the plot routine is called at the end of each iteration. This leads to a very long plot life.

PLOTO is set in the input deck. PLOTO and PRINTO can be reset in the program to initiate the plotting and printing function.

6.3 Interpretation of the Output

Having discussed the layout of printed output we now turn again to the printed output, Figures 6.1 to 6.5, to examine its content and its significance.

The first page of printout, Figure 6.1, contains a summary of all the data introduced through the input deck. No error messages of consequence were issued and a comparison with the data sheets indicates that the data has been introduced correctly.

The second, third and fourth pages (Figure 6.2) contain input values and calculations made with the input. The operating conditions should be checked against the information sheets. Property values generated by the code should be checked against values in standard tables. Correlation data should be verified. The input/output parameters are simply informative. Finally, the geometric data should be verified against drawings or data sheets. The modelled heat transfer area should be examined to ensure that it is not radically different than the prescribed value. Although the correction factor will correct the modelled tube surface, a large discrepancy may indicate an error in treating the tube-free lanes or in the location at the start of the U-bend (IUBEND).

The main grid location (Figure 6.2) and particularly the displaced grid locations should be checked to ensure proper modelling of flow obstacles. For instance, the displaced grid at I=13 for the axial velocity should in this case correspond to the elevation of the first inner baffle. The primary fluid flow, also included on this page, is distributed to reflect the different tube lengths. Scanning the distribution, one should see a drop in primary flow along the K=2 plane with increasing J.

When satisfied with the validity of the input, one can proceed to examine the iteration by iteration output (Figure 6.4). Of prime importance is the line bounded by asterisks. Part of this line contains the overall parameters which must converge on single values - RECIR, PRESS DROP, PRIM and SEC HEAT TRANSFER and QUAL. The last two terms are the sum of the absolute value of the mass imbalance over all control volumes and the maximum mass imbalance at an indicated control volume. These should approach zero at convergence. By examining the line of printout as the solution proceeds, one can assess whether the solution is converging to a single solution or oscillating slowly about the solution.

Assuming that the run has completed normally without any execution errors, we will concentrate on the last several iterations to verify that a converged solution has been obtained. Later in this section we will discuss handling runs that terminate in execution errors.

Comparing iterations 58, 59 and 60, Figures 6.4.3, 4 and 5, we observe that RECIR has converged to the fourth significant figure, which indicates that the pressure distribution has also converged.

Examining the mass flows at various stages in the iteration step, we see that the values are basically stable. Minor changes can be expected due to the nature of the finite difference technique; however, a swinging from one value to another would indicate an inconsistency in the modelling between stages. If the swinging is significant, further debugging of the logic should take place.

In the middle of the mass flow printout is the SUM OF RING (WEDGE) MASS IMBALANCE. As explained in earlier sections, continuity is enforced simultaneously over groups of control volumes. Control volumes are grouped alternatively into wedge and ring geometries. The MASS IMBALANCE should approach zero at convergence; however, the level indicated is considered acceptable.

At the end of the run we also should be satisfied that the pressure drop value is stable, that the heat transferred out of the primary (PRIM H.T.) is equal to that absorbed by the secondary (SEC H.T.) and that the source terms are sufficiently small. The location of the maximum imbalance is given in brackets after the MAX SOURCE. This information can be useful during debugging to indicate trouble areas. If the location remains fixed and the imbalance fairly high, one should examine the region for a modelling error.

The last three lines on Figure 6.4.5 contain local values of thermal and hydraulic variables. These values should be compared with earlier iterations to ensure that they have converged. The positions shown in brackets have been selected to monitor variables because they are particularly sensitive areas.

When we are content that the solution has converged, we should examine the printouts to check numbers against intuition and then examine the plots to verify that flow and quality patterns are consistent. These outputs will not provide additional evidence of convergence but will enable the user to intuitively verify the results. For instance, the quality profiles on the I=2 plane could be superimposed over the velocity vectors to verify that the velocities are concentrating near the point of highest quality. The velocity vectors in the U-bend should indicate an outwards radial flow to the lower resistance regions. The flow around the baffles should be well defined. Having examined the output, we conclude that, for this example, the solution has converged.

6.4 Treatment of Diverging Solutions

If the solution has not converged, we should either restart the program and continue for more iteration or examine the modelling for errors. It may be necessary to use lower relaxation factor to promote convergence.

If the solution terminates on an execution error or will not converge, the user will be required to debug the model. The efficiency of the user's debugging methods will improve only with experience. To assist in debugging, the following potpourri of examples is included:

(a) If the program has terminated before completing one iteration, it is likely that insufficient input data has been given or that the array sizing doesn't match the arrays referenced. One can identify the line in which the error occurred and generally find the error using an "OPT=0" on the FTN card.

(b) If the program fails after the eighth iteration, examine the RECIR subroutine because it is called after the eighth iteration.

(c) If the program terminates with an error message "ARGUMENT LESS THAN ZERO", this is most likely generated by quality values greater than 1 arising from a very high pressure gradient (the user should refer to DENS to see how pressure affects quality). The high pressure gradient generally occurs when a gross inconsistency in the treatment of flow obstacles occurs between various stages of the iteration procedure. Large pressure corrections are required to maintain continuity. The stage within the iteration that contains the inconsistency can be determined by examining the mass flows printout.

(d) Large swings in thermal values generally indicate a problem in the heat transfer subroutine source terms, especially if a new correlation has been introduced. Reduce the relaxation factor for T_W to promote stability.

(e) If the solution is not converging and the reason is not clear, it may prove useful to call for plots for several succeeding iterations. The plots should then be superimposed to identify regions that are oscillating. In this way, the region(s) of possible modelling errors can be pinpointed. One could also call for FPRINT output for several succeeding iterations.

(f) If the FPRINT array is called and columns of zeros appear in the output or if a mode error occurs, check that the common card in EXEC which sets the size of the F-array has been dimensioned correctly.

(g) If the PRIM H.T. is different than the SEC H.T., the problem is most likely located in the SOURCH routine where the heat transfer source terms are calculated. Check that the no-tube regions are handled correctly and that any new correlations are used correctly.

(h) If the results seem to oscillate between two sets of values, check the wedge and ring routines to ensure consistency of treatment. These routines are used on alternate steps.

(i) If the flow oscillates between the hot and cold side shroud windows, examine the treatment of flow obstacles in the downcomer.

(j) If resistances appear to be incorrect, one can print out the DU, DV and DW arrays after the CALCW subroutine. These arrays can be printed using the logic in FPRINT. They contain all the resistances in the model and can be checked to see if any resistances are out of line.

(k) The pressure correction generated in RINGS1 and WEDGES1 can be printed out to identify trouble spots. Printing out the pressure corrections for the CALCPK and CALCPIJ is more involved since the control volumes are not grouped.

(l) When RESTART is set to -1, there should be no control card that attaches a RESTART tape to the program. An ATTACH statement is necessary when RESTART is set to ± 2 and ± 3. If an ATTACH statement is present when RESTART equals -1, the program will run and output will be printed, including any plots, but the RESTART tape requested by negative value of RESTART will not be made and you will get a DMPX. The dayfile will indicate "ILLEGAL I/O REQUEST", the "FILENAME ..." and "FET ADDRESS..." as well as "WRITE NOT AT EOI ON PERMANENT FILE".

(m) Finally, the user should document convergence problems and their solution so that future problems will be easier to track down.

```
************************************     HYPOTHETICAL 600 MW STEAM GENERATOR     ************************************
RESTART   1.000000
NI      36     NJ      10     NK      12

   AKDIV      36
1.E-10 1.E-10 1.E-10 1.E-10 1.E-10 1.E-10 1.E+15 1.E+15 1.E+15 1.E+15 1.E+15 1.E+15 1.E+15 1.E+15 1.E+15 1.E+15 1.E+15
1.E+15 1.E+15 1.E+15 0. 0. 0. 0. 0. 0. 0. 0. 0. 1.8 1.8 1.8 1.8 0. 0. 0.
   BP          3
.03 .18 .56
   ICOLD      36
1 1 1 1 1 1 1 5 1 1 3 1 4 3 4 3 4 3 4 3 7 1 1 2 2 2 2 2 2 2 1 1 1 1 1 1
   IHOT       36
1 1 1 1 1 1 1 6 1 1 1 1 2 1 2 1 2 1 2 1 2 1 1 2 2 2 2 2 2 2 1 1 1 1 1 1
   IIPLOT     36
0 1 0 1 0 1 0 1 0 1 1 0 1 1 1 1 1 1 1 1 1 1 1 1 1 1 1 0 1 0 1 1 1 0
   IMASSF     33
3 4 5 6 7 8 9 10 11 12 13 14 15 16 17 18 19 20 21 22 23 24 25 26 27 28 29 30 31 32 33 34 35
   IFLOWK      8
3 4 5 6 7 8 9 10
   IFLOWI      8
2 -6 14 -21 25 -32 33 -35
   IPRINT     11
1 0 0 0 0 0 0 0 0 0 0
   RELAX      11
.5 .5 .5 1. 1. 1. .25 .5 .5 .2 1.
   TCON       15
0. .01 .02 .03 .05 .1 .15 .2 .22 .25 .3 .35 .4 .5 0.
   X          36
0. .01 .12 .23 .34 .45 .56 .67 .78 .89 1. 1.11 1.46 1.81 2.16 2.51 2.86 3.21 3.56 3.91 4.17 4.26 4.61 5.194 5.76 6.36
6.94 7.53 8.12 8.7 9.07 9.44 9.8 10.2 10.5 10.6
   Y          10
0. .1 .27565 .4513 .6269 .8026 .978 1.1539 1.2845 1.3575
   Z          12
0. 9. 27. 45. 63. 81. 99. 117. 135. 153. 171. 180.
 IDOWNC     6     IDCHNH      7     IFEEDB    13     IFEEDL     8     IFEEDU    10
 IPRHT     20     ISHRD      31     ITFPR      1     IUBEND    30     IVF        1
 JBRCH      4     KCENTC      7     KCENTH     6     KFEEDL     9     LASTEP    60

 AKBL      1600.000         AKBR     1.500000         AKBRL    1.000000         AKBRS    6.000000      AKTP     1600.000
 AKWINCC   13.00000         AKWINDH  13.00000         ARATB    1.2705000E-02    ARATTP   0.            CGAP     7.0000000E-02
 CON1      .9495000         CON2     .1156000         CON4     2030.000         CWALL    16.70000      DIA      1.5875000E-02
 DIAIN     1.3600000E-02    EDFEED   6.5000000E-02    EDNORM   .2200000         EDSHROX  .8000000      FLOB     21000.00
 FLCT      1600.000         FLOWC    386.1870         FLOWRH   23.70000         FLOWTC   2464.930      HTAR     4550.000
 OGAP      3.0000000E-02    PFWB     .3125000         PITCH    2.4511000E-02    PLOTC    1.000000      PPRI     9.879000
 PRINTO    1.000000         PSEC     5.100000         PSHRD    10.10000         QLTU     4.4000000E-02 RADIUS   1.321000
 RECIR     5.300000         RFOUL    2.6420000E-05    RSHELL   1.440000         TINC     176.6000      TPLATE   .6150000
 TRH       251.6000         TUBSHET  .4190000         XDCHN    15.00000         XVANE    16.00000      XL1      9.000000
 XL2       6.250000         YL       6.000000
NO DATA CALLED FOR ARRAY  IEXTRA
NO DATA CALLED FOR ARRAY  REXTRA
  TIMELT   USES PRESET VALUE(S)
```

Figure 6.1: THIRST OUTPUT - Summary of Input Data

```
*************************************     HYPOTHETICAL 600 MW STEAM GENERATOR     *************************************

OPERATING CONDITIONS:

         PRIMARY

         PPRI      9.8790000     N/M2          FLOWTU    2484.9300     KG/S          QLTU     4.40000000E-02

         SECONDARY

         PSEC      5.1000000     N/M2          FLOWC     306.18000     KG/S          TINC     176.67000     CEL
         FLOWRH    23.700000     KG/S          TFW       251.60000     CEL           RECIR    5.3000000

PROPERTY VALUES CALCULATED BY THIRST

         PRIMARY SATURATION VALUES

         TSATU     309.20115     CEL           ENPS      1348548.5     J/KG          ALATU    1177907.6     J/KG
         VFU       1.3'206299E-03 M3/KG        VGU       1.59764798E-02 M3/KG

         SECONDARY SATURATION VALUES

         TSAT      265.17748     CEL           DEN       775.79814     KG/M3         DENSM    25.903825     KG/M3
         ALAT      1631946.1     J/KG          ENSS      1160741.1     J/KG          AMUG     1.80500000E-05 KG/M-S
         AMUS      1.01089552E-04 KG/M-S       CPWS      5051.0885     J/KG-CEL      PRWS     .85645620
         STEN      2.26241618E-02 N/M          DTDP      1.23995400E-05 CEL/(N/M2)   DHDP     6.22190564E-02 (J/KG)/(N/M2)

         SECONDARY SUBCOOLED INLET PROPERTIES

         ENFW      749868.28     J/KG          DENC      893.52101     KG/M3         ENRH     1094156.3     J/KG
      ** OTHER SUBCOOLED PROPERTIES ARE CALCULATED AS NEEDED **


         CONTROL VARIABLES     ITPPU     1  IVF       1
         INPUT VARIABLES

         AKBR      1.5000000        AKBRL     1.0000000        AKBRS     6.0000000        AKTP     1600.0000
         AKBL      1600.0000        AKWINDC   10.000000        AKWINDH   13.000000        ARATB    1.27050000E-02
         ARATTP    0.               CON1      .94950000        CON2      .11560000        CON4     2000.0000
         CWALL     16.700000        FLDB      21000.000        FLDT      1600.0000        RFOUL    2.64200000E-05

         AKDIV

      AT I=  1   1.0E-10     I=  2   1.0E-10     I=  3   1.0E-10     I=  4   1.0E-10     I=  5   1.0E-10
         I=  6   1.0E-10     I=  7   1.0E+15     I=  8   1.0E+15     I=  9   1.0E+15     I= 10   1.0E+15
         I= 11   1.0E+15     I= 12   1.0E+15     I= 13   1.0E+15     I= 14   1.0E+15     I= 15   1.0E+15
         I= 16   1.0E+15     I= 17   1.0E+15     I= 18   1.0E+15     I= 19   1.0E+15     I= 20   1.0E+15
         I= 21   0.          I= 22   0.          I= 23   0.          I= 24   0.          I= 25   0.
         I= 26   0.          I= 27   0.          I= 28   0.          I= 29   0.          I= 30   1.8E+00
         I= 31   1.8E+00     I= 32   1.8E+00     I= 33   1.8E+00     I= 34   0.          I= 35   0.
         I= 36   0.
```

Figure 6.2.1: THIRST OUTPUT - Interpreted Data
(Summary of Operating Conditions)

```
INPUT/OUTPUT AND CONTROL FEATURES

        LASTEP    60      ISTEP       0
        PRINTO     1.0000000       PLOTC        1.0000000             TIMELT     1.0000000                RESTART    1.0000000
        XL1        9.0000000      INCHES          XL2          6.2500000      INCHES               YL          6.0000000      INCHES

        TCON(%)

        0.    1.    2.    3.    5.    10.   15.   20.   22.   25.   30.   35.   40.   50.   0.

        RELAX

        NV( 1)  .500      NV( 2)  .500      NV( 3)  .500      NV( 4) 1.000      NV( 5) 1.000
        NV( 6) 1.000      NV( 7)  .250      NV( 8)  .500      NV( 9)  .500      NV(10)  .200
        NV(11) 1.000

        IPRINT

        NV( 1)  1         NV( 2)  0         NV( 3)  0         NV( 4)  0         NV( 5)  0
        NV( 6)  0         NV( 7)  0         NV( 8)  0         NV( 9)  0         NV(10)  0
        NV(11)  0

        IIPLOT

        IIPLOT( 1) 0      IIPLOT( 2) 1      IIPLOT( 3) 0      IIPLOT( 4) 1      IIPLOT( 5) 0
        IIPLOT( 6) 1      IIPLOT( 7) 0      IIPLOT( 8) 1      IIPLOT( 9) 0      IIPLOT(10) 1
        IIPLOT(11) 1      IIPLOT(12) 0      IIPLOT(13) 1      IIPLOT(14) 1      IIPLOT(15) 1
        IIPLOT(16) 1      IIPLOT(17) 1      IIPLOT(18) 1      IIPLOT(19) 1      IIPLOT(20) 1
        IIPLOT(21) 1      IIPLOT(22) 1      IIPLOT(23) 1      IIPLOT(24) 1      IIPLOT(25) 1
        IIPLOT(26) 1      IIPLOT(27) 1      IIPLOT(28) 1      IIPLOT(29) 1      IIPLOT(30) 0
        IIPLOT(31) 1      IIPLOT(32) 0      IIPLOT(33) 1      IIPLOT(34) 1      IIPLOT(35) 1
        IIPLOT(36) 0

        IMASSF

           3     4     5     6     7     8     9    10    11    12    13    14    15    16    17    18    19    20    21    22
          23    24    25    26    27    28    29    30    31    32    33    34    35

        IPLOTK

           3     4     5     6     7     8     9    10

        IPLOTI

           2    -6    14   -21    25   -32    33   -35
```

Figure 6.2.2: THIRST OUTPUT - Interpreted Data
(Summary of Output Parameters)

```
GEOMETRY

          LOCATIONS

          IDOWNC     6        IDOWNH     7        KCENTC     7        KCENTH     6
          IFEEDB    13        IFEEDL     8        IFEEDJ    10        KFEEDL     3
          IPRHT     20        ISHRD     31        IUBENJ    30        JBRCH      4

          INPUT SIZES AND LOCATIONS

          RADIUS     1.3210000      M          CGAP      7.0000000E-02 M          CGAP     3.0000000E-02  M
          DIA      1.5875000E-02 M             DIAIN     1.3600000E-02 M          PITCH    2.4511000E-02  M
          PSHRD     10.100000                  RSHELL     1.4400000    M          TUBSHET   .41300000     M
          PFWB      .31250000                  TPLATE     .61500000    M          HTAR     4550.0000      M2
          EDNCRM    .22000000       M          EDFEED    6.5000000E-02 M          ECSHRDX   .80000000     M
          XVANE     16.000000       M          XDOWN      15.000000    M
          BF(1)     .83000000       M          BP(2)      .18000000    M          BF(3)      .56000000    M

          CALCULATED SIZES AND LOCATIONS

          XUBEND    8.7000000       M          XPREHT     4.0400000    M          AINC       .32170800    M2

          HEAT TRANSFER AREA AS MODELLED BY THIRST = 4531.761961186  M2

          CORRECTION FACTOR REQUIRED TO FORCE MODELLED AREATO ACTUAL HEAT TRANSFER AREA = 1.004024491791

          LOCATION OF TUBE SUPPORTS ON HOT SIDE

          IHOT( 1)   1      IHOT( 2)   1      IHOT( 3)   1      IHOT( 4)   1      IHOT( 5)   1
          IHOT( 6)   1      IHOT( 7)   1      IHOT( 8)   6      IHOT( 9)   1      IHOT(10)   1
          IHOT(11)   1      IHOT(12)   1      IHOT(13)   2      IHOT(14)   1      IHOT(15)   2
          IHOT(16)   1      IHOT(17)   2      IHOT(18)   1      IHOT(19)   2      IHOT(20)   1
          IHOT(21)   2      IHOT(22)   1      IHOT(23)   1      IHOT(24)   2      IHOT(25)   2
          IHOT(26)   2      IHOT(27)   2      IHOT(28)   2      IHOT(29)   2      IHOT(30)   2
          IHOT(31)   1      IHOT(32)   1      IHOT(33)   1      IHOT(34)   1      IHOT(35)   1
          IHOT(36)   1

          LOCATION OF BAFFLES, TUBE SUPPORTS, AND THERMAL PLATE ON COLD SIDE

          ICOLD( 1)  1      ICOLD( 2)  1      ICOLD( 3)  1      ICOLD( 4)  1      ICOLD( 5)  1
          ICOLD( 6)  1      ICOLD( 7)  1      ICOLD( 8)  5      ICOLD( 9)  1      ICOLD(10)  1
          ICOLD(11)  3      ICOLD(12)  1      ICOLD(13)  4      ICOLD(14)  3      ICOLD(15)  4
          ICOLD(16)  3      ICOLD(17)  4      ICOLD(18)  3      ICOLD(19)  4      ICOLD(20)  3
          ICOLD(21)  7      ICOLD(22)  1      ICOLD(23)  1      ICOLD(24)  2      ICOLD(25)  2
          ICOLD(26)  2      ICOLD(27)  2      ICOLD(28)  2      ICOLD(29)  2      ICOLD(30)  2
          ICOLD(31)  1      ICOLD(32)  1      ICOLD(33)  1      ICOLD(34)  1      ICOLD(35)  1
          ICOLD(36)  1
```

Figure 6.2.3: THIRST OUTPUT - Interpreted Data
(Summary of Geometric Parameters)

```
THE MAIN GRID LOCATIONS

THE AXIAL DISTANCES IN METERS
 I= 1   0.         , I= 2   1.000E-02 , I= 3   1.200E-01 , I= 4   2.300E-01 , I= 5   3.400E-01
 I= 6   4.500E-01 , I= 7   5.600E-01 , I= 8   6.700E-01 , I= 9   7.900E-01 , I=10   8.900E-01
 I=11   1.000E+00 , I=12   1.110E+00 , I=13   1.460E+00 , I=14   1.810E+00 , I=15   2.161E+00
 I=16   2.510E+00 , I=17   2.860E+00 , I=18   3.210E+00 , I=19   3.560E+00 , I=20   3.910E+00
 I=21   4.170E+00 , I=22   4.260E+00 , I=23   4.610E+00 , I=24   5.194E+00 , I=25   5.780E+00
 I=26   6.360E+00 , I=27   6.940E+00 , I=28   7.530E+00 , I=29   8.120E+00 , I=30   8.700E+00
 I=31   9.070E+00 , I=32   9.440E+00 , I=33   9.800E+00 , I=34   1.020E+01 , I=35   1.050E+01
 I=36   1.060E+01

THE RADIAL DISTANCES IN METERS
 J= 1   0.         , J= 2   1.000E-01 , J= 3   2.757E-01 , J= 4   4.513E-01 , J= 5   6.269E-01
 J= 6   8.026E-01 , J= 7   9.780E-01 , J= 8   1.154E+00 , J= 9   1.285E+00 , J=10   1.358E+00

THE CIRCUMFERENTIAL POSITIONS IN DEGREES
 K= 1   0.         , K= 2   9.000E+00 , K= 3   2.700E+01 , K= 4   4.500E+01 , K= 5   6.300E+01
 K= 6   8.100E+01 , K= 7   9.900E+01 , K= 8   1.170E+02 , K= 9   1.350E+02 , K=10   1.530E+02
 K=11   1.710E+02 , K=12   1.800E+02


THE DISPLACED GRID LOCATIONS FOR VELOCITY COMPONENTS

THE AXIAL DISTANCES IN METERS FOR THE AXIAL VELOCITY
 I= 2   0.         , I= 3   6.500E-02 , I= 4   1.750E-01 , I= 5   2.850E-01 , I= 6   3.9[illegible]0E-01
 I= 7   5.0[illegible]0E-01 , I= 8   6.150E-01 , I= 9   7.250E-01 , I=10   8.350E-01 , I=11   9.451E-01
 I=12   1.055E+00 , I=13   1.285E+00 , I=14   1.635E+00 , I=15   1.985E+00 , I=16   2.33[illegible]E+00
 I=17   2.685E+00 , I=18   3.035E+00 , I=19   3.385E+00 , I=20   3.735E+00 , I=21   4.04[illegible]E+00
 I=22   4.215E+00 , I=23   4.435E+00 , I=24   4.902E+00 , I=25   5.487E+00 , I=26   6.0[illegible]E+00
 I=27   6.650E+00 , I=28   7.235E+00 , I=29   7.825E+00 , I=30   8.410E+00 , I=31   8.[illegible]E+00
 I=32   9.255E+00 , I=33   9.620E+00 , I=34   1.000E+01 , I=35   1.035E+01 , I=36   1.[illegible]60E+01

THE RADIAL DISTANCES IN METERS FOR THE RADIAL VELOCITY
 J= 2   0.         , J= 3   1.876E-01 , J= 4   3.635E-01 , J= 5   5.391E-01 , J= 6   7.148E-01
 J= 7   8.903E-01 , J= 8   1.066E+00 , J= 9   1.219E+00 , J=10   1.321E+00

THE CIRCUMFERENTIAL POSITIONS IN DEGREES FOR THE CIRCUMFERENTIAL VELOCITY
 K= 2   0.         , K= 3   1.800E+01 , K= 4   3.600E+01 , K= 5   5.400E+01 , K= 6   7.200E+01
 K= 7   9.000E+01 , K= 8   1.080E+02 , K= 9   1.260E+02 , K=10   1.440E+02 , K=11   1.620E+02
 K=12   1.800E+02
```

PRIMARY FLUID FLOW DISTRIBUTION IN KG/S

J =	2	3	4	5	6	7	8	9
K = 2	.55008	.54130	.53290	.52486	.51714	.50975	.50263	.49751
K = 3	.55058	.54262	.53498	.52763	.52055	.51375	.50717	.50243
K = 4	.55153	.54516	.53899	.53302	.52722	.52160	.51614	.51218
K = 5	.55286	.54872	.54466	.54069	.53679	.53298	.52923	.52650
K = 6	.55443	.55298	.55154	.55011	.54870	.54729	.54589	.54486
K = 7	.55443	.55298	.55154	.55011	.54870	.54729	.54589	.54486
K = 8	.55286	.54872	.54466	.54069	.53679	.53298	.52923	.52650
K = 9	.55153	.54516	.53899	.53302	.52722	.52160	.51614	.51218
K = 10	.55058	.54262	.53498	.52763	.52055	.51375	.50717	.50243
K = 11	.55008	.54130	.53290	.52486	.51714	.50975	.50263	.49751

Figure 6.3: THIRST OUTPUT - Summary of Grid Locations

```
ITERATION NUMBER =  1

MASS FLOWS AFTER SOLUTION OF MOMENTUM EQUATION FOR U VELOCITY

 I  HOT SIDE  COLD SIDE    I  HOT SIDE  COLD SIDE    I  HOT SIDE  COLD SIDE    I  HOT SIDE  COLD SIDE    I  HOT SIDE  COLD SIDE
 3     -.618     -6.474   11   320.635   263.888   19   273.599   261.258   27   268.618   268.618   35   474.409   474.409
 4   118.908    112.136   12   324.658   298.202   20   296.647   258.048   28   268.568   268.568
 5   164.588    190.632   13   277.914   264.774   21   274.018   268.656   29   268.550   268.560
 6   182.394    150.174   14   298.400   258.048   22   303.362   300.839   30   265.051   265.051
 7   188.116    147.588   15   273.884   261.258   23   308.989   307.971   31   244.925   244.925
 8   255.393    253.744   16   296.762   258.048   24   274.342   274.181   32   268.168   266.168
 9   293.950    297.221   17   273.617   261.258   25   269.455   269.429   33   334.248   334.249
10   312.094    318.811   18   296.654   258.048   26   268.732   268.728   34   417.112   417.112

MASS FLOW AFTER K-PLANE SOLUTION OF CONTINUITY EQUATIONFOR P AND CORRECTION OF U VELOCITY

 I  HOT SIDE  COLD SIDE    I  HOT SIDE  COLD SIDE    I  HOT SIDE  COLD SIDE    I  HOT SIDE  COLD SIDE    I  HOT SIDE  COLD SIDE
 3   122.344    131.738   11   301.310   263.452   19   276.674   258.109   27   268.624   268.624   35   478.800   478.488
 4   164.741    168.169   12   303.297   268.626   20   289.138   257.356   28   268.571   268.562
 5   202.528    215.909   13   283.483   259.896   21   280.899   269.084   29   268.526   268.401
 6   218.968    246.993   14   291.279   257.418   22   292.222   284.861   30   264.757   264.541
 7   237.555    260.937   15   277.134   258.065   23   298.905   294.486   31   249.691   251.741
 8   265.333    253.686   16   288.788   257.395   24   275.643   275.528   32   272.942   273.466
 9   272.695    285.173   17   276.627   258.098   25   269.719   269.740   33   329.666   329.124
10   293.606    270.361   18   285.618   257.393   26   268.776   268.780   34   409.892   409.038

MASS FLOW AFTER I-PLANE SOLUTION OF CONTINUITY EQUATIONFOR P AND CORRECTION OF U VELOCITY

 I  HOT SIDE  COLD SIDE    I  HOT SIDE  COLD SIDE    I  HOT SIDE  COLD SIDE    I  HOT SIDE  COLD SIDE    I  HOT SIDE  COLD SIDE
 3    74.805     74.367   11   671.198   320.153   19   525.068   396.747   27   468.088   466.085   35   597.393   597.355
 4   220.149    225.494   12   502.915   476.185   20   658.772   303.277   28   468.062   468.048
 5   297.449    314.696   13   525.394   393.878   21   474.976   478.740   29   467.930   467.884
 6   350.899    385.762   14   630.349   239.372   22   511.242   501.601   30   465.968   466.097
 7   375.652    408.377   15   510.934   338.116   23   493.001   488.633   31   478.915   479.569
 8   507.953    254.057   16   641.752   301.025   24   469.494   468.923   32   485.083   485.139
 9   451.583    437.735   17   520.753   394.293   25   468.432   468.364   33   517.023   516.817
10   471.527    400.273   18   552.574   302.399   26   468.171   468.158   34   538.905   538.335

 SUM OF WEDGE MASS IMBALANCE          4.938

MASS FLOW AFTER EXACT SOLUTION OF CONTINUITY EQUATION USING WEDGES AND RING GEOMETRIES

 I  HOT SIDE  COLD SIDE    I  HOT SIDE  COLD SIDE    I  HOT SIDE  COLD SIDE    I  HOT SIDE  COLD SIDE    I  HOT SIDE  COLD SIDE
 3   120.681    110.037   11   651.114   376.156   19   651.209   376.363   27   513.643   513.629   35   513.632   513.640
 4   258.833    215.270   12   640.985   386.287   20   697.005   330.267   28   513.642   513.630
 5   354.161    281.416   13   654.331   372.941   21   581.973   445.299   29   513.649   513.623
 6   429.793    320.402   14   706.936   320.366   22   548.156   479.116   30   513.520   513.744
 7   506.748    318.701   15   653.310   373.962   23   533.254   494.018   31   513.524   513.745
 8   619.703    254.479   16   706.922   320.350   24   516.722   510.550   32   513.601   513.671
 9   611.694    313.528   17   653.134   374.138   25   514.006   513.266   33   513.606   513.664
10   624.684    351.558   18   706.641   320.631   26   513.683   513.599   34   513.622   513.650

MASS FLOW AFTER SOLUTION OF ENERGY EQUATION AND CORRECTION OF DENSITY

 I  HOT SIDE  COLD SIDE    I  HOT SIDE  COLD SIDE    I  HOT SIDE  COLD SIDE    I  HOT SIDE  COLD SIDE    I  HOT SIDE  COLD SIDE
 3    82.463     78.486   11   427.457   291.649   19   386.856   247.263   27   283.584   294.069   35   281.115   289.133
 4   175.525    151.081   12   416.942   298.664   20   412.761   212.404   28   281.075   296.787
 5   236.762    195.162   13   419.100   318.408   21   338.380   285.815   29   280.636   286.102
 6   258.451    219.865   14   447.468   233.308   22   317.128   303.186   30   280.556   286.427
 7   338.892    215.090   15   405.260   290.229   23   306.006   306.176   31   261.150   286.018
 8   415.021    191.534   16   439.765   218.075   24   292.502   308.002   32   284.144   292.613
 9   406.172    239.340   17   395.577   256.465   25   288.091   302.927   33   281.335   289.356
10   412.343    272.758   18   426.814   208.877   26   285.581   298.051   34   279.963   287.697

****      ****        ****        ****      ****        ****         ****       ****         ****          ****
 RECIR   PRESS DROP  PRIM H.T.  SEC H.T.  AVG OUTLET QUAL  SUM SOURCE  MAX SOURCE (  2 10 11)
5.3000    -4904.13    1329.32    719.99         .35848       4.9296       .0449
****      ****        ****        ****      ****        ****         ****       ****         ****          ****

AXIAL VEL VALUES *** ON HOT SIDE ( 23  5  5)  ON COLD SIDE( 23  5  9)  IN UBEND ( 32  5  5)  IN DOWNCOMER ( 23 10  5)
                            .72917                 .69189                  .47108                 -2.18376

RADIAL VEL VALUES *** IN SHROUD WINDOW (  6 10  5)  ABOVE DIV PLATE ( 21  5  7)  IN PREHEATER ( 16  5  8)  IN U-BEND SECT ( 32  5  4)
                              -.28014                       .12261                      .00392                       .05993

THERMAL VALUES AT ( 25  5  6) *** SEC ENTHALPY  WALL TEMP  PRIMARY TEMP  HEAT FLUX
                                   342130.94     270.77        288.51      .13462
```

Figure 6.4.1: THIRST OUTPUT - Iteration Summaries (Iteration 1)

```
ITERATION NUMBER =  2
MASS FLOWS AFTER SOLUTION OF MOMENTUM EQUATION FOR U VELOCITY
  I  HOT SIDE  COLD SIDE      I  HOT SIDE  COLD SIDE      I  HOT SIDE  COLD SIDE      I  HOT SIDE  COLD SIDE      I  HOT SIDE  COLD SIDE
  3   468.419   401.219      11   702.517   255.325      19   411.354   267.240      27   323.837   357.757      35  3159.196  3077.891
  4   378.759   324.157      12   702.115   447.883      20   724.337   199.838      28   319.077   349.213
  5   400.509   376.298      13   455.133   261.976      21   356.530   343.769      29   314.444   340.495
  6   457.959   510.220      14   772.121   218.188      22   509.315   522.611      30   309.757   329.338
  7   525.380   647.855      15   442.293   259.347      23   710.655   785.857      31   293.201   313.483
  8   370.085   136.392      16   760.070   206.687      24   361.453   415.671      32   350.628   364.981
  9   562.778   355.165      17   426.321   269.058      25   339.352   384.175      33   794.089   793.727
 10   632.766   402.383      18   744.293   199.686      26   330.523   369.231      34  1990.468  1958.166
MASS FLOW AFTER K-PLANE SOLUTION OF CONTINUITY EQUATIONFOR P AND CORRECTION OF U VELOCITY
  I  HOT SIDE  COLD SIDE      I  HOT SIDE  COLD SIDE      I  HOT SIDE  COLD SIDE      I  HOT SIDE  COLD SIDE      I  HOT SIDE  COLD SIDE
  3   111.415   101.136      11   544.778   236.203      19   443.271   169.722      27   323.804   357.692      35   834.822   792.108
  4   249.941   208.214      12   542.085   240.667      20   514.438   168.134      28   319.096   349.233
  5   330.242   261.681      13   498.677   194.834      21   409.999   243.348      29   314.992   340.779
  6   373.748   272.149      14   606.114   187.342      22   456.565   368.494      30   316.933   336.925
  7   393.835   215.862      15   476.327   183.702      23   517.042   488.377      31   311.965   338.289
  8   420.517   136.596      16   592.719   175.673      24   372.562   426.299      32   377.926   336.609
  9   467.772   185.932      17   459.183   174.740      25   340.159   385.399      33   589.571   587.378
 10   513.090   215.873      18   574.068   168.766      26   330.586   369.452      34   804.486   734.173
MASS FLOW AFTER I-PLANE SOLUTION OF CONTINUITY EQUATIONFOR P AND CORRECTION OF U VELOCITY
  I  HOT SIDE  COLD SIDE      I  HOT SIDE  COLD SIDE      I  HOT SIDE  COLD SIDE      I  HOT SIDE  COLD SIDE      I  HOT SIDE  COLD SIDE
  3   121.605   105.066      11   714.499   245.153      19   538.021   271.300      27   383.857   434.084      35   412.058   397.045
  4   228.509   184.888      12   578.463   323.340      20   687.440   169.663      28   380.347   425.540
  5   303.484   234.153      13   591.915   301.145      21   487.831   398.709      29   378.517   418.069
  6   358.521   247.658      14   691.541   163.786      22   614.059   548.815      30   381.156   414.110
  7   386.227   204.831      15   568.386   279.596      23   470.378   469.661      31   420.183   455.961
  8   496.865   136.917      16   685.358   173.935      24   416.421   473.063      32   462.780   489.736
  9   554.461   328.511      17   555.667   270.424      25   395.205   457.236      33   555.615   565.295
 10   582.512   313.697      18   687.109   170.238      26   388.296   444.297      34   564.163   561.461
SUM OF RING MASS IMBALANCE         5.339
MASS FLOW AFTER EXACT SOLUTION OF CONTINUITY EQUATION USING WEDGES AND RING GEOMETRIES
  I  HOT SIDE  COLD SIDE      I  HOT SIDE  COLD SIDE      I  HOT SIDE  COLD SIDE      I  HOT SIDE  COLD SIDE      I  HOT SIDE  COLD SIDE
  3    94.084    77.650      11   784.338   242.934      19   636.606   388.666      27   476.125   551.147      35   521.053   506.219
  4   217.795   178.705      12   627.636   395.636      20   850.551   176.721      28   478.832   546.440
  5   311.561   235.898      13   656.313   370.959      21   539.933   487.339      29   482.362   544.910
  6   392.291   288.774      14   836.736   190.536      22   554.395   472.877      30   487.637   539.635
  7   478.378   324.199      15   649.586   377.686      23   509.440   517.832      31   490.895   536.377
  8   736.050   138.132      16   846.379   180.893      24   474.411   552.861      32   497.423   529.849
  9   589.244   355.509      17   649.137   378.135      25   470.380   556.892      33   508.479   516.793
 10   688.095   367.862      18   850.877   176.395      26   473.163   554.109      34   516.563   516.709
MASS FLOW AFTER SOLUTION OF ENERGY EQUATION AND CORRECTION OF DENSITY
  I  HOT SIDE  COLD SIDE      I  HOT SIDE  COLD SIDE      I  HOT SIDE  COLD SIDE      I  HOT SIDE  COLD SIDE      I  HOT SIDE  COLD SIDE
  3   114.061    97.677      11   907.070   301.738      19   591.359   503.435      27   353.611   806.352      35   373.169   757.512
  4   260.410   217.132      12   701.917   487.103      20   823.303   240.583      28   349.646   811.199
  5   369.592   302.928      13   713.888   415.897      21   479.222   647.108      29   344.882   810.261
  6   462.005   364.331      14   896.935   244.638      22   499.989   645.901      30   333.505   803.073
  7   578.415   425.839      15   653.752   441.924      23   444.845   715.221      31   327.911   793.625
  8   863.620   176.572      16   862.662   240.360      24   385.433   777.287      32   340.349   773.584
  9   652.797   436.322      17   618.955   476.843      25   366.725   796.832      33   359.461   766.265
 10   704.398   451.293      18   838.534   239.253      26   359.196   803.727      34   368.181   760.811

****      ****        ****       ****      ****         ****        ****       ****       ****           ****
 RECIR  PRESS DROP   PRIM H.T.   SEC H.T.   AVG OUTLET QUAL   SUM SOURCE   MAX SOURCE ( 35   8   4)
5.3000  -18955.35    -162.76     -159.17        -.08653       23.3724          .0615
****      ****        ****       ****      ****         ****        ****       ****       ****           ****

AXIAL VEL VALUES *** ON HOT SIDE ( 23   5   5)  ON COLD SIDE( 23   5   9)  IN UBEND ( 32   5   5)  IN DOWNCOMER ( 23 10   5)
                           1.17595                     .98759                 .52110                   -2.18366

RADIAL VEL VALUES *** IN SHROUD WINDOW (  6 10   5)  ABOVE DIV PLATE ( 21   5   7)  IN PREHEATER ( 16   5   8)  IN U-BEND SECT ( 32   5   4)
                               -.45646                      .17208                     .27371                      .12252

THERMAL VALUES AT ( 25   5   6) *** SEC ENTHALPY  WALL TEMP  PRIMARY TEMP  HEAT FLUX
                                     138857.82     271.10        295.45     .18515
```

Figure 6.4.2: THIRST OUTPUT - Iteration Summaries (Iteration 2)

```
ITERATION NUMBER = 58

NEW ESTIMATE OF RECIRCULATION RATIO =  5.39756
 MASS FLOWS AFTER SOLUTION OF MOMENTUM EQUATION FOR U VELOCITY

  I  HOT SIDE  COLD SIDE    I  HOT SIDE  COLD SIDE    I  HOT SIDE  COLD SIDE    I  HOT SIDE  COLD SIDE    I  HOT SIDE  COLD SIDE
  3    94.975      3.862   11   913.237    130.391   19   913.017    130.691   27   521.492    521.995   35   512.489    531.610
  4   249.978     12.002   12   913.118    130.794   20   913.144    130.390   28   508.254    535.224
  5   405.164     17.922   13   913.105    130.688   21   913.012    130.321   29   501.537    541.933
  6   571.966     15.272   14   913.217    130.364   22   873.333    170.232   30   497.895    545.564
  7   777.140    -21.578   15   913.089    130.561   23   801.615    241.958   31   494.608    548.884
  8   913.199    -22.798   16   913.203    130.388   24   675.635    367.905   32   493.436    550.059
  9   913.079     29.024   17   913.041    130.635   25   592.850    450.663   33   495.316    546.297
 10   913.037     79.928   18   913.185    130.480   26   546.729    496.769   34   502.954    540.976
 MASS FLOW AFTER K-PLANE SOLUTION OF CONTINUITY EQUATIONFOR P AND CORRECTION OF U VELOCITY

  I  HOT SIDE  COLD SIDE    I  HOT SIDE  COLD SIDE    I  HOT SIDE  COLD SIDE    I  HOT SIDE  COLD SIDE    I  HOT SIDE  COLD SIDE
  3    95.080      3.827   11   913.149    130.325   19   913.031    130.538   27   521.492    521.996   35   512.399    531.506
  4   250.002     11.766   12   913.140    130.323   20   913.072    130.473   28   508.254    535.224
  5   405.186     17.493   13   913.121    130.266   21   913.021    130.534   29   501.537    541.933
  6   572.006     14.420   14   913.166    130.278   22   873.359    170.228   30   497.900    545.571
  7   777.098    -22.808   15   913.103    130.247   23   801.613    241.955   31   494.608    548.883
  8   913.160    -22.794   16   913.161    130.307   24   675.634    367.899   32   493.445    550.065
  9   913.153     28.274   17   913.054    130.349   25   592.849    450.665   33   495.318    548.291
 10   913.142     79.303   18   913.132    130.415   26   546.729    496.770   34   502.943    540.920
 MASS FLOW AFTER I-PLANE SOLUTION OF CONTINUITY EQUATIONFOR P AND CORRECTION OF U VELOCITY

  I  HOT SIDE  COLD SIDE    I  HOT SIDE  COLD SIDE    I  HOT SIDE  COLD SIDE    I  HOT SIDE  COLD SIDE    I  HOT SIDE  COLD SIDE
  3    95.133      3.936   11   912.896    130.198   19   912.985    130.031   27   521.322    521.778   35   512.187    531.253
  4   249.994     11.672   12   913.075    129.904   20   912.759    130.327   28   506.084    535.017
  5   405.153     17.310   13   913.090    129.978   21   912.960    130.001   29   501.374    541.741
  6   571.965     14.148   14   912.979    130.156   22   873.256    169.576   30   497.761    545.408
  7   777.065    -23.151   15   913.081    130.000   23   801.472    241.406   31   494.467    548.709
  8   913.070    -22.803   16   912.893    130.170   24   675.509    367.600   32   493.342    549.938
  9   913.131     27.871   17   913.023    130.007   25   592.697    450.417   33   495.196    546.139
 10   913.126     78.876   18   912.801    130.244   26   546.564    496.542   34   502.804    540.737
SUM OF RING MASS IMBALANCE          .011
 MASS FLOW AFTER EXACT SOLUTION OF CONTINUITY EQUATION USING WEDGES AND RING GEOMETRIES

  I  HOT SIDE  COLD SIDE    I  HOT SIDE  COLD SIDE    I  HOT SIDE  COLD SIDE    I  HOT SIDE  COLD SIDE    I  HOT SIDE  COLD SIDE
  3    95.051      3.774   11   913.094    130.269   19   913.314    130.349   27   521.437    521.926   35   512.151    531.212
  4   249.654     11.046   12   913.122    130.240   20   912.992    130.471   28   508.202    535.161
  5   404.937     16.793   13   913.130    130.233   21   912.994    130.369   29   501.408    541.375
  6   571.856     13.844   14   913.128    130.235   22   873.324    170.039   30   497.650    545.513
  7   777.068    -23.073   15   913.121    130.242   23   801.571    241.732   31   494.551    548.812
  8   913.072    -22.799   16   913.081    130.282   24   675.586    367.777   32   493.360    549.983
  9   913.128     28.176   17   913.063    130.300   25   592.792    450.571   33   495.239    546.154
 10   913.125     79.203   18   912.980    130.363   26   546.671    496.692   34   502.723    540.640
 MASS FLOW AFTER SOLUTION OF ENERGY EQUATION AND CORRECTION OF DENSITY

  I  HOT SIDE  COLD SIDE    I  HOT SIDE  COLD SIDE    I  HOT SIDE  COLD SIDE    I  HOT SIDE  COLD SIDE    I  HOT SIDE  COLD SIDE
  3    95.076      3.775   11   913.270    130.267   19   913.067    130.347   27   521.471    521.913   35   512.225    531.203
  4   249.718     11.046   12   913.292    130.239   20   912.937    130.530   28   508.235    535.147
  5   405.037     16.792   13   913.281    130.231   21   913.049    130.406   29   501.520    541.860
  6   571.991     13.844   14   913.267    130.230   22   873.378    170.076   30   497.861    545.496
  7   777.227    -23.070   15   913.239    130.238   23   801.624    241.808   31   494.582    548.793
  8   913.234    -22.798   16   913.175    130.276   24   675.635    367.774   32   493.412    549.962
  9   913.300     28.176   17   913.129    130.295   25   592.833    450.562   33   495.247    546.127
 10   913.305     79.203   18   913.038    130.383   26   546.708    496.680   34   502.766    540.510

****      ****       ****       ****       ****       ****           ****        ****         ****        ****
 RECIR   PRESS DROP  PRIM H.T.  SEC H.T.   AVG OUTLET QUAL  SUM SOURCE  MAX SOURCE ( 10   9 11)
5.3976   -11722.58      663.28     661.38        .15737        .0273        .0002
****      ****       ****       ****       ****       ****           ****        ****         ****        ****

AXIAL VEL VALUES *** ON HOT SIDE ( 23  5  5)  ON COLD SIDE( 23  5  9)  IN UBEND ( 32  5  5)  IN DOWNCOMER ( 23 10  5)
                            4.44787                 .98719             2.74394                   -2.36392

RADIAL VEL VALUES *** IN SHROUD WINDOW (  6 10  5)  ABOVE DIV PLATE ( 21  5  7)  IN PREHEATER ( 15  5  8)  IN U-BEND SECT ( 32  5  4)
                                -.83353                  .81779                 .29242                    .66497

THERMAL VALUES AT ( 28  5  6) *** SEC ENTHALPY  WALL TEMP  PRIMARY TEMP  HEAT FLUX
                                    185044.34     273.38       296.07     .17256
```

Figure 6.4.3: THIRST OUTPUT - Iteration Summaries (Iteration 58)

ITERATION NUMBER = 59

NEW ESTIMATE OF RECIRCULATION RATIO = 5.39673

MASS FLOWS AFTER SOLUTION OF MOMENTUM EQUATION FOR U VELOCITY

I	HOT SIDE	COLD SIDE	I	HOT SIDE	COLD SIDE	I	HOT SIDE	COLD SIDE	I	HOT SIDE	COLD SIDE	I	HOT SIDE	COLD SIDE
3	95.045	3.758	11	913.351	130.299	19	913.095	130.453	27	521.488	521.945	35	512.377	531.043
4	249.715	11.016	12	913.295	130.225	20	913.013	130.378	28	508.251	535.178			
5	404.997	16.581	13	913.326	130.336	21	913.048	130.153	29	501.538	541.892			
6	571.875	13.309	14	913.361	130.267	22	873.390	169.864	30	497.906	545.537			
7	776.999	-23.879	15	913.307	130.339	23	801.646	241.599	31	494.608	548.834			
8	913.293	-22.793	16	913.334	130.303	24	675.657	367.783	32	493.451	550.022			
9	913.276	28.271	17	913.196	130.410	25	592.854	450.591	33	495.319	548.233			
10	913.324	78.928	18	913.190	130.416	26	546.726	496.713	34	502.903	540.812			

MASS FLOW AFTER K-PLANE SOLUTION OF CONTINUITY EQUATIONFOR P AND CORRECTION OF U VELOCITY

I	HOT SIDE	COLD SIDE	I	HOT SIDE	COLD SIDE	I	HOT SIDE	COLD SIDE	I	HOT SIDE	COLD SIDE	I	HOT SIDE	COLD SIDE
3	95.084	3.806	11	913.317	130.275	19	913.087	130.499	27	521.468	521.945	35	512.366	531.120
4	249.729	11.211	12	913.318	130.249	20	913.067	130.527	28	508.251	535.178			
5	404.940	16.929	13	913.323	130.226	21	913.045	130.538	29	501.538	541.893			
6	571.639	13.983	14	913.344	130.230	22	873.379	170.071	30	497.906	545.537			
7	777.071	-23.018	15	913.307	130.231	23	801.649	241.763	31	494.614	548.840			
8	913.286	-22.796	16	913.312	130.274	24	675.657	367.772	32	493.457	550.025			
9	913.295	28.191	17	913.194	130.332	25	592.856	450.584	33	495.321	548.228			
10	913.310	79.229	18	913.193	130.422	26	546.727	496.711	34	502.917	540.779			

MASS FLOW AFTER I-PLANE SOLUTION OF CONTINUITY EQUATIONFOR P AND CORRECTION OF U VELOCITY

I	HOT SIDE	COLD SIDE	I	HOT SIDE	COLD SIDE	I	HOT SIDE	COLD SIDE	I	HOT SIDE	COLD SIDE	I	HOT SIDE	COLD SIDE
3	94.993	3.625	11	913.955	130.562	19	913.189	131.352	27	521.743	522.276	35	512.621	531.501
4	249.671	11.587	12	913.455	131.164	20	913.476	130.927	28	508.566	535.490			
5	405.115	17.496	13	913.463	131.024	21	913.146	131.276	29	501.786	542.187			
6	572.022	14.746	14	913.824	130.510	22	873.521	171.047	30	498.130	545.799			
7	777.232	-22.087	15	913.423	130.954	23	801.853	242.656	31	494.858	549.134			
8	913.546	-22.779	16	913.745	130.593	24	675.860	368.251	32	493.667	550.274			
9	913.351	29.282	17	913.311	131.184	25	593.091	450.964	33	495.611	548.567			
10	913.372	80.306	18	913.597	130.798	26	546.977	497.054	34	503.242	541.152			

SUM OF WEDGE MASS IMBALANCE .022

MASS FLOW AFTER EXACT SOLUTION OF CONTINUITY EQUATION USING WEDGES AND RING GEOMETRIES

I	HOT SIDE	COLD SIDE	I	HOT SIDE	COLD SIDE	I	HOT SIDE	COLD SIDE	I	HOT SIDE	COLD SIDE	I	HOT SIDE	COLD SIDE
3	95.087	3.851	11	912.981	130.246	19	912.981	130.246	27	521.402	521.824	35	512.187	531.039
4	249.857	11.593	12	912.981	130.246	20	912.981	130.246	28	508.162	535.065			
5	404.995	17.252	13	912.981	130.246	21	912.981	130.246	29	501.445	541.782			
6	571.793	14.203	14	912.981	130.246	22	873.314	169.913	30	497.808	545.418			
7	776.915	-22.979	15	912.981	130.246	23	801.571	241.655	31	494.513	548.714			
8	912.981	-22.844	16	912.981	130.246	24	675.589	367.638	32	493.347	549.880			
9	912.981	28.186	17	912.981	130.246	25	592.782	450.445	33	495.188	548.039			
10	912.981	79.217	18	912.981	130.246	26	546.647	496.580	34	502.719	540.508			

MASS FLOW AFTER SOLUTION OF ENERGY EQUATION AND CORRECTION OF DENSITY

I	HOT SIDE	COLD SIDE	I	HOT SIDE	COLD SIDE	I	HOT SIDE	COLD SIDE	I	HOT SIDE	COLD SIDE	I	HOT SIDE	COLD SIDE
3	95.082	3.851	11	912.894	130.246	19	912.945	130.243	27	521.388	521.837	35	512.144	531.048
4	249.833	11.593	12	912.899	130.246	20	912.954	130.277	28	508.147	535.078			
5	404.949	17.252	13	912.906	130.245	21	912.938	130.278	29	501.430	541.795			
6	571.726	14.200	14	912.898	130.244	22	873.275	169.945	30	497.736	545.433			
7	776.830	-22.980	15	912.900	130.244	23	801.542	241.680	31	494.562	548.729			
8	912.893	-22.844	16	912.913	130.242	24	675.566	367.655	32	493.334	549.694			
9	912.890	28.167	17	912.924	130.243	25	592.766	450.459	33	495.167	548.049			
10	912.889	79.217	18	912.934	130.244	26	546.632	496.593	34	502.687	540.520			

RECIR	PRESS DROP	PRIM H.T.	SEC H.T.	AVG OUTLET QUAL	SUM SOURCE	MAX SOURCE (7 10 9)
5.3967	-11626.75	663.24	661.26	.15737	.0192	.0002

AXIAL VEL VALUES *** ON HOT SIDE (23 5 5) 4.44737 ON COLD SIDE(23 5 9) .98685 IN UBEND (32 5 5) 2.74956 IN DOWNCOMER (23 10 5) -2.36092

RADIAL VEL VALUES *** IN SHROUD WINDOW (6 10 5) -.83325 ABOVE DIV PLATE (21 5 7) .81794 IN PREHEATER (18 5 8) .29226 IN U-BEND SECT (32 5 4) .66534

THERMAL VALUES AT (25 5 6) *** SEC ENTHALPY 185047.29 WALL TEMP 273.38 PRIMARY TEMP 296.07 HEAT FLUX .17256

Figure 6.4.4: THIRST OUTPUT - Iteration Summaries (Iteration 59)

ITERATION NUMBER = 60

NEW ESTIMATE OF RECIRCULATION RATIO = 5.39756

MASS FLOWS AFTER SOLUTION OF MOMENTUM EQUATION FOR U VELOCITY

I	HOT SIDE	COLD SIDE	I	HOT SIDE	COLD SIDE	I	HOT SIDE	COLD SIDE	I	HOT SIDE	COLD SIDE	I	HOT SIDE	COLD SIDE
3	94.983	3.872	11	913.132	130.364	19	913.016	130.669	27	521.504	521.994	35	512.179	530.689
4	249.932	12.012	12	913.011	130.642	20	913.115	130.378	28	508.263	535.228			
5	405.106	17.917	13	913.043	130.680	21	913.012	130.392	29	501.545	541.940			
6	571.931	15.232	14	913.155	130.351	22	673.344	170.245	30	497.906	545.573			
7	777.104	-21.694	15	913.047	130.518	23	801.626	241.949	31	494.626	548.893			
8	913.100	-22.819	16	913.121	130.384	24	675.659	367.879	32	493.461	550.060			
9	912.975	28.723	17	913.038	130.619	25	592.872	450.644	33	495.330	548.253			
10	912.940	79.918	18	913.108	130.459	26	546.746	496.760	34	502.655	540.703			

MASS FLOW AFTER K-PLANE SOLUTION OF CONTINUITY EQUATIONFOR P AND CORRECTION OF U VELOCITY

I	HOT SIDE	COLD SIDE	I	HOT SIDE	COLD SIDE	I	HOT SIDE	COLD SIDE	I	HOT SIDE	COLD SIDE	I	HOT SIDE	COLD SIDE
3	95.054	3.840	11	913.060	130.308	19	913.029	130.467	27	521.504	521.994	35	512.114	530.574
4	249.948	11.788	12	913.054	130.301	20	913.055	130.423	28	508.263	535.228			
5	405.110	17.517	13	913.055	130.266	21	913.023	130.492	29	501.546	541.940			
6	571.931	14.431	14	913.106	130.275	22	673.357	170.191	30	497.911	545.578			
7	777.015	-22.846	15	913.060	130.256	23	801.624	241.929	31	494.624	548.687			
8	913.080	-22.815	16	913.088	130.303	24	675.658	367.874	32	493.462	550.059			
9	913.062	28.247	17	913.049	130.342	25	592.870	450.647	33	495.310	548.238			
10	913.051	79.291	18	913.071	130.391	26	546.745	496.762	34	502.866	540.692			

MASS FLOW AFTER I-PLANE SOLUTION OF CONTINUITY EQUATIONFOR P AND CORRECTION OF U VELOCITY

I	HOT SIDE	COLD SIDE	I	HOT SIDE	COLD SIDE	I	HOT SIDE	COLD SIDE	I	HOT SIDE	COLD SIDE	I	HOT SIDE	COLD SIDE
3	95.103	3.947	11	912.865	130.210	19	912.982	129.994	27	521.334	521.777	35	512.300	531.401
4	249.938	11.705	12	913.016	129.991	20	912.780	130.276	28	508.093	535.020			
5	405.679	17.360	13	913.033	130.037	21	912.966	129.990	29	501.363	541.746			
6	571.895	14.209	14	912.959	130.185	22	873.271	169.579	30	497.770	545.413			
7	777.012	-23.132	15	913.037	130.034	23	801.495	241.393	31	494.478	548.708			
8	913.015	-22.821	16	912.886	130.186	24	675.534	367.575	32	493.349	549.923			
9	913.052	27.946	17	913.010	130.031	25	592.719	450.400	33	495.174	548.082			
10	913.044	78.956	18	912.806	130.235	26	546.580	496.535	34	502.719	540.616			

SUM OF RING MASS IMBALANCE .010

MASS FLOW AFTER EXACT SOLUTION OF CONTINUITY EQUATION USING WEDGES AND RING GEOMETRIES

I	HOT SIDE	COLD SIDE	I	HOT SIDE	COLD SIDE	I	HOT SIDE	COLD SIDE	I	HOT SIDE	COLD SIDE	I	HOT SIDE	COLD SIDE
3	95.026	3.797	11	913.077	130.287	19	913.017	130.346	27	521.444	521.919	35	512.155	531.208
4	249.604	11.093	12	913.059	130.304	20	912.936	130.427	28	508.226	535.158			
5	404.865	16.859	13	913.076	130.287	21	913.065	130.359	29	501.490	541.873			
6	571.791	13.911	14	913.105	130.258	22	873.337	170.026	30	497.853	545.511			
7	777.020	-23.022	15	913.082	130.282	23	801.592	241.772	31	494.558	548.605			
8	913.084	-22.810	16	913.071	130.293	24	675.611	367.752	32	493.391	549.973			
9	913.057	28.246	17	913.052	130.311	25	592.812	450.552	33	495.223	548.141			
10	913.054	79.281	18	912.989	130.374	26	546.684	496.680	34	502.732	540.631			

MASS FLOW AFTER SOLUTION OF ENERGY EQUATION AND CORRECTION OF DENSITY

I	HOT SIDE	COLD SIDE	I	HOT SIDE	COLD SIDE	I	HOT SIDE	COLD SIDE	I	HOT SIDE	COLD SIDE	I	HOT SIDE	COLD SIDE
3	95.055	3.797	11	913.332	130.288	19	913.173	130.342	27	521.504	521.933	35	512.188	531.211
4	249.683	11.093	12	913.304	130.306	20	913.083	130.421	28	508.264	535.168			
5	405.004	16.858	13	913.311	130.289	21	913.149	130.348	29	501.547	541.881			
6	571.975	13.911	14	913.326	130.257	22	873.467	170.031	30	497.907	545.517			
7	777.251	-23.024	15	913.293	130.281	23	801.702	241.785	31	494.610	548.810			
8	913.334	-22.809	16	913.271	130.289	24	675.696	367.772	32	493.444	549.977			
9	913.315	28.248	17	913.237	130.308	25	592.883	450.571	33	495.276	548.141			
10	913.319	79.281	18	913.158	130.371	26	546.746	496.697	34	502.771	540.633			

RECIR	PRESS DROP	PRIM H.T.	SEC H.T.	AVG OUTLET QUAL	SUM SOURCE	MAX SOURCE (10 9 11)
5.3976	-11720.64	663.26	661.34	.15736	.0233	.0602

AXIAL VEL VALUES *** ON HOT SIDE (23 5 5) 4.44723 ON COLD SIDE(23 5 9) .98733 IN UBEND (32 5 5) 2.74979 IN DOWNCOMER (23 10 5) -2.36408

RADIAL VEL VALUES *** IN SHROUD WINDOW (6 10 5) -.83373 ABOVE DIV PLATE (21 5 7) .81795 IN PREHEATER (16 5 8) .29235 IN U-BEND SECT (32 5 4) .66502

THERMAL VALUES AT (25 5 6) *** SEC ENTHALPY 185001.37 WALL TEMP 273.38 PRIMARY TEMP 296.06 HEAT FLUX .17256

Figure 6.4.5: THIRST OUTPUT - Iteration Summaries (Iteration 60)

AXIAL VELOCITY - M/SEC

K = 2

I \ J	2	3	4	5	6	7	8	9	10
3	[illegible]	3.993E-01	4.959E-01	4.126E-01	3.161E-01	2.762E-01	1.597E-01	-8.135E-02	-3.688E-01
4	[illegible]	9.598E-01	1.197E+00	9.947E-01	7.965E-01	7.122E-01	4.257E-01	-2.233E-01	-9.925E-01
5	[illegible]	1.452E+00	1.824E+00	1.462E+00	1.191E+00	1.097E+00	7.044E-01	-3.337E-01	-1.619E+00
6	[illegible]	1.857E+00	2.391E+00	1.796E+00	1.492E+00	1.402E+00	1.010E+00	-3.401E-01	-2.254E+00
7	[illegible]	2.238E+00	2.935E+00	1.991E+00	1.705E+00	1.638E+00	1.390E+00	-7.894E-02	-2.904E+00
8	[illegible]	2.650E+00	3.605E+00	2.065E+00	1.891E+00	1.760E+00	1.573E+00	8.322E-01	-3.546E+00
9	[illegible]	2.874E+00	3.935E+00	2.317E+00	2.068E+00	1.883E+00	1.651E+00	7.745E-01	-3.565E+00
10	[illegible]	2.962E+00	4.075E+00	2.621E+00	2.235E+00	1.995E+00	1.716E+00	8.165E-01	-3.463E+00
11	[illegible]	2.980E+00	4.116E+00	2.893E+00	2.406E+00	2.104E+00	1.777E+00	9.251E-01	-3.421E+00
12	[illegible]	3.032E+00	4.114E+00	3.140E+00	2.634E+00	2.279E+00	1.917E+00	1.103E+00	-3.379E+00
13	[illegible]	2.811E+00	3.733E+00	3.404E+00	2.953E+00	2.554E+00	2.230E+00	1.527E+00	-3.296E+00
14	[illegible]	2.937E+00	3.965E+00	3.750E+00	3.335E+00	2.909E+00	2.551E+00	1.929E+00	-3.170E+00
15	[illegible]	2.864E+00	3.760E+00	3.871E+00	3.601E+00	3.264E+00	3.010E+00	2.128E+00	-3.056E+00
16	[illegible]	3.169E+00	4.058E+00	4.190E+00	3.911E+00	3.546E+00	3.240E+00	2.434E+00	-2.951E+00
17	[illegible]	3.315E+00	4.125E+00	4.348E+00	4.143E+00	3.848E+00	3.616E+00	2.523E+00	-2.853E+00
18	[illegible]	3.602E+00	4.425E+00	4.644E+00	4.409E+00	4.073E+00	3.775E+00	2.794E+00	-2.762E+00
19	[illegible]	3.914E+00	4.619E+00	4.825E+00	4.617E+00	4.325E+00	4.089E+00	2.826E+00	-2.682E+00
20	[illegible]	4.236E+00	4.883E+00	5.022E+00	4.767E+00	4.438E+00	4.127E+00	3.007E+00	-2.608E+00
21	[illegible]	4.616E+00	5.002E+00	5.040E+00	4.784E+00	4.490E+00	4.240E+00	2.900E+00	-2.554E+00
22	[illegible]	4.593E+00	4.955E+00	4.993E+00	4.761E+00	4.487E+00	4.247E+00	2.912E+00	-2.514E+00
23	[illegible]	4.437E+00	4.852E+00	4.915E+00	4.721E+00	4.462E+00	4.179E+00	3.005E+00	-2.475E+00
24	[illegible]	4.215E+00	4.525E+00	4.597E+00	4.475E+00	4.293E+00	4.062E+00	2.782E+00	-2.41[illegible]E+00
25	[illegible]	4.097E+00	4.308E+00	4.351E+00	4.253E+00	4.100E+00	3.898E+00	2.607E+00	-2.352E+00
26	[illegible]	4.151E+00	4.279E+00	4.284E+00	4.183E+00	4.039E+00	3.853E+00	2.563E+00	-2.307E+00
27	[illegible]	4.305E+00	4.378E+00	4.353E+00	4.243E+00	4.102E+00	3.925E+00	2.614E+00	-2.273E+00
28	[illegible]	4.510E+00	4.556E+00	4.516E+00	4.401E+00	4.261E+00	4.092E+00	2.734E+00	-2.249E+00
29	[illegible]	4.691E+00	4.736E+00	4.720E+00	4.642E+00	4.536E+00	4.391E+00	2.986E+00	-2.235E+00
30	[illegible]	4.527E+00	4.662E+00	4.830E+00	4.913E+00	5.004E+00	5.063E+00	3.779E+00	-2.223E+00
31	[illegible]	3.471E+00	4.121E+00	4.554E+00	4.864E+00	5.259E+00	5.851E+00	5.721E+00	-2.226E+00
32	[illegible]	2.791E+00	3.123E+00	3.522E+00	3.930E+00	4.081E+00	4.669E+00	7.929E+00	-2.224E+00
33	[illegible]	1.978E+00	1.959E+00	1.922E+00	2.040E+00	2.647E+00	5.217E+00	6.513E+00	-2.224E+00
34	[illegible]	9.242E-01	6.714E-01	1.149E+00	1.684E+00	2.604E+00	5.382E+00	8.589E+00	-2.223E+00
35	[illegible]	7.490E-01	7.525E-01	1.078E+00	1.666E+00	2.637E+00	5.455E+00	8.544E+00	-2.223E+00
36	[illegible]	7.570E-01	7.605E-01	1.085E+00	1.691E+00	2.641E+00	5.452E+00	6.532E+00	-2.224E+00

K = 3

I \ J	2	3	4	5	6	7	8	9	10
3	1.230E-01	2.153E-01	3.415E-01	3.973E-01	2.833E-01	2.442E-01	1.396E-01	-8.514E-02	-3.515E-01
4	3.394E-01	6.476E-01	9.414E-01	9.421E-01	7.383E-01	6.573E-01	3.991E-01	-2.104E-01	-9.312E-01
5	5.093E-01	1.056E+00	1.530E+00	1.399E+00	1.132E+00	1.046E+00	6.954E-01	-2.865E-01	-1.512E+00
6	9.912E-01	1.370E+00	2.124E+00	1.756E+00	1.461E+00	1.387E+00	1.037E+00	-2.551E-01	-2.116E+00
7	1.735E+00	1.789E+00	2.722E+00	1.986E+00	1.719E+00	1.663E+00	1.427E+00	1.523E-02	-2.768E+00
8	2.187E+00	2.253E+00	3.384E+00	2.053E+00	1.910E+00	1.786E+00	1.609E+00	8.686E-01	-3.436E+00
9	2.211E+00	2.402E+00	3.685E+00	2.291E+00	2.087E+00	1.910E+00	1.677E+00	7.803E-01	-3.411E+00
10	2.165E+00	2.462E+00	3.793E+00	2.570E+00	2.252E+00	2.019E+00	1.733E+00	8.082E-01	-3.381E+00
11	2.099E+00	2.317E+00	3.805E+00	2.819E+00	2.415E+00	2.124E+00	1.787E+00	9.152E-01	-3.348E+00
12	2.024E+00	2.327E+00	3.787E+00	3.037E+00	2.629E+00	2.291E+00	1.922E+00	1.096E+00	-3.312E+00
13	1.963E+00	2.224E+00	3.421E+00	3.276E+00	2.924E+00	2.552E+00	2.223E+00	1.531E+00	-3.239E+00
14	1.627E+00	2.249E+00	3.577E+00	3.611E+00	3.297E+00	2.901E+00	2.550E+00	1.940E+00	-3.121E+00
15	1.625E+00	2.371E+00	3.468E+00	3.730E+00	3.554E+00	3.249E+00	3.008E+00	2.135E+00	-3.012E+00
16	1.533E+00	2.642E+00	3.758E+00	4.045E+00	3.865E+00	3.534E+00	3.241E+00	2.447E+00	-2.907E+00
17	2.073E+00	2.944E+00	3.863E+00	4.214E+00	4.097E+00	3.833E+00	3.618E+00	2.532E+00	-2.612E+00
18	2.077E+00	3.159E+00	4.144E+00	4.538E+00	4.366E+00	4.063E+00	3.783E+00	2.610E+00	-2.723E+00
19	2.820E+00	3.615E+00	4.382E+00	4.709E+00	4.584E+00	4.323E+00	4.103E+00	2.643E+00	-2.646E+00
20	2.918E+00	3.914E+00	4.657E+00	4.921E+00	4.746E+00	4.445E+00	4.150E+00	3.034E+00	-2.578E+00
21	3.974E+00	4.408E+00	4.840E+00	4.973E+00	4.779E+00	4.508E+00	4.271E+00	2.928E+00	-2.527E+00
22	3.983E+00	4.388E+00	4.794E+00	4.919E+00	4.747E+00	4.496E+00	4.271E+00	2.933E+00	-2.498E+00
23	3.643E+00	4.234E+00	4.687E+00	4.628E+00	4.690E+00	4.456E+00	4.190E+00	3.013E+00	-2.464E+00
24	3.745E+00	4.090E+00	4.408E+00	4.523E+00	4.437E+00	4.270E+00	4.054E+00	2.777E+00	-2.402E+00
25	3.788E+00	4.017E+00	4.230E+00	4.300E+00	4.224E+00	4.084E+00	3.892E+00	2.604E+00	-2.346E+00
26	3.953E+00	4.097E+00	4.226E+00	4.250E+00	4.166E+00	4.033E+00	3.855E+00	2.566E+00	-2.344E+00
27	4.174E+00	4.264E+00	4.338E+00	4.329E+00	4.235E+00	4.102E+00	3.934E+00	2.622E+00	-2.273E+00
28	4.414E+00	4.475E+00	4.521E+00	4.497E+00	4.396E+00	4.264E+00	4.103E+00	2.743E+00	-2.251E+00
29	4.609E+00	4.658E+00	4.702E+00	4.696E+00	4.629E+00	4.530E+00	4.392E+00	2.986E+00	-2.237E+00
30	4.447E+00	4.497E+00	4.613E+00	4.747E+00	4.864E+00	4.960E+00	5.027E+00	3.757E+00	-2.230E+00
31	2.734E+00	3.324E+00	3.943E+00	4.400E+00	4.741E+00	5.151E+00	5.733E+00	5.708E+00	-2.227E+00
32	2.563E+00	2.729E+00	3.009E+00	3.362E+00	3.748E+00	3.879E+00	4.446E+00	7.831E+00	-2.225E+00
33	1.977E+00	1.954E+00	1.916E+00	1.856E+00	1.945E+00	2.484E+00	4.975E+00	6.439E+00	-2.224E+00
34	7.906E-01	8.152E-01	8.609E-01	1.126E+00	1.632E+00	2.458E+00	5.117E+00	8.506E+00	-2.224E+00
35	7.512E-01	6.832E-01	7.161E-01	1.059E+00	1.652E+00	2.496E+00	5.171E+00	6.459E+00	-2.223E+00
36	7.562E-01	6.508E-01	7.235E-01	1.065E+00	1.657E+00	2.500E+00	5.169E+00	8.447E+00	-2.224E+00

Figure 6.5: THIRST OUTPUT - Detailed Output (Velocity Field)

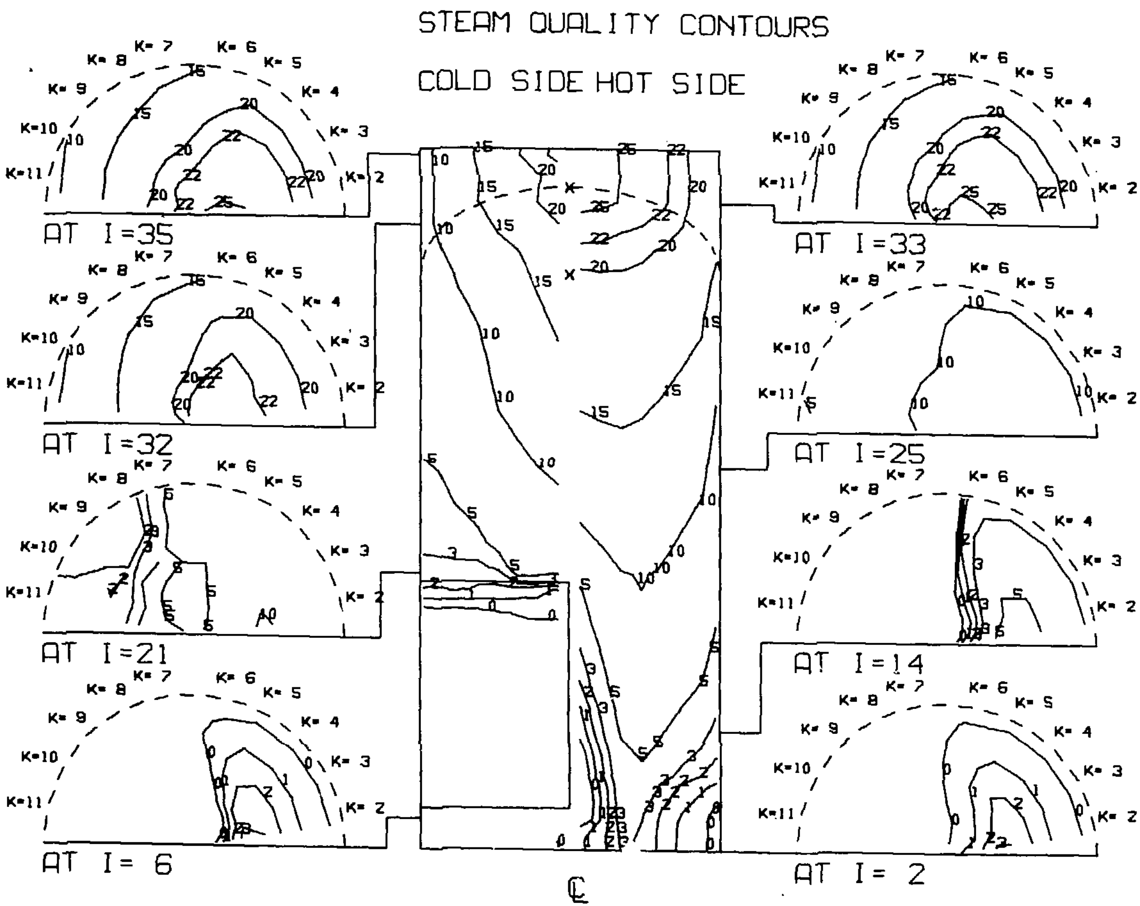

Figure 6.6.1: THIRST OUTPUT - Composite Plots
(Quality Distribution)

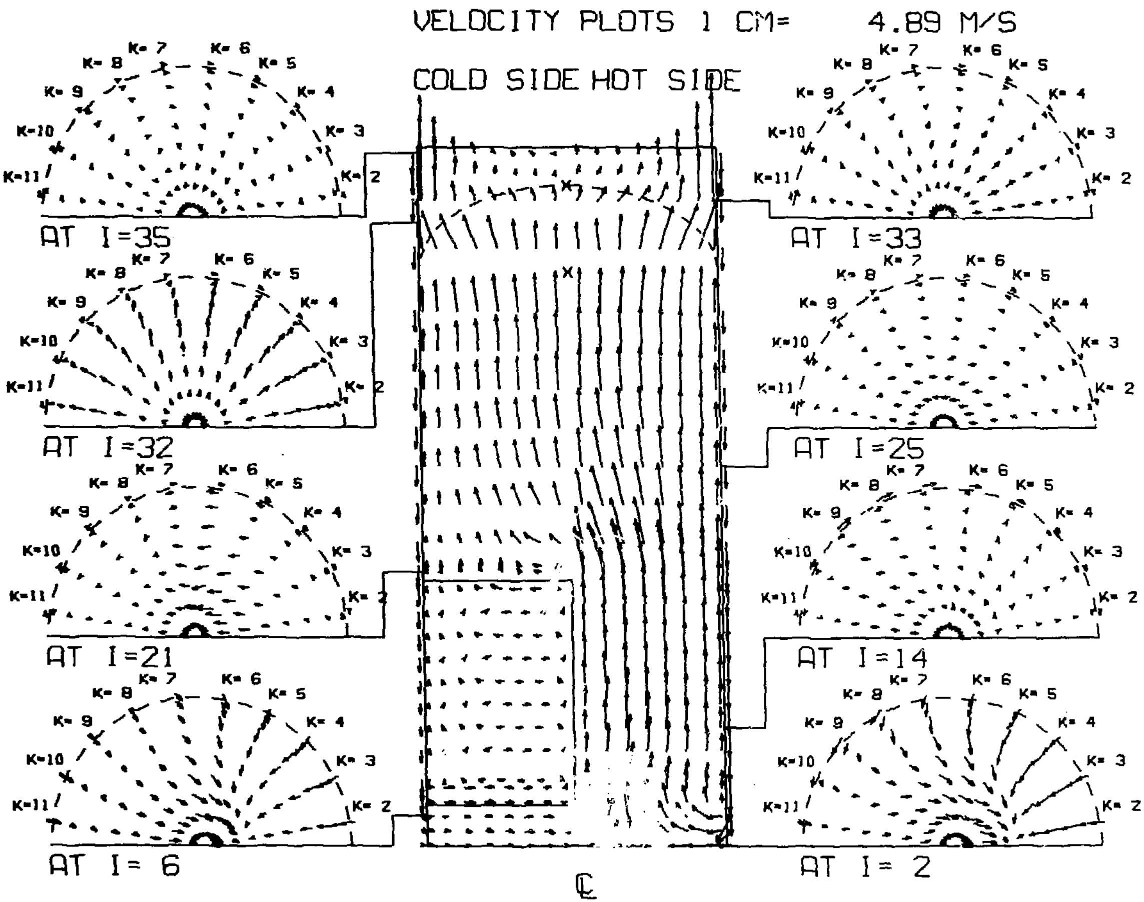

Figure 6.6.2: THIRST OUTPUT - Composite Plots
(Velocity Distribution)

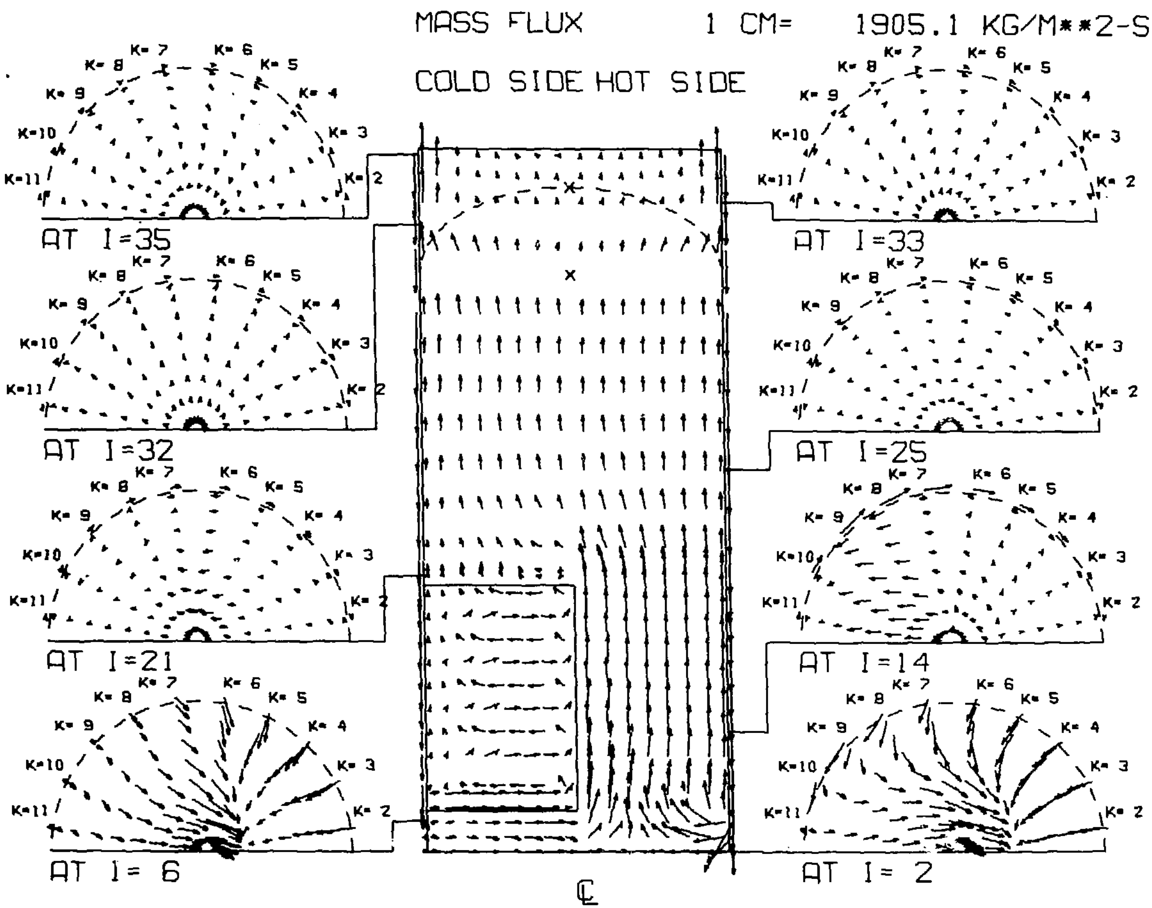

Figure 6.6.3: THIRST OUTPUT - Composite Plots
(Mass Flux Distribution)

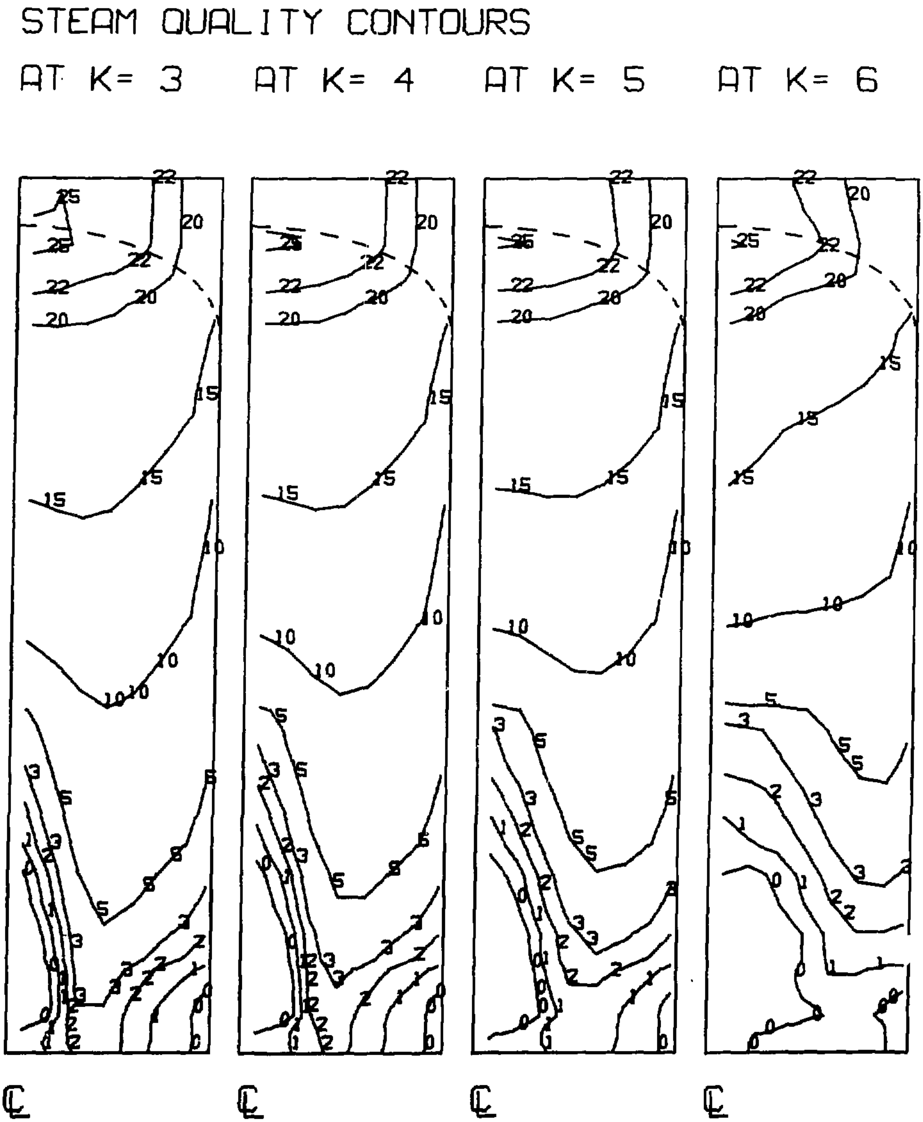

Figure 6.7.1: THIRST OUTPUT - Radial Plane Plots
(Quality Distribution)

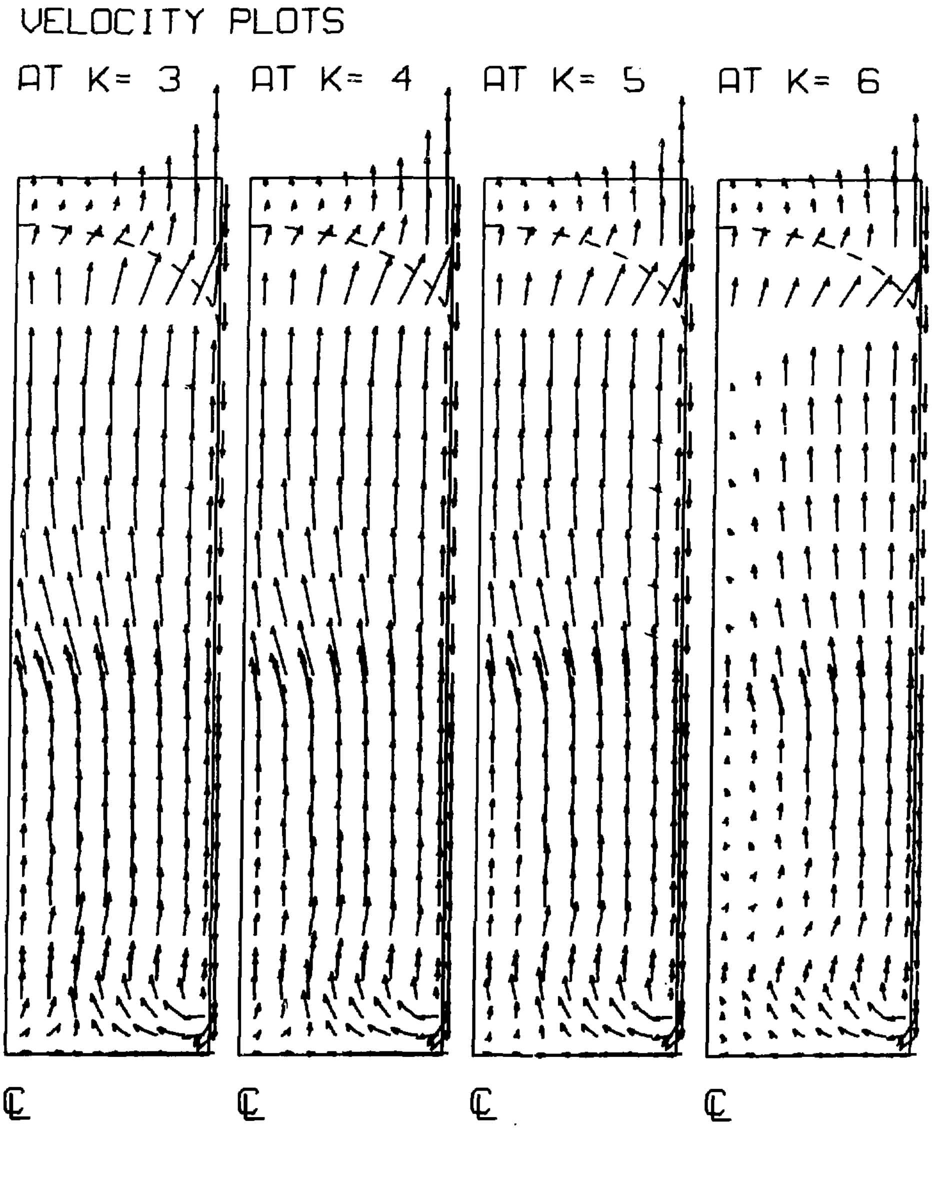

Figure 6.7.2: THIRST OUTPUT - Radial Plane Plots
(Velocity Distribution)

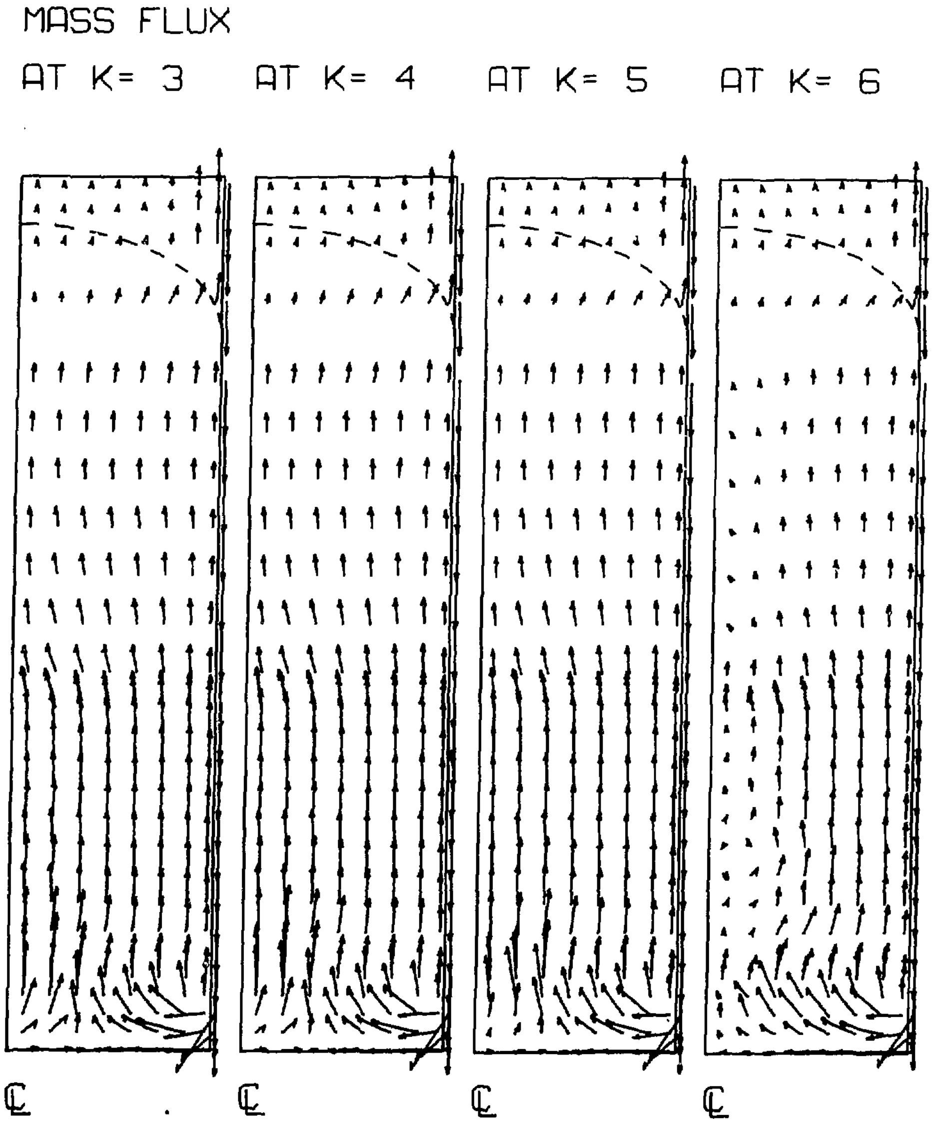

Figure 6.7.3: THIRST OUTPUT - Radial Plane Plots
(Mass Flux Distribution)

7. THERMAL-HYDRAULIC DATA

This chapter details the content and sources of (i) the thermodynamic property data for light and heavy water, and (ii) the empirical correlations used in the THIRST code. Normally the user will not change these. However, if it is desired to investigate the possible effect of introducing different correlations, this may be accomplished by simple coding changes to the routines mentioned below.

The user can easily insert his own property functions to cover different temperature and pres: ure ranges or different fluids. Pertinent information related to each property or parameter calculated in PROPRTY is listed in Table 7.1.

7.1 Thermodynamic Properties

Heavy water and light water saturation and subcooled properties* as well as property-related parameters are calculated in the function subprogram PROPRTY. Saturation properties are computed from polynomial functions of user-specified saturation pressures** whereas subcooled properties are calculated from polynomial functions of temperature and/or enthalpy.

The user can easily insert his own property functions to cover different temperature and pressure ranges or different fluids. Pertinent information related to each property or parameter calculated in PROPRTY is listed in Table 7.1.

* Heavy water primary properties are based on an AECL proprietary program. Light water secondary properties are based on the ASME steam tables.

** THIRST is set up to handle a two-phase primary fluid. For steam generators which have a subcooled primary fluid entering the tube bundle, the primary inlet pressure is specified rather than a saturation pressure. The subcooling is specified by defining a negative thermodynamic quality.

TABLE 7.1: Fluid Properties and Parameters

PROPERTY OR PARAMETER	FORTRAN NAME IN PROPRTY	ACCURACY OF POLYNOMIAL EXPRESSION (%)	COMMENTS
<u>Secondary Fluid Saturation Properties</u>:			
Pressure (MPa)	PSEC	specified by user	- Secondary Fluid Saturation Properties are expressed as polynomial functions of the user-specified secondary saturation pressure PSEC. Each function is valid over the pressure range of 4 MPa to 6 MPa. The properties are calculated in the function subprogram PROPRTY, ENTRY PROP1.
Liquid Density (kg/m^3)	DEN	0.00	
Steam Density (kg/m^3)	DENSM	0.01	
Saturation Temperature (°C)	TSAT	0.03	
Enthalpy of Vaporization (J/kg)	ALAT	0.01	
Liquid Saturation Enthalpy (J/kg)	ENSS	0.01	- DTDP is the derivative of the TSAT versus PSEC expression.
Liquid Viscosity (kg·m^{-1}·s^{-1})	AMUS	0.05	- DHDP is the derivative of the ENSS versus PSEC expression.
Liquid Specific Heat (J·kg^{-1}·°C^{-1})	CPWS	0.00	
Liquid Prandtl Number	PRWS	0.02	
Steam Viscosity (kg·m^{-1}·s^{-1})	AMUG	0.00	
Surface Tension (N/m)	STEN	0.02	
Change in Saturation Temperature per Unit Change in Pressure (°C/Pa)	DTDP	--	

TABLE 7.1: Fluid Properties and Parameters (Cont'd)

PROPERTY OR PARAMETER	FORTRAN NAME IN PROPRTY	ACCURACY OF POLYNOMIAL EXPRESSION (%)	COMMENTS
Change in Saturation Liquid Enthalpy per Unit Change in Pressure	DHDP		
Chen Correlation Parameters:	AKBO XTTK		- The Chen correlation parameters are defined in Section 7.3. The two parameters are expressed as functions of various saturation properties.
<u>Primary Fluid Saturation Properties (Heavy Water):</u>			
Pressure (MPa)	PPRI	user-specified	- Primary Fluid Saturation Properties are expressed as polynomial functions of the user-specified primary saturation pressure, PPRI. Each function is valid for heavy water over the pressure range of 7 MPa to 11 MPa. The properties are calculated in PROPRTY, ENTRY PROP1.
Saturation Temperature (°C)	TSATU	0.01	
Liquid Saturation Enthalpy (J/kg)	ENPS	0.02	
Enthalpy of Vaporization (J/kg)	ALATU	0.03	
Liquid Specific Volume (m^3/kg)	VFU	0.07	
Steam Specific Volume (m^3/kg)	VGU	0.47	

TABLE 7.1: Fluid Properties and Parameters (Cont'd)

PROPERTY OR PARAMETER	FORTRAN NAME IN PROPRTY	ACCURACY OF POLYNOMIAL EXPRESSION (%)	COMMENTS
Feedwater Subcooled Properties:			
Feedwater Temperature (°C)	TINC	user-specified	- The subcooled feedwater properties are calculated from the user-specified temperatures TINC and TRH. The properties are calculated in PROPRTY, ENTRY PROP1 and are valid for the temperature range of 150°C to saturation.
Reheater Drains Temperature (°C)	TRH	user-specified	
Feedwater Enthalpy (J/kg)	ENFW	0.1 at 5 MPa 0.2 at 4 to 6 MPa	
Reheater Drains Enthalpy (J/kg)	ENRH	0.1 at 5 MPa 0.2 at 4 to 6 MPa	
Feedwater Density (kg/m^3)	DENC	0.1 at 5 MPa 0.2 at 4 to 6 MPa	

TABLE 7.1: Fluid Properties and Parameters (Cont'd)

PROPERTY OR PARAMETER	FORTRAN NAME IN PROPRTY	ACCURACY OF POLYNOMIAL EXPRESSION (%)	COMMENTS
<u>Primary Subcooled Properties (Heavy Water):</u>			
Temperature (°C)	PROP (ENTRY PROP2)	0.01 at 9 MPa 0.30 at 7 to 11 MPa	- The primary temperature and the heat transfer coefficient parameter are calculated from polynomial functions of enthalpy. They are valid over the temperature range of 245°C to saturation. - The heat transfer coefficient parameter (RCONVA) is defined in Section 7.3.
Heat Transfer Coefficient Parameter, RCONVA $\left[(W\cdot m^{-1}\cdot {}^\circ C^{-1})^{0.67}\ (kg\cdot m^{-1}\cdot s^{-1})^{-0.47}\ (J\cdot kg^{-1}\cdot {}^\circ C^{-1})^{0.33}\right]$	PROP (ENTRY PROP3)	0.12 at 9 MPa 0.50 at 7 to 11 MPa	
<u>Secondary Subcooled Properties (Light Water):</u>			
Liquid Viscosity $(kg\cdot m^{-1}\cdot s^{-1})$	PROP (ENTRY PROP4)	0.96 at 5 MPa 2.5 at 4 to 6 MPa	- All subcooled properties (ENTRY PROP4 to PROP8 inclusive) are calculated as polynomial functions of enthalpy and are valid over the temperature range of 150°C to saturation.

TABLE 7.1: Fluid Properties and Parameters (Cont'd)

PROPERTY OR PARAMETER	FORTRAN NAME IN PROPRTY	ACCURACY OF POLYNOMIAL EXPRESSION (%)	COMMENTS
Temperature (°C)	PROP (ENTRY PROP5)	0.1 at 5 MPa 0.1 at 4 to 6 MPa	
Liquid Specific Heat ($J \cdot kg^{-1} \cdot {}^\circ C^{-1}$)	PROP (ENTRY PROP6)	0.3 at 5 MPa 0.6 at 4 to 6 MPa	
Liquid Prandtl Number	PROP (ENTRY PROP7)	0.5 at 5 MPa 1.1 at 4 to 6 MPa	
Liquid Density (kg/m^3)	PROP (ENTRY PROP8)	0.1 at 5 MPa 0.2 at 4 to 6 MPa	
Derivative of Saturation Pressure with Respect to Temperature for Chen Correlation ($Pa \cdot {}^\circ C^{-1}$), (Section 7.3).	PROP (ENTRY PROP9)		

7.2 Range of Application

The thermal-hydraulic data in the THIRST code is limited to the following range of operating conditions:

<u>Primary</u> - heavy water; 7 MPa to 11 MPa inlet pressure; subcooled to two-phase inlet (the overall temperature drop should be such that the outlet temperature is not less than 245°C

<u>Secondary</u> - light water; 4 MPa to 6 MPa mean pressure; feedwater temperature range of 150°C to saturation

If it becomes necessary to investigate different fluids or conditions outside of the above ranges, the user must redefine the appropriate property polynomial functions in the PROPRTY subprogram.

7.3 Empirical Correlations for Flow and Heat Transfer

All the fluid flow and heat transfer correlations used in THIRST are given in Tables 7.2 to 7.6.

The secondary side smooth bundle friction factors and heat transfer coefficients are calculated in the function subprograms FRIC and HTF, respectively. These relationships are valid for equilateral triangle tube bundle arrays with pitch-to-diameter ratios ranging from 1.3 to 1.7. The user can easily insert his own correlations if those coded are unsuitable for his application.

Tube support plates and baffle plates are assumed to resist the flow only in the axial direction. The tube support plate pressure loss is assumed to result entirely from the sudden area change through the plate; friction resistance is ignored. The baffle plate pressure loss is a combination of shock loss plus frictional loss in the reduced area. The value of the loss factors are determined by the user. The method for calculating these factors is shown in the data sheets.

Two-phase pressure drop correlations, in the form of multipliers, are coded in the subroutine TWOPH. The user can choose various combinations of these multipliers by setting the appropriate value for the index ITPPD.

The mixture density distribution is calculated in the subroutine DENS. The user has the option of calculating density using the homogeneous, the Smith*, or the Chisholm* void fraction relationships by setting the appropriate value of the index IVF.

The Chen* correlation is the only two-phase heat transfer relationship used in THIRST. Because of their non-linear nature, boiling heat transfer correlations require considerable coding work to ensure convergence and stability. In view of this, it is recommended that the user consult with the authors if he wishes to insert another boiling heat transfer relationship.

---

* These correlations are discussed in detail in reference 5.

TABLE 7.2: Single Phase Pressure Drop Correlations*

CORRELATION	COMMENTS
$f = \begin{cases} (-3.3 + 22.8\ p/d)/R_e; \\ \quad \text{for } R_e < (-25 + 172.2\ p/d)^{1.416} \\ 0.132\ R_e^{-0.294};\ R_e < 25000 \\ 0.066\ R_e^{-0.227};\ R_e > 25000 \end{cases}$ $\frac{\Delta P}{\Delta \ell} = 2\ \frac{f}{d_e}\ \frac{G^2}{\rho_f}$	<u>Smooth Bundle Parallel Flow Pressure Drop</u>: - calculated in the function subprogram FRIC. - ENTRY FRIC1: calculates the p/d-dependent coefficient PDA(1). This is done from START, once per program run. - ENTRY FRIC11: calculates the friction factor as a function of Reynolds number. This is done as required from SOURCU, SOURCV, and SOURCW.
$f_c = 28.1\ (p/d)^{-6.8}\ R_c^{\ m}$ $m = 0.62\ [\ell n\ (p/d)^{-0.92}]$ $\frac{\Delta P}{\Delta \ell} = 2\ \frac{f_c}{0.866p}\ \frac{G_{max}^2}{\rho_f}$	<u>Smooth Bundle Cross-Flow Pressure Drop</u>: - calculated in the function subprogram FRIC. - ENTRY FRIC2: calculates the p/d-dependent coefficient PDA(2). This is done from START, once per program run. - ENTRY FRIC3: calculates the p/d-dependent exponent PDA(3). This is done from START, once per program run. - ENTRY FRIC12: calculates the friction factor as a function of Reynolds number. This is done as required from SOURCU, SOURCV, and SOURCW.

* The pressure gradient is related to the source term by $S = -\Delta P/\Delta \ell$.

TABLE 7.2: Single Phase Pressure Drop Correlations (Cont'd)

CORRELATION	COMMENTS
$f = \begin{cases} 64/R_e; & R_e < 2000 \\ 0.316\ R_e^{-0.25}; & R_e \geq 2000 \end{cases}$ $\frac{\Delta P}{\Delta \ell} = \left(\frac{f}{2d_e}\right) \frac{G^2}{\rho_f}$	<u>Downcomer Annulus Pressure Drop</u>: - calculated in the function subprogram FRIC. - ENTRY FRIC13: calculates the friction factor as a function of Reynolds number. This is done as required from SOURCU, and SOURCW.
$\Delta P = \frac{K_t\ G^2}{2\rho_f}$ K_t = tube support loss factor based on approach area	<u>Tube Support or Broach Plate Pressure Drop</u>: - the loss factor is stored as AKBR in code. - K_t based on the contraction into the support plate and the expansion out of the plate. dt is based on the approach area before the contraction.

TABLE 7.2: Single Phase Pressure Drop Correlations (Cont'd)

<table>
<tr><th>CORRELATION</th><th>COMMENTS</th></tr>
<tr><td>

$$\Delta P = \left[K_b + \left(\frac{A_2}{A_1}\right)^2 \frac{f_1 t}{c}\right] \frac{G^2}{2\rho_f}$$

K_b = baffle loss factor based on approach area
A_2 = approach area
A_1 = local area
t = baffle thickness
c = diametral clearance
$f_1 = 0.316 \left(\frac{G_1 c}{\mu}\right)^{-0.25}$, local friction factor
G_1 = local mass flux

</td><td>

Baffle Pressure Drop

- K_b is the shock loss factor based on a contraction into the baffle and expansion out of the baffle. It is based on the approach area.

- f_1 is the friction factor which varies with Reynolds number. The constant portion is stored in FLD (see data sheets for discussion of FLD calculation).

</td></tr>
</table>

TABLE 7.2: Single Phase Pressure Drop Correlations (Cont'd)

CORRELATION	COMMENTS
$\Delta P = \frac{K_w G^2}{2\rho_f}$ K_w = downcomer window loss factor	<u>Downcomer Window Loss Factor</u> - K_w is determined by the user and is stored as AKWINDH for the hot side and AKWINDC for the cold side. - It includes the downcomer-to-window contraction shock loss plus the 90° elbow (due to change in flow direction) shock loss. K_w is based on the window area.

TABLE 7.3: Separator Pressure Loss

CORRELATION	COMMENTS
$\Delta P = \dfrac{C_1 W^2}{2\rho_h}$ $C_1 = K_s/A_s^2$ K_s = separator loss factor A_s = total separator throat area W = total mass flow through separators ρ_h = homogeneous mixture density	C_1 = CON1. CON1 is calculated by the user and read in as input. The separator loss factor K_s and the total separator area A_s should be available as design specifications for the steam generator of interest.

TABLE 7.4: Two-Phase Pressure Drop Correlations

CORRELATION	COMMENTS
$\left(\frac{\Delta P}{\Delta \ell}\right)_{tp} = \phi^2 \left(\frac{\Delta P}{\Delta \ell}\right)_{\ell o}$	- All two-phase pressure drop multipliers are calculated in the subroutine TWOPH, and called from the SOURCU, SOURCV and SOURCW subroutines.
homogeneous: $\phi^2 = 1 + x\rho_f \left[\frac{1}{\rho_g} - \frac{1}{\rho_\ell}\right]$	- Three types of pressure drop are calculated in the program: area change (i.e., expansion and contraction losses), cross flow, and parallel flow. The corresponding two-phase multipliers are TWOA, TWOC and TWOP.
Thom: $\phi^2 = (1-x)^{1.8} \left[1 + \frac{C}{X} + \frac{1}{X^2}\right]$ $C = 1.1 \left[\left(\frac{\rho_f}{\rho_g}\right)^{1/2} + \left(\frac{\rho_g}{\rho_f}\right)^{1/2}\right] - 0.2$	- The user can use the listed correlations as follows: ITPPD = 1 - use Thom's correlation for all three pressure drops ITPPD = 2 - use Baroczy's correlation for all three pressure drops ITPPD = 3 - use the homogeneous expression for area change, Baroczy's for parallel flow, and Ishihara's for cross flow
$X^2 = \left(\frac{1-x}{x}\right)^{1.8} \left(\frac{\rho_g}{\rho_f}\right)\left(\frac{\mu_f}{\mu_g}\right)^{0.2}$	- Note that each multiplier is multiplied by DR (=RHOM/DEN). This is necessary because all pressure drop calculations in SOURCU, SOURCV and SOURCW are based on the mixture density RHOM instead of the liquid density DEN.

TABLE 7.4: Two-Phase Pressure Drop Correlations (Cont'd)

CORRELATION	COMMENTS
Baroczy:	
$\phi^2 = 1 + (\varepsilon^2 - 1)\left[Bx^{0.9}(1-x)^{0.9} + x^{1.8}\right]$	
$B = 55/\sqrt{G} \quad ; \quad G > 500$	
$\quad = 2.45 \quad ; \quad G \leq 500$	
$\varepsilon^2 = \left(\frac{\mu_g}{\mu_f}\right)^{0.2} \cdot \frac{\rho_f}{\rho_g}$	
Ishihara:	
$\phi^2 = (1-x)^{1.8}\left[1 + \frac{8}{X} + \frac{1}{X^2}\right]$	

TABLE 7.5: Void Fraction Relationships

CORRELATION	COMMENTS
$\rho_m = \alpha\rho_g + (1-\alpha)\ \rho_f$ $\alpha = \dfrac{\beta}{\beta + S(1-\beta)}$ $\beta = \dfrac{x}{x + \dfrac{\rho_g}{\rho_f}(1-x)}$ homogeneous: $S = 1$ Chisholm: $S = \left[1 + x\left(\dfrac{\rho_f}{\rho_g} - 1\right)\right]^{\frac{1}{2}}$ Smith: $S = 0.4 + 0.6\left[\dfrac{\dfrac{\rho_f}{\rho_g} + 0.4\left(\dfrac{1-x}{x}\right)}{1 + 0.4\left(\dfrac{1-x}{x}\right)}\right]^{\frac{1}{2}}$	- The mixture density, based on one of three different void fraction relationships, is calculated in the subroutine DENS. - The user can choose one of the three relationships by setting IVF as follows: IVF = 1 - homogeneous expression IVF = 2 - Chisholm correlation IVF = 3 - Smith correlation

TABLE 7.6: Heat Transfer Correlations

CORRELATION	COMMENTS
parallel flow: $\frac{hd}{k} = (0.023)\ (C)\ R_e^{0.8}\ \ P_r^{0.4}$ $C = 0.58 + 0.4\ (p/d)$ cross flow: $\frac{hd}{k} = 0.36\ R_c^{0.6}\ P_r^{0.36}$	Single Phase Secondary Side: - calculated in the function subprogram HTF. - ENTRY HTF1: calculates the parallel flow p/d-dependent coefficient, HTPL. This is done from START, once per program run. - ENTRY HTF2: calculates the parallel flow Reynolds-number-dependent portion of the Nusselt number. This is done from SOURCH as required. - ENTRY HTF3: calculates the cross-flow Reynolds-number-dependent portion of the Nusselt number. This is done from SOURCH, as required.
Chen Correlation: $h_{tp} = h_{\ell} + h_{nb}$	Saturated Boiling Heat Transfer, Secondary Side: - calculated in the subroutine SOURCH. The saturation pressure and temperature-dependent terms are calculated in the function PROP. These terms are valid for light water in the range of 4 MPa to 6 MPa saturation pressure.

TABLE 7.6: Heat Transfer Correlations (Cont'd)

CORRELATION	COMMENTS
Chen Correlation Cont'd: $h_\ell = \begin{cases} \left(\frac{k_f}{d_e}\right)(0.023)\left[\frac{(1-x)Gd_e}{\mu_f}\right]^{0.8} Pr^{0.4} F_c; \text{ parallel flow} \\ \left(\frac{k_f}{d}\right)(0.36)\left[\frac{(1-x)G_{max}d}{\mu_f}\right]^{0.6} Pr^{0.36} F_c; \text{ cross-flow} \end{cases}$ $F_c = \begin{cases} 0.35 + 2.43\left(\frac{1}{X_{tt}}\right)^{0.73} + \frac{0.199}{\exp\left[\frac{10}{X_{tt}} - 1\right]}; \frac{1}{X_{tt}} \geq 0.1 \\ 1.0; \frac{1}{X_{tt}} < 0.1 \end{cases}$	- ENTRY PROP1: AKBO and XTTK are calculated: $AKBO = 0.00122\left[\frac{k_f^{0.79}\left(c_p\right)_f^{0.45}\rho_f^{0.49}}{\sigma^{0.5}\mu_f^{0.29}H_{fg}^{0.24}\rho_g^{0.24}}\right]$ $XTTK = \left(\frac{\rho_g}{\rho_f}\right)^{1/2}\left(\frac{\mu_f}{\mu_g}\right)^{0.1}$ - ENTRY PROP9: calculates $(dP/dT)_{SAT}$ so that ΔP_{SAT} can be calculated. $(dP/dT)_{SAT}$ is the derivative of the saturation pressure versus saturation temperature relationship.

TABLE 7.6: Heat Transfer Correlations (Cont'd)

CORRELATION	COMMENTS
$X_{tt} = \left(\frac{1-x}{x}\right)^{0.9} \left(\frac{\rho_g}{\rho_f}\right)^{\frac{1}{2}} \left(\frac{\mu_f}{\mu_g}\right)^{0.1}$	
$h_{nb} = 0.00122 \left[\frac{k_f^{0.79} \left(c_p\right)_f^{0.45} \rho_f^{0.49}}{\sigma^{0.5} \mu_f^{0.29} H_{fg}^{0.24} \rho_g^{0.24}}\right] B$	
$B = \Delta T_{SAT}^{0.24} \; \Delta P_{SAT}^{0.75} \; S_c$ $S_c = \begin{cases} 1\ 0; & \left(R_e\right)_\ell < 2000 \\ \left(1.\ldots\ .121 \left[10^{-4} \; F_c^{1.25} \left(R_e\right)_\ell\right]^{1.17}\right)^{-1} & \\ ; & \left(R_e\right)_\ell \geq 2000 \end{cases}$	

TABLE 7.6: Heat Transfer Correlations (Cont'd)

CORRELATION	COMMENTS
$\frac{hd}{k_f} = 0.023 \left(\frac{Gd_i}{\mu_f}\right)^{0.8} \left(\frac{C_p\mu}{k}\right)_f^{0.33} \lambda$ $\lambda = \left[1 + x(v_{fg}/v_f)\right]^{1/2}$	<u>Primary (tube-side) Heat Transfer Correlation</u>: - The parameter λ is a two-phase heat transfer coefficient multiplier. It is activated when the primary flow is two-phase. - The temperature-dependent parameters k_f, μ_f and $(C_p)_f$ are calculated in the function subprogram PROP (ENTRY PROP3) as: $\text{RCONVA} = k_f^{0.67}\ \mu_f^{-0.47}\ (C_p)_f^{0.33}$ $\approx F$ (primary enthalpy) RCONVA is based on heavy water properties over the temperature range of 245°C to 315°C. It is valid in the pressure range of 7 MPa to 11 MPa to an accuracy of 0.5%. - Note that h is the primary-side heat transfer coefficient referred to the tube outside surface.

TABLE 7.6: Heat Transfer Correlations (Cont'd)

CORRELATION	COMMENTS
$h_w = \dfrac{2k_w}{d \, \ell n(d/d_i)}$	<u>Wall Heat Transfer Coefficient</u>: - The wall resistance referred to the tube outside diameter, RWALL = $\dfrac{1}{h_w}$ is calculated in START. CWALL = k_w, the thermal conductivity of the tube wall material is specified by the user in READIN.
$\text{RFOUL} = \dfrac{1}{h_{foul}}$	<u>Fouling Resistance</u>: - RFOUL is specified by the us-r in READIN.

8. GEOMETRICAL RESTRICTIONS AND POSSIBLE VARIATIONS

The basic steam generator geometry as illustrated in Figure 1.1 has obvious geometric restrictions. Foremost is the restriction to cylindrical coordinate geometry. However, a number of minor geometrical changes can be made quite readily, enabling the code to accept a wider variety of designs.

8.1 Tube Bundles

The tube bundle is U-shaped with a spherical U-bend. Porosities and control volume centroids for the U-bend region are calculated in the subroutine VOLL. If the design of interest has a non-spherical U-bend geometry (i.e., square - elliptic) major modifications of NEW as well as some changes in SOURCU to SOURCH will be necessary. The user is advised to consult the authors before such modifications are undertaken.

The user can specify any tube bundle outer diameter and tube-free lane width. There are no provisions in the code to handle cylindrical tube-free areas in the centre region, however.

Porosities and single-phase fluid flow correlations are based on an equilateral triangle pitch arrangement. The user should modify the correlations in FRIC and HTF if other arrangements are of interest. If the arrangement is square, ATR in the subroutine START must be redefined as ATR = 0.5 * PITCH ** 2.

8.2 Preheater

The preheater geometry is defined by specifying the following: thermal-plate elevation, top of preheater, elevation, feedwater inlet opening and baffle plate cuts. The feedwater inlet opening can extend over the full 90° circumferential arc on the cold side*. Baffle cuts must be parallel to the divider plate. Code modifications are required if other types of cuts (i.e., normal to divider plate) or other baffles (i.e., triple segmental) are considered.

8.3 Tube Supports

The user can specify any number of horizontal tube supports up to the start of the U-bend. The code can handle a vertical U-bend tube support if it is located midway between the hot and cold sides.

8.4 Downcomer Windows

The downcomer window heights on the hot and cold sides can be specified independently. Once specified, each window extends over the full 90° circumferential arcs on the hot and cold sides.

8.5 Separators

The three-dimensional modelled region can be extended to just below the separator deck. The separators are treated as a one-dimensional resistance.

---

* Remembering that only ½ of the steam generator is modelled.

9. ADAPTATION OF THIRST TO A NEW DESIGN

As discussed in earlier chapters, THIRST has been generalized to accept minor geometric changes and most sizing changes. As the user becomes more familiar with the code, alterations to handle radically different designs will become easier to make. Initially, the user is advised to return to the authors for advice on preparation of modification decks to handle radically new designs. An example of such modification is now considered.

In order to eliminate problems that can arise with a pre-heater, several steam generator designs introduce the feedwater through a distribution ring located at the top of the downcomer annulus, below the liquid free surface. The colder relatively dense feedwater mixes with the saturation liquid coming from the separators and flows down the annulus to the shroud windows. The average density in the downcomer is increased thus the recirculation ratio increases. The log-mean temperature difference (LMTD) of the units is reduced, however, and thus we would expect a drop in overall heat transfer without the preheater.

This section considers a design which does not contain a preheater but introduces the feedwater at the top of the downcomer. All dimensions remain the same as the original values. All operating conditions remain the same. This unit may not be well designed since the basic layout normally would be altered when feedwater is introduced at the top. However, it will serve to illustrate the extent of code modifications.

Altering the code to handle new geometries requires both data and code logic changes. To simplify the logic changes we will locate the last I-plane just below the feedwater distribution ring. The downcomer flow rate is thus increased by the amount of the feedwater flow. The downcomer enthalpy is also reduced because the feedwater is subcooled. Both of these parameters serve as boundary conditions to the model.

To illustrate the changes required, we must look at how the downcomer flow is determined. In the code, a subroutine called RECIR estimates the recirculation ratio which will balance the driving head against the flow-dependent pressure losses. Recirculation ratio is defined as

$$\text{RECIR} = \frac{\text{FLOW OF SATURATED LIQUID OUT OF THE SEPARATORS}}{\text{INLET FLOW}}$$

where the inlet flow is the sum of feedwater and reheater drain flows.

If we add the feedwater flow to this liquid separator flow, we have the flow in the downcomer annulus

DOWNCOMER FLOW = RECIR * (INLET FLOW) + FEEDWATER FLOW

In terms of code variables, we have

FLOWH = RECIR * (FLOWC + FLOWRH) + FLOWC

The code then determines the velocity at the boundary by dividing the new downcomer volumetric flow rate by the annulus area.

The downcomer enthalpy is calculated by summing the individual flows coming into the downcomer multiplied by their enthalpy values, and divided by the total downcomer flow

$$\text{ENTH. OF D.C.} = \frac{\text{FLOW FROM SEP * SAT. ENTH. + PREHEATER FLOW * PREH. ENTH. + FEEDWATER FLOW * FEEDWATER ENTH.}}{\text{TOTAL DOWNCOMER FLOW}}$$

In THIRST the liquid saturation enthalpy is set to zero and all other enthalpy values are relative to this zero level. Thus, the above expression reduces to the following form in terms of code variables

$$\text{SUBH} = \frac{\text{FLOWRH * SUBRH + FLOWC * ENC}}{\text{FLOWH}}$$

The enthalpy value at the I-plane is set to this value, and thus the boundary conditions handle the introduction of feedwater into the downcomer.

The code changes required to incorporate these changes are

<u>In START</u> - initializing subroutine

```
*D START.112
   FLOWH = RECIR * (FLOWC + FLOWRH) + FLOWC
```
(this statement initializes the downcomer flow rate to include the feedwater flow)

```
*D START.114
   FLOTOT = FLOWH
```
(this statement tells the program that the total flow is equal to the downcomer flow as all the inlet flows occur at the top of the downcomer)

```
*D START.159, also *D START.260
   SUBH = -(FLOWRH * SUBRH + FLOWC * ENC)/FLOWH
```
(this statement initializes the downcomer enthalpy value)

<u>In RECIR</u> - calculating the recirculation ratio

```
*D RECIRC.65, RECIRC.66
   FLOWH = RECIR * (FLOWC + FLOWR1) + FLOWC
   FLOTOT = FLOWH

*D RECIRC.67
   SUBH = -(FLOWRH * SUBRH + FLOW * ENC)/FLOWH
```

We now have introduced the feedwater in the top of the downcomer. Our next task is to eliminate the preheater and the feedwater inlet. For the most part, we will leave the data the same if it is not related to the preheater. The following chart contains the essential changes to remove the preheater.

Data No.	Name	Reason for Change	New Values
8	ICOLD	Set plate loss locations to the same as in IHOT.	7*1,6,3*1, 5*(1,2),2*1, 7*2,6*1
12	IFEEDB	Remove preheater bubble by reducing its height to I=1.	1
13	IFEEDU	Set upper limit of feedwater window to the I=2.	2
14	IFEEDL	Make the lower limit feedwater window greater than the upper limit so that no control volumes lie between the two.	10
15	IPRHT	Set the top of preheater to I=1 for the plotting routine.	1

Other data values that deal with the preheater could be altered; however, the changes made above ensure that these data values are never used. An example is AKBC, the baffle resistance, which is not used because ICOLD never equals 3 or 4.

These changes were inserted as illustrated in Figures 7.1 and 7.2. Results are summarized in Figures 7.3 and 7.4. Two major prediction changes are evident:

(1) The recirculation climbed from 5.4 to 7.06.
(2) The heat transfer dropped from 662 to 577.

The quality profiles undercut the larger subcooled region on the cold side. Mass flux plots indicate a uniform flow distribution across the bundle.

In concluding this chapter, it should be pointed out again that these changes were to illustrate the flexibility of the code and not to compare two design types. Each design could be altered to maximize its performance. Although the number of changes required to handle this new configuration were small, it required a good overall understanding of the code to identify them. We therefore stress that when faced with radically different designs, the user is advised to consult with the authors.

```
UNLABELED CLOFL              IDENT     NPRHTR                          UPDATE 1.3-498.       80-07-08  21.14.01.      PAGE    1

*****    *IDENT NPRHTR
/////    *DELETE START.112
                  FLCWH=RECIR*(FLOWC+FLOWRH)+FLOWC
/////    *DELETE START.114
                  FLCTOT=FLOWH
/////    *DELETE START.159
                  SUBH=-(FLOWRH*SUBRH+FLOWC*ENC)/FLOWH
/////    *DELETE START.496,START.534
/////    *DELETE RECIRC.65,RECIRC.67
                  FLOWH=RECIR*(FLOWC+FLOWRH)+FLOWC
                  FLCTOT=FLOWH
                  SUBH=-(FLOWRH*SUBRH+FLOWC*ENC)/FLOWH
/////    *DELETE SOURCU.107

         MODIFICATIONS / CONTROL CARDS


START           FLCWH=RECIR*(FLOWC+FLOWRH)                                        START      112       D
START           FLCWH=RECIR*(FLOWC+FLOWRH)+FLOWC                                  NPRHTR       1     I
START           FLCTOT=FLOWC+FLOWH                                                START      114       D
START           FLCTOT=FLOWH                                                      NPRHTR       2     I
START           SUBH=-FLCWRH*SUBRH/FLOWH                                          START      159       D
START           SUBH=-(FLOWRH*SUBRH+FLOWC*ENC)/FLOWH                              NPRHTR       3     I
START     CALCULATE PERCENT AREAS OCCUPIED BY BAFFLES                             START      496       D
START     C      NN=1    INNER BAFFLE                                             START      497       D
START     C      NN=2    OUTER BAFFLE                                             START      498       D
START     C     NN = 3    LAST BAFFLE AT PREHEATER EXIT                           START      499       D
START           DO 900 NN=1,3                                                     START      500       D
START               DO 900 K=KCENTC,N                                             START      501       D
START                   DO 900 J=2,MM                                             START      502       D
START                       BP=RADIUS                                             START      503       D
START                       T1=ZW(K)                                              START      504       D
START                       T2=ZW(K+1)                                            START      505       D
START                       AA=DAA=1.0                                            START      506       D
START                       II=1                                                  START      507       D
START                       IF (BP(NN) .GT. YV(J+1)) GOTO 860                     START      508       D
START                           BR=BP(NN)/COS(PI-ZW(K+1))                         START      509       D
START                           IF (BR .GT. YV(J+1)) GOTO 860                     START      510       D
START                               II=2                                          START      511       D
START                               T1=PI-ACOS(BP(NN)/YV(J+1))                    START      512       D
START                               IF (BP(NN) .LT. YV(J)) T2=PI-ACOS(BP(NN)/YV(J))   START  513       D
START                               IF (ZW(K) .GT. T1) T1=ZW(K)                   START      514       D
START                               IF (ZW(K+1) .LT. T2) T2=ZW(K+1)               START      515       D
START                               IF (T2 .LT. T1) GOTO 860                      START      516       D
START                                   AA=YV(J+1)*YV(J+1)-YV(J)*YV(J)            START      517       D
START                                   DAA=AA*(T1-ZW(K))-YV(J)*YV(J)*(T2-T1)+BP(NN)*BP(   START  518   D
START                                   NN)*             (TAN(T2-PI)-TAN(T1-PI))  START      519       D
START                                   AA=AA*(ZW(K+1)-ZW(K))                     START      520       D
START        860            CONTINUE                                              START      521       D
START                       IF (NN .EQ. 2) GOTO 880                               START      522       D
START                           IF (NN .EQ. 3) GOTO 890                           START      523       D
START     C      INNER BAFFLES                                                    START      524       D
START        870                IF(T2 .LT. T1) DAA=0.0                            START      525       D
START                           BFIN(J-1,K-KCENTH)=DAA/AA                         START      526       D
START                           GOTO 900                                          START      527       D
START     C      OUTER BAFFLES                                                    START      528       D
START        880            IF (T2 .LT. T1) DAA=0.0                               START      529       D
START                       BFOU(J-1,K-KCENTH)=1.0-DAA/AA                         START      530       D
START                       GOTO 900                                              START      531       D
START        890            IF (T2 .LT. T1) DAA=0.0                               START      532       D
START                       BLAST(J-1,K-KCENTH)=DAA/AA                            START      533       D
START        900 CONTINUE                                                         START      534       D


RECIRC          FLCWH=RECIR*(FLOWC+FLOWRH)                                        RECIRC      65       D
RECIRC          FLCTOT=FLOWH+FLOWC                                                RECIRC      66       D
RECIRC          SUBH=-FLCWRH*SUBRH/FLOWH                                          RECIRC      67       D
RECIRC          FLCWH=RECIR*(FLOWC+FLOWRH)+FLOWC                                  NPRHTR       4     I
RECIRC          FLCTOT=FLOWH                                                      NPRHTR       5     I
RECIRC          SUBH=-(FLOWRH*SUBRH+FLOWC*ENC)/FLOWH                              NPRHTR       6     I


SOURCU          GOTO(70,90),KHCCO                                                 SOURCU     107       D
```


Figure 7.1: THIRST OUTPUT MODIFIED DESIGN - Code Changes

```
*************************************      NO PREHEATER 600 MW STEAM GENERATOR      *************************************
 RESTART   1.000000
 NI       36      NJ       10      NK       12

    AKDIV       36
0. 0. 0. 0. 0. 0. 0. 0. 0. 0. 0. 0. 0. 0. 0. 0. 0. 0. 0. 0. 0. 0. 0. 0. 0. 0. 0. 0. 0. 0. 0. 0. 0. 0. 0. 0.
    ICOLD       36
1 1 1 1 1 1 1 6 1 1 1 1 2 1 2 1 2 1 2 1 2 1 1 2 2 2 2 2 2 1 1 1 1 1 1
    IHOT        36
1 1 1 1 1 1 1 6 1 1 1 1 2 1 2 1 2 1 2 1 2 1 1 2 2 2 2 2 2 2 1 1 1 1 1
    IJPLOT      36
0 1 0 1 0 1 0 1 0 1 1 0 1 1 1 1 1 1 1 1 1 1 1 1 1 1 1 1 0 1 0 1 1 1 0
    IPASSF      33
3 4 5 6 7 8 9 10 11 12 13 14 15 16 17 18 19 20 21 22 23 24 25 26 27 28 29 30 31 32 33 34 35
    IFLOTK      8
3 4 5 6 7 8 9 10
    IPLCTI      8
2 -6 14 -21 25 -32 33 -35
    IFRINT      11
1 9 0 0 0 0 0 0 0 0 0
    RELAX       11
.5 .5 .5 1. 1. 1. .25 .5 .5 .2 1.
    TCON        15
0. .01 .02 .03 .05 .1 .15 .2 .22 .25 .3 .35 .4 .5 0.
    X           36
0. .01 .12 .23 .34 .45 .56 .67 .78 .89 1. 1.11 1.46 1.81 2.16 2.51 2.86 3.21 3.56 3.91 4.17 4.26 4.61 5.194 5.78 6.36
6.94 7.53 8.12 8.7 9.07 9.44 9.6 10.2 10.5 10.6
    Y           10
0. .1 .27565 .4512 .6269 .8026 .978 1.1539 1.2845 1.3575
    Z           12
0. 9. 27. 45. 63. 81. 99. 117. 135. 153. 171. 180.
    BP          3
0. 0. 0.

  IDCHNC     6        IDCHNH     7        IFEEDB     2        IFEEDL    10        IFEEDU     2
  IPRHT      0        ISHRO     31        ITFFD      1        IUBEND    30        IVF        1
  NBRCH      4        KCENTC     7        KCENTH     6        KFEEDL     2        LASTEP    60

  ITMELT   0.                   AKBL     0.                   AKBR     1.500000          AKBRL    1.000000          AKBRS    6.000000
  AKTP     0.                   AKWINDC  10.00000             AKWINDH  13.00000          ARATB    0.                ARATTP   0.
  CGAP     7.0000000E-02        CON1     .9495000             CON2     .1156500          CON4     2000.000          CWALL    16.70000
  DIA      1.5875000E-02        DIAIN    1.3677900E-02        EDFEED   0.                EDNORM   .2200000          EDSHROX  .8000000
  FLDB     0.                   FLDT     0.                   FLCWC    306.1800          FLOWRH   23.70000          FLOWTU   2484.930
  HTAR     4550.000             OGAP     3.0000000E-02        PFWB     0.                PITCH    2.4511000E-02     FLOTO    1.000000
  RPRI     9.879000             PRINTO   1.000000             PSEC     5.100000          PSHRC    14.10000          QLTU     3.4000000E-02
  RADIUS   1.321000             RECIR    5.300000             RFOUL    2.6427000E-05     RSHELL   1.440000          TINC     176.6700
  TPLATE   .6150000             TRH      281.6700             TUBSHET  .4190000          XDOWN    13.00000          XL1      9.000000
  XL2      6.250000             XVANE    16.00000             YL       6.300000

 NO DATA CALLED FOR ARRAY  IEXTRA

 NO DATA CALLED FOR ARRAY  REXTRA
```

Figure 7.2: THIRST OUTPUT MODIFIED DESIGN - Data Summary

ITERATION NUMBER = 60

NEW ESTIMATE OF RECIRCULATION RATIO = 7.06239

MASS FLOWS AFTER SOLUTION OF MOMENTUM EQUATION FOR U VELOCITY

I	HOT SIDE	COLD SIDE	I	HOT SIDE	COLD SIDE	I	HOT SIDE	COLD SIDE	I	HOT SIDE	COLD SIDE	I	HOT SIDE	COLD SIDE
3	77.899	64.581	11	642.877	689.057	19	774.467	551.789	27	633.583	691.505	35	650.085	670.740
4	209.146	203.209	12	654.590	677.681	20	799.824	527.312	28	621.604	703.710			
5	327.278	342.957	13	673.286	654.512	21	760.600	566.348	29	611.999	712.374			
6	433.102	509.623	14	703.656	625.578	22	762.346	567.251	30	604.421	715.615			
7	541.713	678.724	15	722.718	603.645	23	776.607	552.080	31	595.590	729.451			
8	643.498	685.196	16	768.267	559.702	24	724.813	601.516	32	592.353	732.441			
9	635.153	695.873	17	760.705	565.427	25	681.807	643.989	33	600.176	726.338			
10	635.435	696.216	18	808.061	519.426	26	652.743	672.734	34	625.560	702.204			

MASS FLOW AFTER K-PLANE SOLUTION OF CONTINUITY EQUATIONFOR P AND CORRECTION OF U VELOCITY

I	HOT SIDE	COLD SIDE	I	HOT SIDE	COLD SIDE	I	HOT SIDE	COLD SIDE	I	HOT SIDE	COLD SIDE	I	HOT SIDE	COLD SIDE
3	80.058	70.619	11	641.640	688.119	19	774.605	551.913	27	633.576	691.506	35	646.579	672.432
4	209.860	202.712	12	653.081	676.608	20	799.546	527.230	28	621.000	703.703			
5	326.898	343.041	13	673.546	654.781	21	760.801	566.483	29	612.009	712.374			
6	429.846	505.230	14	703.143	625.211	22	762.025	565.878	30	604.544	715.778			
7	532.777	667.415	15	722.959	604.043	23	776.195	551.518	31	595.466	729.296			
8	643.501	685.369	16	767.863	559.283	24	724.862	601.506	32	592.340	732.436			
9	634.435	694.828	17	760.843	565.576	25	681.810	644.014	33	599.558	725.937			
10	634.339	695.264	18	807.733	519.022	26	652.734	672.714	34	623.911	704.966			

MASS FLOW AFTER I-PLANE SOLUTION OF CONTINUITY EQUATIONFOR P AND CORRECTION OF U VELOCITY

I	HOT SIDE	COLD SIDE	I	HOT SIDE	COLD SIDE	I	HOT SIDE	COLD SIDE	I	HOT SIDE	COLD SIDE	I	HOT SIDE	COLD SIDE
3	80.692	74.674	11	631.171	678.849	19	770.627	538.548	27	628.408	681.800	35	646.812	675.581
4	208.477	199.359	12	642.543	666.087	20	794.265	511.655	28	615.790	694.620			
5	323.851	338.129	13	665.057	645.646	21	756.826	552.445	29	606.917	704.128			
6	425.476	500.166	14	694.207	613.159	22	756.397	548.642	30	599.906	712.087			
7	527.388	661.630	15	717.078	593.238	23	770.629	533.749	31	590.754	721.855			
8	637.663	679.627	16	760.788	545.516	24	720.696	568.860	32	588.614	726.724			
9	625.150	686.643	17	756.207	553.294	25	677.111	632.858	33	595.331	719.345			
10	624.055	686.748	18	801.792	504.109	26	647.711	652.393	34	620.675	696.383			

SUM OF RING MASS IMBALANCE .167

MASS FLOW AFTER EXACT SOLUTION OF CONTINUITY EQUATION USING WEDGES AND RING GEOMETRIES

I	HOT SIDE	COLD SIDE	I	HOT SIDE	COLD SIDE	I	HOT SIDE	COLD SIDE	I	HOT SIDE	COLD SIDE	I	HOT SIDE	COLD SIDE
3	76.537	69.503	11	635.561	682.400	19	772.653	545.306	27	631.161	685.859	35	645.219	672.742
4	196.234	186.753	12	647.343	673.618	20	797.258	520.703	28	618.547	695.414			
5	315.796	326.138	13	665.941	649.020	21	756.741	559.220	29	609.566	705.393			
6	418.327	491.949	14	698.740	619.220	22	759.594	558.367	30	601.966	715.980			
7	523.678	658.086	15	719.785	598.175	23	773.865	544.096	31	592.847	721.114			
8	638.185	679.776	16	754.788	553.173	24	722.815	595.146	32	589.647	726.314			
9	628.702	689.259	17	756.525	559.432	25	679.495	638.465	33	596.424	721.537			
10	628.272	689.669	18	805.217	512.744	26	650.264	667.676	34	620.781	697.186			

MASS FLOW AFTER SOLUTION OF ENERGY EQUATION AND CORRECTION OF DENSITY

I	HOT SIDE	COLD SIDE	I	HOT SIDE	COLD SIDE	I	HOT SIDE	COLD SIDE	I	HOT SIDE	COLD SIDE	I	HOT SIDE	COLD SIDE
3	76.539	69.489	11	635.620	682.274	19	772.835	544.617	27	631.371	684.512	35	645.273	671.578
4	196.304	186.718	12	647.355	670.500	20	797.389	519.592	28	618.649	697.186			
5	315.936	326.082	13	669.397	648.909	21	758.942	557.470	29	609.887	706.297			
6	418.467	491.860	14	699.132	619.119	22	759.809	556.464	30	602.268	713.989			
7	523.804	657.970	15	720.117	598.379	23	774.065	541.981	31	593.146	723.174			
8	638.341	679.645	16	754.954	553.056	24	723.052	592.581	32	589.967	726.459			
9	628.832	689.125	17	756.709	559.306	25	679.731	635.847	33	596.719	719.618			
10	628.359	689.557	18	805.340	512.460	26	650.531	665.202	34	620.857	695.681			

RECIR	PRESS DROP	PRIM H.T.	SEC H.T.	AVG OUTLET QUAL	SUM SOURCE	MAX SOURCE (3 2 11)
7.0624	-8652.12	577.76	573.07	.10470	.2453	.0036

AXIAL VEL VALUES *** ON HOT SIDE (3 5 5) .13504 ON COLD SIDE(3 5 3) .11424 IN UBEND (32 5 5) 2.75007 IN DOWNCOMER (3 10 5) -.35194

RADIAL VEL VALUES *** IN SHROUD WINDOW (6 10 5) -.83893 ABOVE DIV PLATE (10 5 7) -.07193 IN PREHEATER (7 5 8) -.56381 IN U-BEND SECT (32 5 4) .66679

THERMAL VALUES AT (8 5 6) *** SEC ENTHALPY -18998.94 WALL TEMP 273.13 PRIMARY TEMP 309.23 HEAT FLUX .28868

FIGURE 7.3: THIRST OUTPUT MODIFIED DESIGN - Final Iteration Results Graphical Output

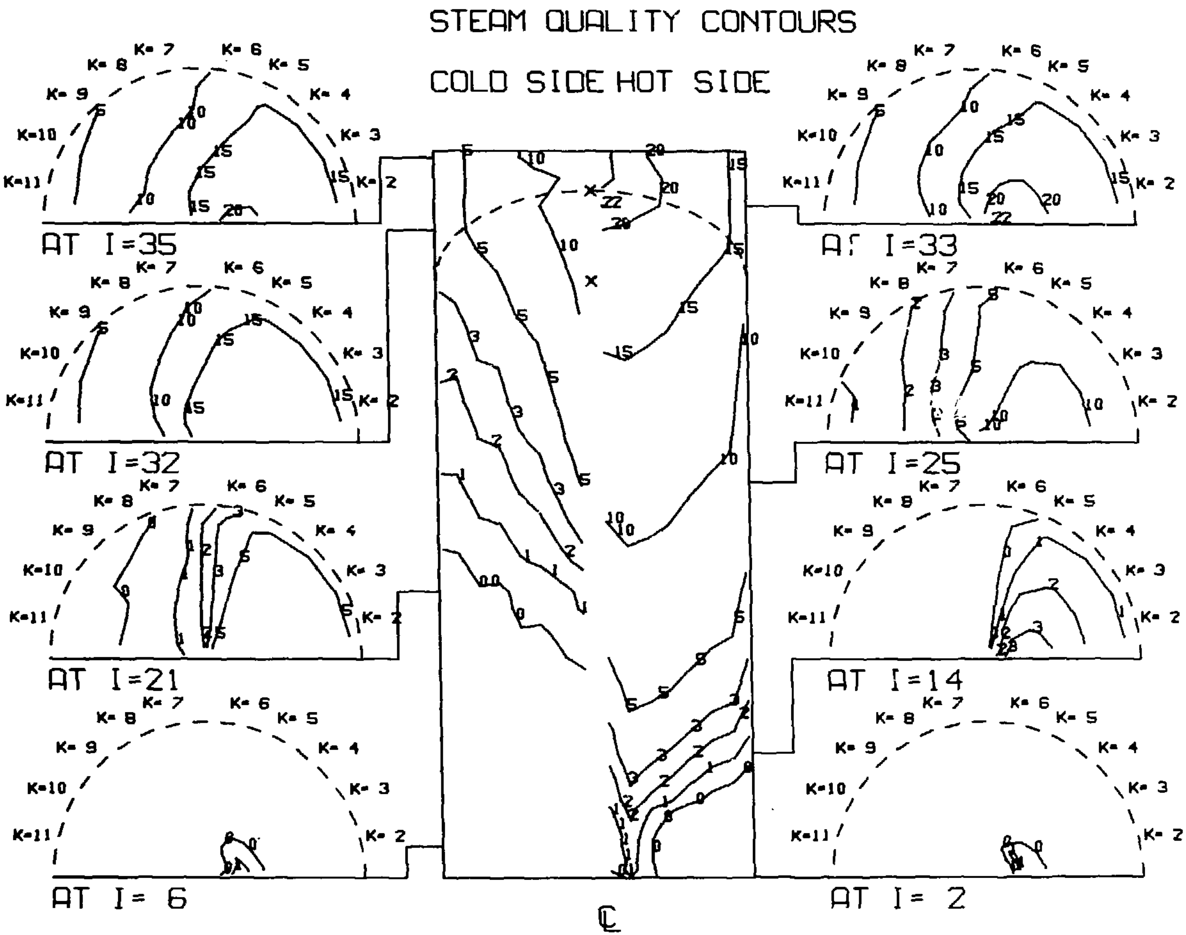

Figure 7.4.1: THIRST OUTPUT MODIFIED DESIGN - Final Iteration Results Graphical Output (Quality Distribution)

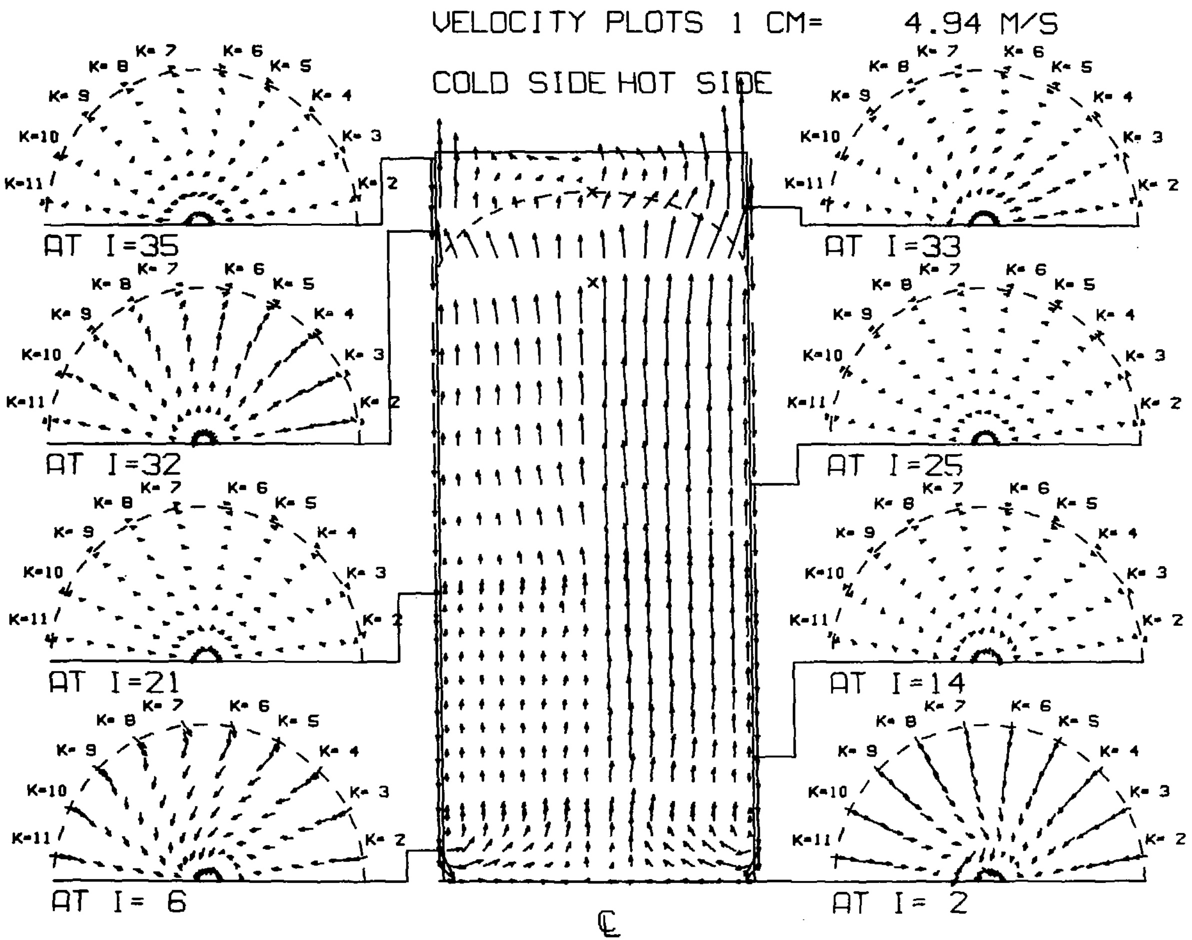

Figure 7.4.2: THIRST OUTPUT MODIFIED DESIGN - Final Iteration Results Graphical Output (Velocity Distribution)

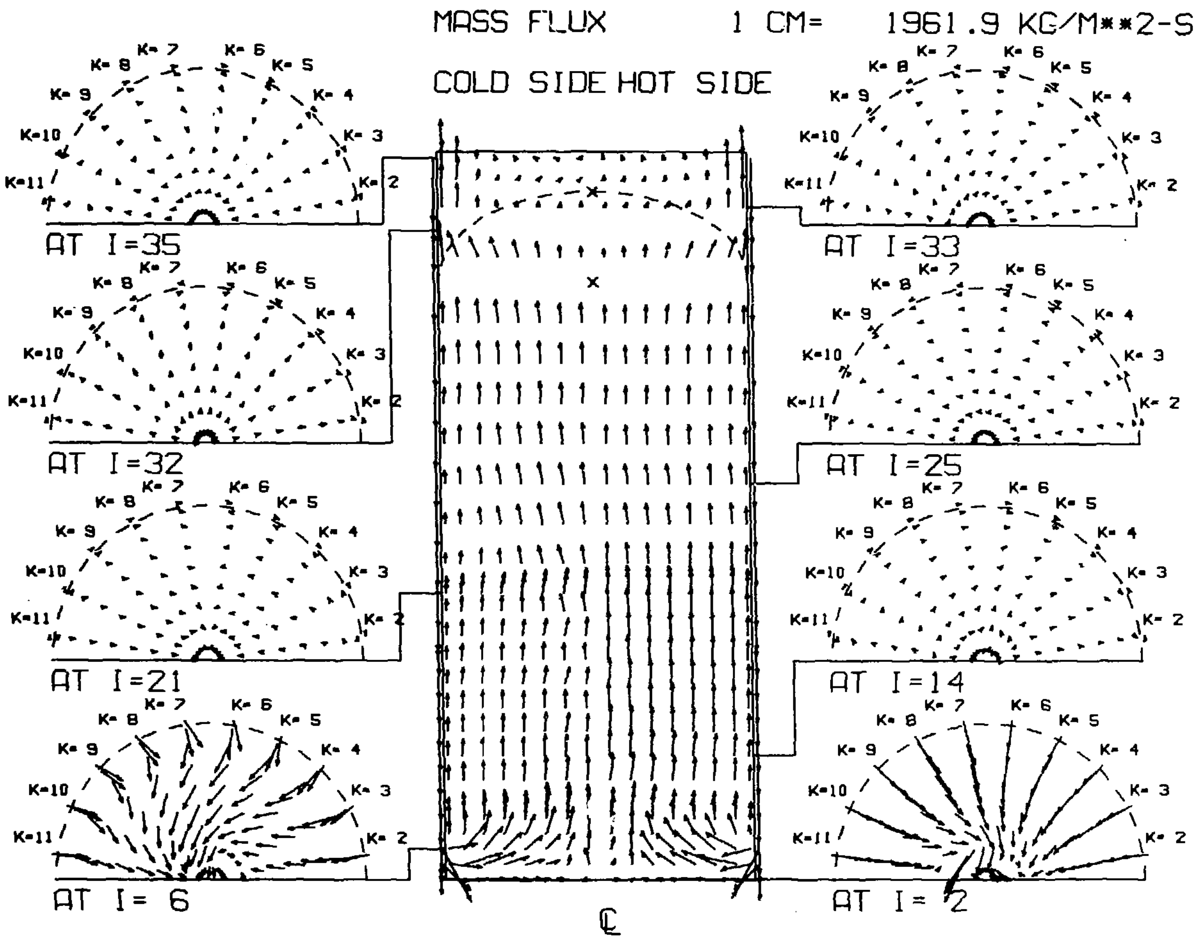

Figure 7.4.3: THIRST OUTPUT MODIFIED DESIGN - Final Iteration Results Graphical Output (Mass Flux Distribution)

APPENDIX A

LOGIC STRUCTURE OF THE THIRST CODE

This appendix discusses the logic structure of the code, including the outer and inner iteration sequences, the pressure correction, and the function of the subroutines.

A.1 The Outer Iteration Sequence

The executive subroutine orchestrates the outer iteration sequence, computing in turn each velocity component from the associated momentum equation to obtain velocity and pressure corrections as described in Section 3, computing the enthalpy from the energy equation and finally obtaining new densities from the equation of state.

A.2 The Inner Iteration Sequence used in CALCU, CALCV, CALCW and CALCH

Because it is possible to set up all the conservation equations in general transport form, the solution of each equation follows the same general sequence. The problem is to solve the matrix equation 3.6.

$$A_p \phi_p + \Sigma A_i \phi_i = SU$$

$$i = n, s, e, w, h, \ell$$

$$A_n = +C_n \; , \quad A_S = -C_S \quad \text{etc.}$$

$$A_p = \Sigma A_i + S_p$$

This is accomplished by setting up the alternating direction tridiagonal solution in a plane as described in Section 3.4.

The general sequence used in CALCU and CALCV is given in Table A-2. However, as W is a θ velocity, the K-planes must be incorporated more implicitly in CALCW. The sequence in CALCW is identical to Table A-2, except that it is done by I-planes and uses routines SOLVE3 and SOLVE4, which set up the tridiagonal systems in KJ and I, respectively.

The energy equation solution CALCH also uses the same sequence as Table A-2.

TABLE A-1

THIRST LOGIC STRUCTURE EXECUTIVE ROUTINE ITERATION SEQUENCE

Routine Called	Purpose	Equations
READIN	Read all data.	--
INIT	Initialize all array pointers.	--
START	Compute all geometry and initial correlations	--
RECIRC	Compute recirculation.	
CALCU	Compute U vector from axial momentum equation	2.3
CALCV	Compute V vector from radial momentum equation	2.4
CALCW	Compute W vector from azimuthal equation	2.5
EXITT	Force exit axial velocities to be positive	
CALCP	Compute pressure and velocity corrections from continuity equation	2.2
CALCH	Compute enthalpy distribution from energy equation	2.6
DENS	Compute densities from equation of state	
MASSFLO	Compute axial mass flows	
BOUND	Impose exit plane boundary values	
OUTPUT	Output summary	
REPEAT (Y: return to RECIRC; N: continue)	Repeat unless time or no. of iterations is about to expire	
FPRINT	Final output	
WSTART	Write tape for Restart	
STOP		

TABLE A-2

GENERAL SOLUTION OF TRANSPORT EQUATIONS

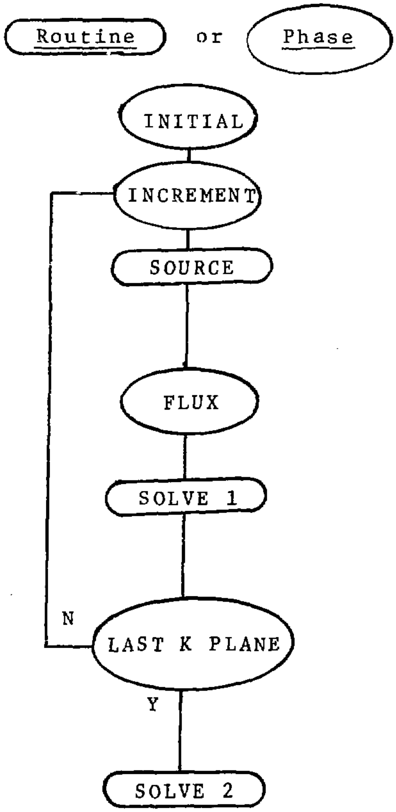

Purpose

Compute K = 1 boundary flux.

Start next K plane.

Call appropriate SOURCE routine to evaluate resistances and assemble S_U and S_P terms.

Compute all flux terms to complete definition of Equation 3.6.

Incorporate under-relaxation. Set up the system $A\phi = B$ using tridiagonal in x and solve using forward and backward sweeps through r.

Repeat tridiagonal in r and sweep in x. Assemble coefficients in the K plane preparatory for a K block solution.

Set up the system $A\phi = B$ using tri-diagonal in θ. Perform one solution using coefficients assembled above thus correcting the above results for K variation.

A.3 The Pressure and Velocity Correction Routine CALCP

The pressure and velocity correction obtains pressure corrections by embedding the velocity corrections in the continuity equation as described in Chapter 2. The sequence is shown in Table A-3.

First, the continuity equation is solved for the embedded pressure corrections as in Section 2.4. Then, each velocity is corrected following equation 2.21, and finally, the new values of pressure are computed. As mentioned in Section 3, unlike the other variables, pressure is under-relaxed if necessary after the linear equation solution rather than before.

The solution of the embedded continuity equation in routine CALCPK is performed exactly in the sequence of Table A-2, except of course, there are no source terms to evaluate in the continuity equation.

In standard applications of the Spalding and Patankar technique, this pressure correction would be performed several times, and then the sequence would pass on to the energy equation as shown in Table A-1.

However, CRNL experience has shown that convergence can be promoted more rapidly if further pressure correction is done using an alternative iteration sequence. In this sequence, a further standard pressure correction is performed in CALCPI. This imposes continuity over the I-planes following the modified sequence used in CALCW.

TABLE A-3

THE PRESSURE AND VELOCITY CORRECTION SEQUENCE

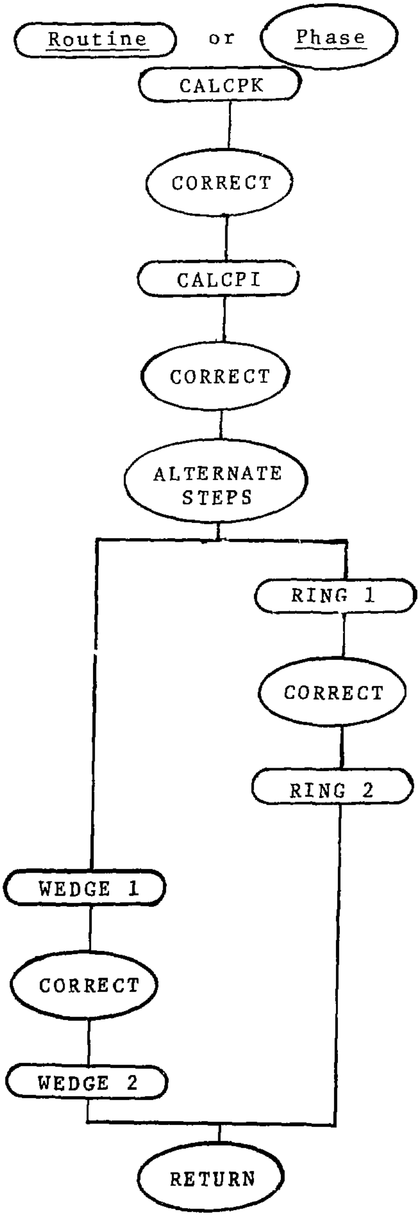

Purpose

Solve continuity equation for pressure corrections by K planes.

Apply velocity corrections and compute new pressures.

Solve continuity equation for pressure corrections by I planes.

Apply velocity corrections and compute new pressures.

Solve continuity equation for pressure corrections by rings.

Apply velocity corrections and compute new pressures.

Adjust W velocities for continuity in neighbouring rings.

Solve continuity equation for pressure correction by wedges.

Apply velocity corrections and compute new pressures.

Adjust V velocities for continuity in neighbouring wedges.

Finally, continuity is imposed, on alternate iteration steps, over 'wedges' and 'rings'. In the latter two cases, the resulting equations are not solved by alternating direction tridiagonal iteration, but by direct solution of the banded linear equation set. This is done fully by Gaussian elimination using the decomposition and back substitution routines MATSET and SOLN.

A.4 Auxiliary Routines

The routines that form the inner and outer iteration sequences call a number of auxiliary routines, which have not yet been described. They are listed here:

Routine	Function
RSTART	Read Restart tape
SOMOD	Find maximum source term
FRIC	Multiple entry routine for all single-phase friction factors
HTF	Multiple entry routine for all single-phase heat transfer
PRPRTY	Multiple entry routine for all fluid thermodynamic properties
TWOPH	Multiple entry routine for all two-phase pressure drop correlations
VOLL	Compute control volume parameters in tube filled regions
BCUT	Compute fraction of control volume in the tube free lane, or occupied by a baffle

APPENDIX B

REFERENCES AND ACKNOWLEDGEMENTS

References

[1] S.V. Patankar, "Computer Analysis of Distributed Resistance Flows, 1. Introduction to the DRIP Computer Program", CHAM Report B262, Combustion Heat and Mass Transfer Ltd., 1975.

[2] R.H. Shill, Private Communication, September, 1977.

[3] W.W.R. Inch and R.H. Shill, "Thermal-Hydraulics of Nuclear Steam Generators", ASME Nuclear Engineering Division Conference, San Francisco, August 1980.

[4] W.W.R. Inch, D.A. Scott and M.B. Carver, "Steam Generator Thermal-Hydraulics Analytical and Experimental", AECL-6885, presented at the 5th Symposium on Engineering Applications of Mechanics, University of Ottawa, 1980.

[5] L.N. Carlucci, "Thermal-Hydraulic Analysis of the Combustion Engineering System 80 Steam Generator", EPRI Report NP 1546, project S-130-1, June 1980.

[6] W.W.R. Inch, "Thermal-Hydraulic Analysis of the Combustion Engineering Series 67 Steam Generator, EPRI Report NP 1678, project S-130-1, Jan. 1981.

[7] M.B. Carver, "Thermal-Hydraulic Analysis of the stinghouse 51 Steam Generator, EPRI report in press, proje S-130-1, March 1981.

[8] S.V. Patankar and D.B. Spalding, "A Calculation Procedure for Heat, Mass and Momentum Transfer in Three-Dimensional Parabolic Flows", Int. J. Heat Transfer, 15, p.1787, 1972.

[9] F.H. Harlow and J.E. Welch, "Numerical Calculation of Time Dependent Viscous Incompressible Flow", Physics Fluids, 8, p.2182, 1965.

[10] M.B. Carver and H.W. Hinds, "The Method of Lines and Advective Equation", Simulation, 31, p.59, 1978.

[11] M.B. Carver, "Pseudo-Characteristic Method of Lines Solution of the Conservation Equations, J. Comp. Physics, 35, 1, p.57, 1980.

Acknowledgements

The authors wish to acknowledge the early work by R.H. Shill on steam generator codes, much of which laid the foundations of the current THIRST code. N.M. Sandler has been of invaluable assistance in the computer programming, among other contributions he designed the plotting and read in sections. D.G. Stewart and C. Taylor have also contributed towards restructuring and rationalizing code content.

The monumental task of deciphering, typing and revising this manuscript might have foundered but for the efficient and cheerful efforts of Mrs. M.L. Schwantz.

ISSN 0067 - 0367

To identify individual documents in the series we have assigned an AECL- number to each.

Please refer to the AECL- number when requesting additional copies of this document

from

Scientific Document Distribution Office
Atomic Energy of Canada Limited
Chalk River, Ontario, Canada
KOJ 1JO

Price $9.00 per copy

ISSN 0067 - 0367

Pour identifier les rapports individuels faisant partie de cette série nous avons assigné un numéro AECL- à chacun.

Veuillez faire mention du numéro AECL- si vous demandez d'autres exemplaires de ce rapport

au

Service de Distribution des Documents Officiels
L'Energie Atomique du Canada Limitée
Chalk River, Ontario, Canada
KOJ 1JO

Prix $9.00 par exemplaire

1167–81